

POLITECNICO DI MILANO

MASTER'S THESIS

BIOMEDICAL ENGINEERING - ELECTRONICS
TECHNOLOGIES

Electronic, Information and Bioengineering Department

**Tactile display with tunable
stiffness based on
magnetorheological effect**

Supervisor:

Prof. Andrea ALIVERTI

Co-Supervisor:

Prof. Miki NORIHISA

Author:

Nicolò LORENZONI

783734

in collaboration with

KEIO UNIVERSITY OF SCIENCE AND TECHNOLOGY

Miki MEMS Laboratory

ACADEMIC YEAR 2013/2014

“I am enough of an artist to draw freely upon my imagination. Imagination is more important than knowledge. Knowledge is limited. Imagination encircles the world.”

Albert Einstein

POLITECNICO DI MILANO

Extended Abstract

Keio University of Science and Technology

Master's Degree in Biomedical Engineering - Electronics Technologies

Tactile display with tunable stiffness based on magnetorheological effect

by Nicolò LORENZONI

In the last decades visual and auditory senses have been the topics of researches that have produced interesting devices and nowadays there are widespread and well consolidated technologies for both of them whereas *haptics* is not equally well known. Haptic technologies involve the interaction of the tactile sense both as pure mechanical and thermal or pain perception. Tactile sense is for sure more vivid and realistic since can give a massive quantity of information without any sounds or glimpse. Nowadays haptic system are mainly applied in communication system as simple buzzing signal for mobile phone, in gaming and entertainment (Buttkicker™) to immerge the spectator into a stunning realism and in the more serious industrial field as in cockpit to deliver through a vibrating handles life threatening and critical condition.

Haptic devices are of course following the meteoric rise of technologies and today, more than ever before, are finding their way in medical field becoming vital part of many medical training and research applications. The hands of the surgeons are progressively being substituted by robotic and minimally invasive arms, which can operate through small natural or artificial holes. It must be said that machines at the same time deprive the operators of the plurality of information that can be transmitted by the sense of touch and the tactile feedback that doctor was used to use is no longer available since the direct contact is missing.

For this reason engineers and researcher in the last two decades started to propose a multiplicity of devices that try to fill the gap between machine and human during medical operation for true-to-life simulation of the tactile experience in the virtual environments. The requirements that a haptic device has to fulfil are extremely demanding. It has to substitute the multitude of sensation that human acquire by the sense of touch: in fact, simultaneously the shape and the surface of the object are analysed. By touching it we are able to characterize the physical properties of the surface saying if it is rough or smooth and at the same time to discriminate the mechanical properties of that object classifying it as soft or hard. In this sense haptic devices if indented as add-ons in medical diagnosis as well as bridge between doctor and patient after the decoupling caused by the technologies have to fulfil the capability to recreate a vivid sensation as much as close to the realty with a remarkably high level of accuracy that is not negotiable. Of course haptic feedback is not always necessary since it depends on the work considered. But as mentioned above for professions such as medical that require high manual trades haptic feedback plays an important role and optimize the interface between real world and the telemanipulated-programmed machine. Thus, the state of art of virtual reality medical devices should not leave out of consideration the involvement and usage of the sense of touch. Nowadays the most commonly available haptic interfaces can be defined as force producing (Wristalyzer™ or SensAble Phantom Omni™). In fact force is a concept that is related with everyday experience and allows a simple introduction to the workings of haptic technology. However, tactile perception is not exclusively bound to the use of force but there are several ways to describe and realize haptic devices such as elongation, frequencies, mechanical tension and sheared forces that could be other ways, maybe easier, to translate the mechanical interaction with the object.

Many medical disciplines are nowadays using tactile analysis and doctors still draw conclusion based on their tactile feeling even though the patient prefers the distinctiveness of a real image. For example during medical analysis for tumour detection *palpation* of tissues is still preferred: it is well known that tumours are stiffer than normal tissues, moreover CT scanning cannot detect tumours smaller than 5 mm and endoscope can only make diagnosis on surface of tissues. Thus, stiffness information is still a key factor for medical applications for diagnosis and therapy. Sometimes the plurality of information that derives from palpation is not easily accessible or even not accessible at all. In this scenario is required a

breakthrough solution that brings out through an on-tip sensor the tissue's natural mechanical properties and allows to reproduce them in a virtual environment, such as a haptic display. This device would vary its mechanical characteristics to faithfully reproduce the properties of the considered tissue for a simulation of the tactile sensation that an operator would receive when palpating that generic tissue. It is obvious that to replicate human tissues a simple time-invariant system would not be sufficient but for the design of such devices is demanded to deal with a selectable and reconfigurable haptic properties since the stiffness of tissues can span in a wide range of values. The focus of this thesis is on the design of novel polymer tactile display or *tactor* with magnetorheological fluid fill-in. Magnetorheological effect allows changing the stiffness of the device by applying a magnetic field. The stiffness enhancement is sensed touching the devices through a large displacement PDMS membrane. The basic idea is to create a display capable of changing its mechanical behaviour as response to an external electrical signal. The fast response-time and the non-abrasive characteristic of the fluid give the chance for real-time application and long life devices. Final purpose of the project is to design -using MEMS techniques- a programmable device whose controlled surface is intended for interface with human touch. As already speculated the widespread applications of this kind of devices make it useful when a tactile feedback is needed in order to improve the quality of the virtual reality in medical applications.

Like in any other process the final design of the tactor derives from an optimization of different elements influenced by each other. Since the very first steps of the project it has been followed the idea of designing a device accordingly to the requirement of simplicity, low power consumption and low costs. Between the manifold methods and techniques to communicate the haptic information through the display, smart magnetic materials (SMM) such as magnetorheological fluid (MR) have been chosen. When exposed to a magnetic field, the rheology of the fluid reversibly and instantaneously changes from a free-flowing liquid to a semi-solid with controllable yield strength. The phenomenon is consequence of the disposing of particles that will be aligned according to the distribution of the magnetic field. Inter alia the alignment of magnetic particles increases the stiffness of the liquid and by increasing the magnitude of magnetic field it can be further enhanced the material's rigidity by the attraction force of particles. In order to create a proper case for fluid containment and membrane bonding polymethylmethacrylate (PMMA) which is a plastic material formed by polymers of

methyl methacrylate has been shaped through a laser-cut assisted machine. Unlike the chamber's shape the choice of the thickness called for a very hard study to hammer out a workable compromise since the stiffness displayed is not linearly proportional to the thickness of the case.

When it came to chose a low price and easy to pattern material for membranes, polydimethylsiloxane (PDMS) won hands down: widely used in microfluidics, is optically transparent, flexible and cheap enough for not denting the budgets. The fabrication process of PDMS membrane consisted of preparing a glass plate coated with a solution that facilitated the peeling off. When the plate is ready PDMS is spin-coated on the glass at the proper speed to obtain $100\mu m$ membrane. Thereafter the membrane is bonded with the case through a UV-curable resin: previously spin coated on another glass plate, the resin is transferred to the PMMA case and eventually exposed to UV-light. To transfer the MR fluid inside the chamber different encapsulation's methods have been tested. If the fluid is poured directly into the chamber and then the membrane is sealed with the UV-resin chances are that also air bubbles are encapsulated. Thus, after trying the bond-in-liquid-technique (BiLT) to get rid of the mentioned problem it has been opted for a syringe encapsulation with two air-escape holes and to bond the PDMS membrane before liquid encapsulation.

Of course the tactile display needs an actuator and its selection is quite delicate since influences the quality of the haptic impression. The main feature that the actuator for this haptic display should have is the capability to generate high (above $250mT$) and variable magnetic field. In fact, to generate adequate stiffness through the alignment of nanoparticles the MR fluids needs a substantial quantity of magnetic flux and the variability is necessary to span in a wide range of stiffness value. In other words the straightforward on-off solution would not fulfilling the purpose. Even though current controlled solenoids were quite attractive their magnetic intensity is not even close to the necessary. Neodymium magnets coupled with voice coil actuator (VCA) have been chosen. Between a wide set of actuation solutions such as ultrasonic actuators, stepper-motor, pneumatic and hydraulic system VCAs stand out because can be easily made oneself and chances are that the actuator cannot be found off-the-shelf. To electronically control the VCAs through an Arduino™ board the choice was oscillating between supervised *neural network*, due to the high non-linearity of the system and the principle of equivalent area (PEA). PEA uses the pulse-width-modulation (PWM), which is frequently

combined with a dual H-bridge to provide two-operation mode, thus two active direction of movement and enough output current from the microcontroller's pins to the coil. The tactor's spatial resolution was linked with the magnetic field containment: if the magnetic flux is well confined the iron particles' cluster obtained is smaller, better defined in the 3D space and it may result in a more punctual haptic perception. Unfortunately, there is no known material that totally blocks or contains magnetic field. It can only be redirected away from the objects to be protected providing an alternative path for the magnetic field lines. Hence, solutions as redirection through high-permeability alloys, septa, magnet's polarities, iron discs and self-made MR fluids have been covered. Once assembled, the device's quality has to be quantified and the usage of tools that enable the engineer to judge the quality of the technical design is an advantage. To quantify the haptic perception micro-strain tester and teslameter were precious instrumentation to draw graphical results.

In conclusion the haptic display proposed in this thesis fulfil the coding of volumetric information with low complexity, good spatial resolution, low delay in data processing, repeatability and accuracy. When MR fluid reacts against an external magnetic field and changes its mechanical property the display through the PDMS membranes can create hard spots in soft surfaces, like a tumour in tissues. The spatial resolution of about 7 mm (referred to FWHM) is consistent with the diameter of the smallest lymph node and the hardness of the spot is within the values of natural tissues ranging of several hundreds of kPa . Using voice coil actuator for magnet positioning the action is fast enough to consider negligible the delay of implementation. The hardness displayed along the device has a small standard deviation and doesn't scatter widely (a good repeatability has been achieved) giving a stable haptic perception.

As already speculated, using MEMS techniques, this thesis work proposes a novel design for a miniature tactile display conveying stiffness information. Based on magnetorheological (MR) fluids its stiffness can be varied by magnetic flux and sensed touching the liquid through a large displacement PDMS membrane. Using MR fluids has been possible to simplify and miniaturize the actuation and avoid bulky electronic. The overall project is divided essentially in two parts. The first is completely dedicated on the discussion of the technical process to design the display itself. The second one is committed on the actuation system, one of the

most important elements of haptic devices. The detailed contents of chapters are shown below.

- Chapter 1: An introduction is dedicated to an historical overview on haptic perception from the purely philosophical approach of ancient greek up to the modern technologies. Moreover, a small section is dedicated to frame different haptic devices and to explore the terminology linked to them.
- Chapter 2: The first chapter deals with the choice of the materials. Fluids, structure, membrane and actuators are here analyzed. The usage of each component instead of others is studied and justified.
- Chapter 3: This chapter is almost fully dedicated on different ways of positioning the actuator. After the analysis and comparing different solutions a detail study on confining magnetic flux density is reported.
- Chapter 4: In this section are described the techniques used to assembly the tactile display after that all components have been chosen. Further a precise measurement protocol is described parallel to the design of the supports for testing.
- Chapter 5: All the graphs and results are here reported and discussed.
- Chapter 6: The last chapter gives a final overall evaluation of the project. Moreover, open topics are here analyzed with future prosppections, directions and developments of the experimental project of this thesis.

This thesis work was done while in candidature for a Master's degree at Politecnico di Milano. The experimental work was entirely done at Keio University of Tokyo from March 2013 till the end of September 2013. Where I have consulted or quoted published work this is always clearly attributed, the source is always given. With the exception of such quotations, this thesis is entirely my own work. Due to a limited time available few topics are still on going and their final solutions are not presented in this thesis work.

This thesis work has already been presented at the following conferences:

- *SICE (The Society of Instrument and Control Engineers) IA (Industrial Applications) Division Annual Conference 2014.*
- *JSME (Japan Society of Mechanical Engineers) 5th micro and nano technology and science conference.*
- *ICEP(International Conference on Electronics Packaging) 2014 Toyama, Japan.*

Moreover, it is under review for:

- *H. Ishizuka, N. Lorenzoni and N. Miki, "Tactile display for presenting stiffness distribution using magneto-rheological fluid" - Mechanical Engineering Journal.*
- *H. Ishizuka, N. Lorenzoni and N. Miki, "Tactile display to reproduce stiffness distribution of biological tissues using Magnetorheological Fluid" - Eurohaptics 2014.*

POLITECNICO DI MILANO

Sommario Esteso

Keio University of Science and Technology

Laurea in Ingegneria Biomedica - Tecnologie Elettroniche

Display tattile con rigidità sintonizzabile basato sull'effetto magnetoreologico

di Nicolò LORENZONI

Negli ultimi decenni i sensi visivo ed uditivo sono stati oggetto di un'intensa ricerca che ha prodotto dispositivi interessanti, ad oggi tecnologie diffuse e ben consolidate, mentre il *tatto* non ha seguito lo stesso percorso. Le tecnologie aptiche coinvolgono l'interazione del senso tattile sia come pura percezione meccanica sia termica o di dolore. Il senso tattile è sicuramente più vivido e realistico dei primi due poiché può dare una quantità enorme d'informazioni senza sentire od osservare alcunché. Oggi le interfacce aptiche trovano principalmente applicazione in sistemi di comunicazione, come può essere la semplice vibrazione di un telefono cellulare, nel settore dei videogiochi e dell'intrattenimento (Buttkicker™), per immergere lo spettatore in un ambiente più realistico possibile e nel campo industriale, ad esempio nelle cabine di guida di macchine o aerei per avvisare attraverso maniglie vibranti situazioni di pericolo di vita e condizioni critiche.

I dispositivi tattili stanno seguendo la rapida crescita dello sviluppo tecnologico e oggi, più che mai, stanno trovando la loro strada in campo medico diventando parte vitale di molte applicazioni medicali. Le mani dei chirurghi sono progressivamente sostituite da robot minimamente invasivi, i quali possono operare attraverso piccoli fori naturali o artificiali. Va detto però che le macchine contemporaneamente privano gli operatori della pluralità d'informazioni che possono essere trasmesse dal senso del tatto e il feedback tattile al quale il medico era abituato non è più disponibile, mancando un contatto diretto.

Per questo motivo ingegneri e ricercatori nell'arco degli ultimi due decenni stanno proponendo una molteplicità di dispositivi che cercano di colmare il divario creatosi tra macchina ed umano durante le operazioni medicali, per una simulazione il più realistica possibile (*true-to-life*) dell'esperienza tattile nell'ambiente virtuale. I requisiti che un dispositivo aptico deve soddisfare sono quindi molto esigenti. Deve, infatti, sostituire la moltitudine di sensazioni che si acquisirebbero naturalmente come ad esempio l'analisi contemporanea della forma e della superficie dell'oggetto. Toccando un elemento si è in grado di caratterizzare le proprietà fisiche della superficie dicendo se sia ruvida o liscia e allo stesso tempo discriminare le proprietà meccaniche di tale oggetto classificandolo come morbido o duro. In questo senso, i dispositivi tattili se si prefigurano di essere elementi di supporto nella diagnosi medica, come ponte tra medico e paziente dopo il disaccoppiamento causato dalle tecnologie, devono avere la capacità di ricreare una sensazione aptica quanto più vicina alla realtà con un livello di accuratezza molto elevato dal quale non si può prescindere. Naturalmente il feedback tattile non è sempre necessario giacché dipende dal lavoro considerato. Ma, come detto sopra per professionisti come medici il cui mestiere richiede un'elevata interazione manuale, il feedback tattile gioca un ruolo importante nell'ottimizzare l'interfaccia tra il mondo reale e la macchina telemanipolata e programmata. Pertanto, lo stato dell'arte dei dispositivi medici per realtà virtuale non dovrebbe prescindere dal coinvolgimento e dall'utilizzo del senso del tatto. Oggi le interfacce aptiche più comunemente disponibili possono essere definite come produttori di forza (WristalyzerTM o SensAble Phantom OmniTM). Ciò è dovuto al fatto che la forza è un concetto strettamente legato con l'esperienza quotidiana e consente una semplice introduzione al funzionamento della tecnologia aptica. Tuttavia, la percezione tattile non è destinata ad essere espressa esclusivamente con l'uso di una forza, ma vi sono diversi metodi per descrivere e realizzare dispositivi tattili quali allungamento, frequenze e tensioni meccaniche che potrebbero rappresentare altri modi, forse più facili, di tradurre l'interazione tattile con l'oggetto.

Molte discipline mediche ancora oggi utilizzano l'analisi tattile tramite la quale i medici traggono conclusioni sulla base della loro sensibilità ed esperienza tattile nonostante il paziente generalmente preferisca il carattere distintivo di un'immagine diagnostica reale. Ad esempio la palpazione, per il rilevamento di eventuali forme tumorali dei tessuti, è ancora molto diffusa: è noto che i tumori sono più rigidi rispetto ai tessuti normali, inoltre la CT non può rilevare tumori inferiori a 5 mm e l'endoscopio può solo fare diagnosi tessutali superficiali. Per quanto

detto, le informazioni sulla rigidità (*stiffness*) dei tessuti ad oggi sono ancora un fattore chiave per applicazioni mediche per la diagnosi e la terapia. A volte però, la pluralità d'informazioni che deriva dalla palpazione non è facilmente accessibile o non fruibile del tutto. In questo scenario è richiesta una soluzione innovativa che misuri attraverso un sensore in punta di catetere le proprietà meccaniche naturali del tessuto e che ne permetta la loro riproduzione in un ambiente virtuale, quale ad esempio un display tattile. Questo dispositivo potrebbe variare le proprie caratteristiche meccaniche al fine di riprodurre fedelmente quelle del tessuto biologico considerato per una simulazione della sensazione tattile che un operatore riceverebbe palpando quello stesso tessuto. È ovvio che per replicare tessuti umani, semplici sistemi tempo-invarianti non siano sufficienti, ma per la realizzazione di tali dispositivi è richiesto affrontare la progettazione d'interfacce con proprietà tattili selezionabili e riconfigurabili poiché la rigidità dei tessuti può estendersi in un ampio intervallo di valori. Il focus di questa tesi è proprio la progettazione di un display tattile con rigidità sintonizzabile che sfrutta l'effetto magnetoreologico di un fluido per portare l'informazione di *stiffness*. L'effetto magnetoreologico permette di modificare la rigidità del dispositivo applicando un campo magnetico. L'incremento di rigidità è rilevato toccando il display attraverso una membrana polimerica (PDMS). L'idea di base è di creare un'interfaccia aptica in grado di cambiare il suo comportamento meccanico come risposta ad un segnale elettrico esterno. Il tempo di risposta veloce e la caratteristica non abrasiva del fluido danno la possibilità ad applicazioni in tempo reale e a dispositivi di lunga durata. Lo scopo finale del progetto è di realizzare, utilizzando tecniche MEMS, un dispositivo programmabile la cui superficie regolabile è intesa ad interfacciarsi con il tocco umano. Come già ipotizzato, dispositivi di questo tipo si rendono utili quando un feedback tattile è necessario, al fine di migliorare la qualità della realtà virtuale esse siano applicazioni mediche o meno.

Come in qualsiasi altro processo, il progetto finale del display tattile deriva da un'ottimizzazione di diversi elementi che s'influenzano a vicenda. Fin dai primi passi della realizzazione è stata seguita l'idea di progettare un dispositivo che rispondesse a requisiti di semplicità, basso consumo e costi contenuti. Tra molteplici metodi e tecniche utilizzabili per rappresentare l'informazione tattile, una soluzione interessante è stata trovata nei materiali magnetici intelligenti (SMM), in particolare nei fluidi magnetoreologici (MR). In questi ultimi, quando esposti ad un campo magnetico, la reologia del fluido reversibilmente e istantaneamente

cambia da uno stato liquido ad uno semi-solido con rigidità controllabile. Il fenomeno è conseguenza dell'allineamento delle nano particelle di ferro secondo la distribuzione del campo magnetico. La nuova distribuzione delle particelle magnetiche aumenta la rigidità del liquido e incrementando l'intensità del campo magnetico può essere ulteriormente incrementata la forza di attrazione delle particelle e quindi della rigidità generata. Al fine di possedere una camera (*case*) per il corretto contenimento del liquido e allo stesso tempo facilmente incollabile con la membrana è stato modellato, tramite una macchina per il taglio assistito al laser, il polimetilmetacrilato (PMMA) ovvero una materia plastica formata da polimeri di metacrilato di metile. Diversamente dalla forma, la scelta dello spessore della camera ha richiesto uno studio molto meticoloso per trovare un compromesso plausibile poiché la rigidità visualizzata non è linearmente proporzionale allo spessore del *case*.

Quando si è trattato di scegliere un materiale dal prezzo ridotto e facilmente modellabile per la realizzazione della membrana, il polidimetilsilossano (PDMS) ha vinto a mani basse: ampiamente usato in micro fluidica, è otticamente trasparente, flessibile e abbastanza a buon mercato per non intaccare i bilanci. Il processo di fabbricazione della membrana PDMS consiste nel preparare un vetrino rivestito con una soluzione che facilita lo spellamento di quest'ultima. Quando il piattino è pronto, il PDMS liquido è distribuito uniformemente per centrifugazione ad una precisa velocità (processo di *spin-coating*), fino ad ottenere un rivestimento di circa $100\mu m$. In seguito la membrana è legata al *case* attraverso una resina fotosensibile ai raggi UV: prima rivestita per centrifugazione su un'altra lastrina di vetro, la resina è trasferita sul contenitore di PMMA e quindi esposta a luce ultravioletta. Per trasferire il liquido MR all'interno della camera diversi metodi d'incapsulamento sono stati testati. Se il liquido fosse versato direttamente nella camera e il tutto sigillato con la membrana sarebbero incapsulate anche molte bolle d'aria. Così, dopo aver provato la tecnica d'incapsulamento direttamente nel liquido (BiLT) per sbarazzarsi del problema di cui sopra, si è scelto un incapsulamento a siringa con due fori per la fuga d'aria creati ad hoc sulla struttura di PMMA e di incollare la membrana PDMS prima di incapsulare il liquido.

Naturalmente il display tattile richiede un attuatore e la sua scelta è molto delicata poiché influenza la qualità dell'impressione tattile finale. La caratteristica principale che l'attuatore per l'interfaccia aptica in oggetto deve avere è la capacità di generare un elevato (sopra i $250mT$) e variabile campo magnetico. Infatti,

per generare un'adeguata rigidezza attraverso l'allineamento delle nano particelle i fluidi MR hanno bisogno di una quantità sostanziale di flusso magnetico mentre la variabilità è necessaria per la rappresentazione di una vasta gamma di valori di *stiffness*. In altre parole la semplice soluzione on-off non soddisferebbe lo scopo. Anche se i solenoidi controllati in corrente sono molto attraenti, la loro intensità magnetica non è nemmeno lontanamente vicina a quella necessaria. Per lo scopo si sono scelti magneti al neodimio accoppiati con una bobina-attuatore (Voice Coil Actuator). Tra una vasta gamma di soluzioni di attuazione, quali ultrasuoni, pneumatici, con sistema idraulico e motori passo-passo, i VCA spiccano perché possono essere facilmente realizzati "in casa" e le probabilità che l'attuatore necessario non sia disponibile sul mercato sono molto alte. Per controllare elettronicamente i VCA attraverso una scheda Arduino™, la scelta è oscillata tra una *rete neurale supervisionata*, a causa dell'elevata non linearità del sistema e il principio delle aree equivalenti (PEA). Il PEA utilizza la Pulse Width Modulation (PWM), ed è spesso combinata con un circuito integrato a doppio ponte H per fornire due modi di funzionamento, quindi due direzioni attive di movimento, e una corrente di uscita al piedino del microcontrollore sufficiente allo spostamento della bobina.

La risoluzione spaziale del display aptico è fortemente connessa al contenimento del campo magnetico: se il flusso magnetico risulta ben confinato allora l'insieme delle particelle di ferro ottenuto sarà più piccolo, meglio definito nello spazio e provocherà una percezione tattile più puntuale. Purtroppo, non vi è alcun materiale noto che blocchi totalmente o equivalentemente contenga il campo magnetico. Quest'ultimo può solo essere reindirizzato lontano dagli oggetti da proteggere fornendo un percorso alternativo alle linee di flusso. Detto ciò, si sono affrontate soluzioni per l'indirizzamento e il controllo del campo tramite leghe ad alta permeabilità, vasche di contenimento, polarità dei magneti, dischi di ferro e fluidi MR fatti da sé. Una volta assemblato, la qualità del dispositivo deve essere quantificata e l'utilizzo di strumenti che consentono al progettista di giudicare la qualità del progetto tecnico è di enorme vantaggio. Per quantificare la percezione tattile, il tester a micro-deformazione e il teslametro sono stati strumenti preziosi per rappresentare graficamente i risultati.

In conclusione, il display tattile proposto in questa tesi cerca di riprodurre le informazioni meccaniche dei tessuti tramite una soluzione a bassa complessità, buona

risoluzione spaziale, basso ritardo nel trattamento dei dati, ripetibilità e precisione. Quando il fluido MR reagisce per risposta ad un campo magnetico esterno e cambia le proprie proprietà meccaniche, il display attraverso una membrana PDMS crea punti duri su una superficie morbida, similmente ad un tumore nei tessuti. La risoluzione spaziale di circa 7 mm (intesa come FWHM) è coerente con il diametro del più piccolo linfonodo e i valori di rigidità mostrata spaziano all'interno del *range* naturale dei tessuti umani variando di diverse centinaia di *kPa*. Il posizionamento del magnete tramite l'uso di una bobina-attuatore è abbastanza veloce da considerare trascurabile il ritardo di attuazione. La percezione tattile offerta dall'interfaccia è stabile poiché i valori rappresentati dal dispositivo hanno una piccola deviazione standard, segno di una buona ripetibilità.

Come già anticipato, utilizzando tecniche MEMS, questo lavoro di tesi propone un nuovo design per un display tattile allo scopo di trasmettere informazioni sulle caratteristiche meccaniche dei tessuti. Basandosi sull'utilizzo di un fluido magnetoreologico (MR) la sua rigidità può essere variata da un flusso magnetico e quindi rilevata toccando il liquido attraverso una membrana polimerica PDMS ad elevata deformazione. Utilizzando il fluido MR è stato possibile semplificare e miniaturizzare l'azionamento ed evitare ingombranti soluzioni elettroniche. Il progetto complessivo è suddiviso essenzialmente in due parti. La prima è completamente dedicata alla discussione del processo tecnico che ha portato alla progettazione del display stesso. La seconda fa invece perno sul sistema di azionamento, uno degli elementi più importanti nei dispositivi tattili. I contenuti dettagliati dei capitoli sono riportati di seguito.

- Capitolo 1: L'introduzione è dedicata ad una *overview* sulla percezione aptica da un approccio puramente filosofico degli antichi greci fino alle più moderne tecnologie. Inoltre, è stata dedicata una piccola sezione per inquadrare i dispositivi aptici e la terminologia ad essi connessa.
- Capitolo 2: Il primo capitolo tratta con la scelta dei materiali. Fluidi, struttura, membrana ed attuatori vengono analizzati. L'utilizzo di ogni componente, piuttosto che un altro è studiato e giustificato.
- Capitolo 3: Questo capitolo è interamente dedicato a diversi modi di posizionamento dell'attuatore magnetico. Dopo l'analisi e il confronto di diverse soluzioni è riportato uno studio dettagliato sul come confinare la densità di flusso magnetico.

- Capitolo 4: In questa sezione vengono descritte le tecniche utilizzate per l'assemblaggio del display tattile, dopo che la scelta di tutti i componenti è stata ultimata. Inoltre, un protocollo preciso di misura è descritto parallelamente alla progettazione dei supporti utilizzati per i test.
- Capitolo 5: Tutti i grafici ed i risultati sono qui riportati e discussi.
- Capitolo 6 : L'ultimo capitolo fornisce una valutazione finale complessiva del progetto. Vengono poi qui analizzati i temi aperti assieme alle prospettive, direzioni future e possibili sviluppi del progetto sperimentale di tesi.

Questo lavoro di tesi è stato fatto in candidatura per una laurea specialistica presso il Politecnico di Milano. Il lavoro sperimentale è stato interamente realizzato alla Keio University di Tokyo, da Marzo 2013 fino alla fine di Settembre 2013. Dove è stato consultato o citato lavoro già pubblicato ciò è sempre chiaramente attribuito e la fonte è sempre data. Con l'eccezione di tali quotazioni, questa tesi è frutto del mio lavoro. A causa di un periodo limitato a disposizione alcuni argomenti sono ancora in fase di studio e le loro soluzioni definitive non sono presentate in nella seguente tesi.

Il lavoro è già stato presentato alle seguenti conferenze:

- *SICE (The Society of Instrument and Control Engineers) IA (Industrial Applications) Division Annual Conference 2014.*
- *JSME (Japan Society of Mechanical Engineers) 5th micro and nano technology and science conference.*
- *ICEP(International Conference on Electronics Packaging) 2014 Toyama, Japan.*

Inoltre, sotto revisione per:

- *H. Ishizuka, N. Lorenzoni and N. Miki, "Tactile display for presenting stiffness distribution using magneto-rheological fluid" - Mechanical Engineering Journal.*

- *H. Ishizuka, N. Lorenzoni and N. Miki, "Tactile display to reproduce stiffness distribution of biological tissues using Magnetorheological Fluid" - Eurohaptics 2014.*

Acknowledgements

Foremost, I would like to express my sincere gratitude to my advisor Prof. Norihisa Miki for the continuous support during my research period at his laboratory at Keio University. I would also like to thank him for the motivation, the enthusiasm and the help he gave me to shape my interest and ideas in all the time of research. I would like to express my deep gratitude and respect to Prof. Andrea Aliverti that gave me confidence and carte blanche to my experience abroad. A sincere appreciation goes to Hiroki Isihzuka, my fellow in this amazing project. I would like to thank him for his continuous help, for the stimulating discussions and support in all stages of this project. His attitude to research inspired me.

My greatest appreciation and friendship goes to my closest friend, Koya Mikami, who was always a great support in all my struggles and frustrations in my new life in Japan. We spend amazing moments together wakeboarding and clubbing. Of course a massive thanks to all members of Miki Laboratory who made the lab a friendly environment for working and gave me the chance to get a deeper knowledge of Japanese culture. I have amazing memories of the climb of Fuji-San and the relaxing onsen we went all together after, the wine experience at Kosemura's house and all the farewell parties where Kota Sampei aka "The Japanese monster" got drunk every time. Big thanks to Dr. Gunawan Prihandana for from which I had always something to learn. Despite the immense distance from home, I never felt like a foreigner in a foreign land.

Cheers to all the people that made my stay in Japan more enjoyable. So thanks to Lorenzo, Hamza, Angelos, Valeria, Mario and Nouha. A special and sincere thanks to Marco Huebner for being a great reliable person to whom I could always talk about my concerns and excitements with whom I have spent amazing and unforgettable moments. Even though we have seen each other few times in the past two years I am still grateful to Federico and Beatrice.

Last but not least expression of gratitude to Elena for her continuous love and supports in my decisions and of course my family: my parents for giving birth to me at the first place, for always believing in me and supporting me spiritually throughout my life without whom I could not have made it here.

Contents

Extended Abstract	ii
Sommario Esteso	ix
Acknowledgements	xvii
Contents	xviii
List of Figures	xx
1 Introduction	1
1.1 Historical prospective	1
1.2 Framing haptic science	6
1.2.1 Terminology	9
2 Materials and Technologies	13
2.1 Fluid	15
2.2 Case	21
2.3 Membrane	25
2.3.1 Piston-like membrane	28
2.3.2 Fluid encapsulation	29
2.3.2.1 BILT	31
2.3.2.2 Syringe encapsulation	33
2.4 Magnetic field generation	35
2.4.1 Solenoids	38
2.4.2 Permanent magnets	39
3 Actuators	41
3.1 Actuation systems	45
3.1.1 Voice coil actuation (VCA)	49
3.2 Solution for the magnetic field confinement	52
3.2.1 Re-routing for shielding	52
3.2.2 Septa	55

3.2.3	Iron nanoparticles	60
3.2.4	Magnet's polarities	61
4	Assembly	64
4.1	Control of the actuator	69
4.2	Tools for measurements	75
5	Experimental results	79
6	Conclusions	96
6.1	Open topics and future directions	96
6.2	Final conclusions on the device	101
A	Conference Paper	104
B	Journal Paper	105
	Bibliography	107

List of Figures

1.1	Human and the corresponding robotic hand [1].	2
1.2	West equipped with vibrators for the spatial coding of positioning and bearing data [2].	3
1.3	Example of haptic technologies.	4
1.4	The Mako Rio™ is a surgeon interactive tactile surgical simulation platform that with a robotic arm allows the insertion and alignment of implants through a minimal incision.	5
1.5	The climax of video-laparoscopic telemanipulation technologies can be found in the DaVinci™ robotic system.	6
1.6	Overview about the disciplines participatin in haptic research [3].	7
1.7	Human senses with a detail on haptic [3].	8
1.8	Haptic device.	10
1.9	Tactor device.	11
1.10	Haptic simulator.	11
1.11	Haptic assistive system.	12
2.1	Main components of the tactile display and correspondent chapters.	14
2.2	MR fluid used to control the response of a car suspension.	16
2.3	Physical detail of the electromagnetic control for a piston-like suspension.	16
2.4	The figures depicts at the electronic microscope the MR fluid in normal condition (top) and crossed by a magnetic flux (bottom) where all particles are alligned.	18
2.5	Detail of the effect of increasing the magnetic flux on the particles' chains [4].	18
2.6	Lord™MRF-122EG fluid datasheet.	19
2.7	Yield stress vs. Magnetic Field Strength.	20
2.8	Ferrofluid when magnetic field is applied.	21
2.9	First type of PMMA case for MR fluid. The dimensions are 30 x 30 mm.	22
2.10	Single chamber acrylic base for MR fluid.	23
2.11	First attempt to create a thin PDMS membrane.	25
2.12	PDMS membrane on glass substrate cured in advance.	26
2.13	Relation between spin coater speed and thickness of the resluting membrane [5].	27

2.14	On the top is represented the section of the device with already the magnetic field generators arrayed at the bottom. The figure above represents the detail of the piston-like membrane.	28
2.15	PMMA mold used to create the cylindrical membrane.	29
2.16	Process for generic fluid encapsulation.	30
2.17	Result of first encapsulation process.	31
2.18	Result of BILT encapsulation process.	32
2.19	Fabrication process of the tactile display. (a) Bonding of each layer with glue or UV curable resin. (b) Encapsulation of MR fluid through one channel and removal of air through another one. (c) Sealing of channels with glue and peeling off glass substrate.	33
2.20	Display obtained with syringe/two hole encapsulation process.	34
2.21	Magnetic flux lines.	35
2.22	Coils arrayed under the bottom acrylic plate as actuators for changing magnetic field intensity.	36
2.23	Physical principle of operation of a solenoid.	38
2.24	Coils of different dimension used for tests.	38
2.25	Effect on iron particles when magnetic flux is applied.	40
3.1	Schematic cross-sectional views of (a) HDAM and (b) vibrational Braille code display [6].	42
3.2	Stiffness vs distance distribution.	43
3.3	The first study-case is linear actuators. Usually this kind of devices calls for huge space inside the system hence, usually work standing alone.	45
3.4	The data sheet refers to the bottom device in figure 3.3. Even though the stroke of the end effector is a strong feature and attractive as shown in the data sheet the dimension is not suitable for intended application. Other strengths are velocity up to 150 mm/s, self-locking at rest, integrated linear encoder and integrated linear guiding system so the device is really attractive.	46
3.5	Pen cylinder above allows reducing the dimension of the end effector and the structure as well. It's "pen-like" easily to be arrayed. The main issue is the actuation control: controlling air with a pump and compressed air is suitable for on-off application but when a precise positioning is required, generate a precise signal could be challenging.	46
3.6	This linear actuator is ultra miniaturized but still compared to "usual" linear actuator as the ones pictured in figure 3.3. For the case in object 16 mm diameter is still too big.	47
3.7	TULA Ultrasonic actuators allow moving the end effector really fast and precisely. Moreover, the device is shrunked to a likely dimension suitable for but the stroke module is too low. This kind of devices is widely used for precision positioning such as cameras but when it comes to move a 5x5 mm magnet is not suitable anymore.	47
3.8	C2946 Voice coil actuator.	48

3.9	The idea of how integrating the device under the display is shown in figure and the dimension are scaled.	48
3.10	Moving-coil actuator [3].	49
3.11	Technical specification of VCA used for tactile display.	51
3.12	VCAs.	51
3.13	Stiffness distribution generated on the display using a neodymium magnet.	52
3.14	3D stiffness distribution generated on the display using a neodymium magnet.	53
3.15	Sheets of Permalloy, Mu-Metal™ or soft ferromagnetic metal coatings. The permeability of Mumax 350000/500000 $\frac{H}{m}$ versus 3000 $\frac{H}{m}$ of iron.	53
3.16	Saturation induction: Mumetal™ is a very good magnetic shielding in certain applications where very low fields ($\leq 1Gauss$) are required but it saturates at about 0.2 to 0.4 T, while soft iron saturates at about 1.4 T which is a better choice for the intended application	54
3.17	By only exposing one pole end area of the magnet to the surrounding, it still have a complete field interaction between north and south poles, but this north-south interaction is executed inside the shielded volume.	55
3.18	Waffles.	56
3.19	Manufacturing of polymer microneedles: (a) Exposure with one slit and multiple slits, (b) after exposure, (c) developing after short-term exposure, (d) developing after long-term exposure, (e) molding, and (f) formation of polymer microneedles [7].	57
3.20	SU-8 thickness relation with spincoater's RPM speed.	58
3.21	Mask used for creating septa.	58
3.22	FolchLab's solution for PDMS peeling off.	59
3.23	1 mm deep and thick PDMS septa, bonded with UV-curable resin at the bottom PMMA plate.	60
3.24	Effect of using extra iron particles. Three different quantities have been studied and repulsive force has been analyzed along the display's axis.	61
3.25	Through a simulator is possible to distinguish the difference in the combined magnetic field by changing the magnet's polarity.	62
3.26	Tool for magnet's polarity test. It's shaped using a PMMA plate and cut by a laser-assisted machine.	63
4.1	Tactile display.	65
4.2	PMMA structure to test the tactile display.	65
4.3	Extrusion of structure's components.	66
4.4	Technical sheet for the desing of the VCA's container. The shape recalls a motor cylinder.	67
4.5	Detail of the VCA's container.	68
4.6	Basic structure of a neural network.	69

4.7	PCA's basic concept.	71
4.8	First PCA's method [8].	71
4.9	Second PCA's method [8].	72
4.10	Third PCA's method [8].	72
4.11	Internal schematic of L293D	74
4.12	Picture shows final device assembled and connected to the Arduino board.	74
4.13	Tools for measurements.	75
4.14	Young's Modulus between stress P, below proportional limit and R or preload.	76
4.15	Experimental setup for measuring the relation between magnetic flux and stiffness.	77
4.16	Detail of the loading cell, tactile display and strain machine.	78
5.1	Experimental setup for measuring the relation between magnetic flux intensity and distance from bottom acrylic plate.	80
5.2	Experimental setup for measuring the relation between stiffness and distance from bottom acrylic plate.	81
5.3	The figure represents the relation between the stiffness and the correspondent magnetic flux intensity. The graph is obtained as combination of the two previous ones.	82
5.4	Speed test.	83
5.5	Plot stiffness versus magnet distance: the highest stiffness is generated by the 4 mm acrylic plate.	85
5.6	Measurement position and direction.	87
5.7	3x3 mm diameter force's distribution.	88
5.8	4x4 mm diameter force's distribution.	89
5.9	5x5 mm diameter force's distribution.	90
5.10	6x6 mm diameter force's distribution.	91
5.11	7x7 mm diameter force's distribution.	92
5.12	The information are then summarized in one graph where is possible to compare the maximum repulsive force (stiffness or equivalently Young's Module) and the FWHM.	93
5.13	3D qualitative Young's Modulus distribution.	95
6.1	(a) shows the basic tactile display. To improve the spatial resolution of the device is possible to use an iron disc bonded with PDMS membrane (b) or glued directly inside the bottom acrylic plate (c).	97
6.2	Detail of the ferromagnetic effect on the iron disc that translate the same magnetic field from the top of the magnet inside the chamber.	98
6.3	Picture shows Young's Modulus distribution. Using the iron disc the highest stiffness' value is substantially increased.	98
6.4	Relation of Q-factor with magnetic flux intensity. The Q-factor, hence the shape of the stiffness distribution is improved with the use of the iron disc.	99

6.5	Subjective sensations on spot's size displayed in relation with the magnetic flux intensity.	100
6.6	Picture shows the minimum detectable stiffness at 310 mT.	100
6.7	Tactile display with tunable stiffness and magnetorehological fluid filled-in based on voice coil actuation.	103

*Dedicated to all those people that believed and are still
believing in me*

Chapter 1

Introduction

1.1 Historical prospective

HAPTICS is derived from the Greek term “*haptios*” and describes something which can be touched or more generally the “sense of touch”. The influence that haptics has on the human being beyond technological descriptions is wide and ranges from minor interactions in everyday life, e.g. drinking from a glass or writing a text, to a means of social communication, e.g. shaking hands or giving someone a pat on the shoulder [3].

During human history the meaning and understanding of the haptic sense has changed continuously and have taken different shapes. Aristotele underlines the importance of touch [9] in his *De Anima*:

“Some classes of animals have all the senses, some only certain of them, others only one, the most indispensable, touch.”

In the sixteenth century haptic start to evoke the most erotic and seductive of the five senses leading to the further danger of succumbing to any number of vices; among them the most treacherous deadly sin of lust [10].

“Sight differs from touch by its virginity, such as hearing differs from smell and taste: and in the same way their lust-sensation differs.” [11]

Even though sense of touch has been stigmatized as sense of forbidden due to the pleasure that can be gained by it, in the eighteenth century Kant gives a different interpretation and the philosopher emphasizes its central function in human life experience:

“This sense is the only one with an immediate exterior perception; due to this it is the most important and the most teaching one, but also the roughest. Without this sensing organ we would be able to grasp our physical shape, whose perception the other two first class senses (sight and hearing) have to be referred to, to generate some knowledge from experience.”[12]

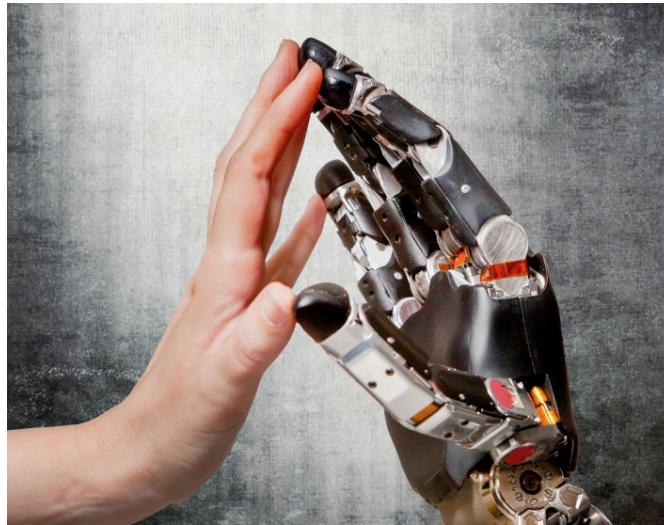


FIGURE 1.1: Human and the corresponding robotic hand [1].

It is easy to understand the huge difference of using only vision and hearing when interacting with objects in daily life: interpretation of what we see and hear can be improved substantially with tactile feedback. Only touch enables us to feel and classify impressions collected with the help of other senses, put them into context and understand spatial concepts [3]. Despite of the substantial improvement gained by using tactile feedback, in the last decades the researches were focused

on the visual and the auditory senses, producing interesting devices but overlooking *haptic* field. Tactile sense is for sure more vivid and realistic since can give a massive quantity of information without any sound or glimpse.



FIGURE 1.2: West equipped with vibrators for the spatial coding of positioning and bearing data [2].

Nowadays tactile feedback devices can be widely used ranging from communication system (as simple buzzing signal for mobile phone) to gaming and entertainment where an enhancement of user interfaces with machines tries to improve the quality of *virtual reality* and to immerse the spectator into a stunning realism. Alongside the numerous examples of haptic interfaces in the industrial field (as in cockpits to deliver through a vibrating handles life threatening and critical conditions) haptic devices are finding their way in medicine. In fact, modern robotic machines depriving the operators of the plurality of information that can be transmitted by the sense of touch highlight the necessity to design alternative systems able to substitute the direct and natural haptic interaction. Thus, haptic interfaces are having the same meteoric rise of other modern technologies and today, more than ever, are becoming topics of research and vital part of many medical applications: the state of art of medical devices for virtual reality should not leave out of consideration the involvement and usage of the sense of touch.



(a) Novint Falcon™ haptic system for gaming.



(b) Buttkicker™ haptic system for entertainment.

FIGURE 1.3: Example of haptic technologies.

The hands of the surgeons are progressively being substituted by robotic and minimally invasive arms, which can operate through small natural or artificial holes but conjointly in many medical disciplines high manual skills are still required and a virtual environments become useful in simulated training for surgeons, telemanipulation [13], diagnostics and therapy or for a direct surgical application like the transplantation of a heart, the sawing of the cranium or the punctuation of the spinal cord [3]. Haptically felt data can be useful also for home care: for example in internet access for the visually impaired where a simulated tactile image maybe required for the user to actually feel [13]. For this reason engineers and researchers in the last two decades started to propose a multiplicity of devices [14–16] that try to fill the gap between machine and human during medical operation for true-to-life simulation of the tactile experience in the virtual-surgical operations trough an engineering expression of haptic sensation in terms of forces, elongations, frequencies, mechanical tensions and shear-forces [3]. Although, as listed before, there are

several ways to describe and realize haptic devices nowadays the most commonly available haptic interfaces can be defined as force producing (Wristalyzer™ or Sens-Able Phantom Omni™). In fact, force is a concept that is related with everyday experience and allows a simple introduction to the workings of haptic technology.



FIGURE 1.4: The Mako Rio™ is a surgeon interactive tactile surgical simulation platform that with a robotic arm allows the insertion and alignment of implants through a minimal incision.

Haptic interfaces as already speculated could be used not only in telemanipulation, as a bridge between doctors and patients after the decoupling caused by the technology, but also as add-ons for medical diagnosis and therapy (intended as haptic assistive system). Such devices still recreate a vivid sensation as much as close to the realty simulating the real world in a programmed machine. In fact, despite a wide range of technologies, today many medical disciplines are using tactile analysis and doctors still draw conclusion based on their tactile feeling even

though the patient prefers the distinctiveness of a real image. For example during medical analysis for tumour detection *palpation* of tissues is still widely used since tumours are stiffer than normal tissues, moreover CT scanning cannot detect tumours smaller than 5 mm and endoscope can only make diagnosis on surface of tissues. In this scenario a device able to recreate the physical characteristics of real object, such as the mechanical and surface properties, would be of great help.

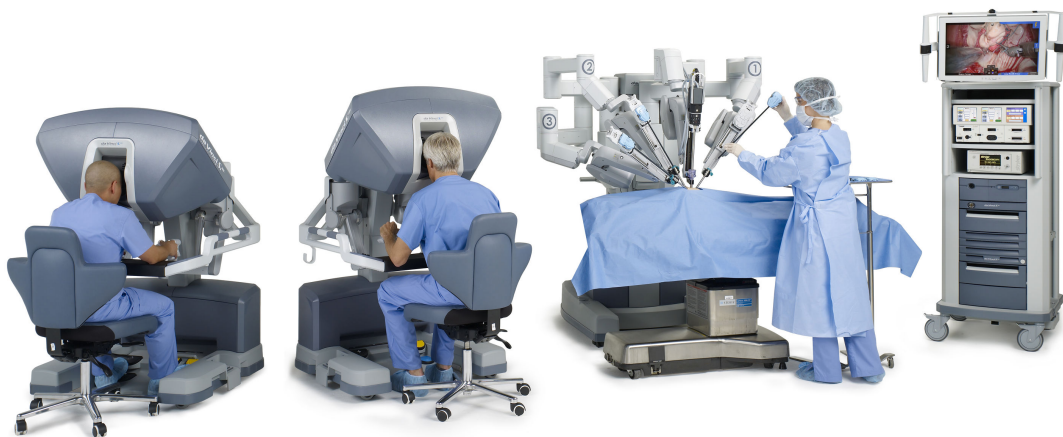


FIGURE 1.5: The climax of video-laparoscopic telemanipulation technologies can be found in the DaVinci™ robotic system.

1.2 Framing haptic science

When speaking about haptic research a multiplicity of disciplines, studies, products and technologies are involved since different aspects are connected to its field. In order to put the following thesis project into a proper scenario figure 1.6 might be clarifying. Haptic world, hence all the disciplines and the studies connected, could be divided into three big fields: *haptic perception*, *haptic measure* and *haptic synthesis*.

The “haptic perception” is the focus of research of disciplines such as psychophysics that is the scientific study of the relation between stimulus and sensation [17] and

neurobiology which is the scientific study of the nervous system [18]: the arrow underlines the fact that a result in psychophysics can be explained and justified by the neurobiology and vice versa.

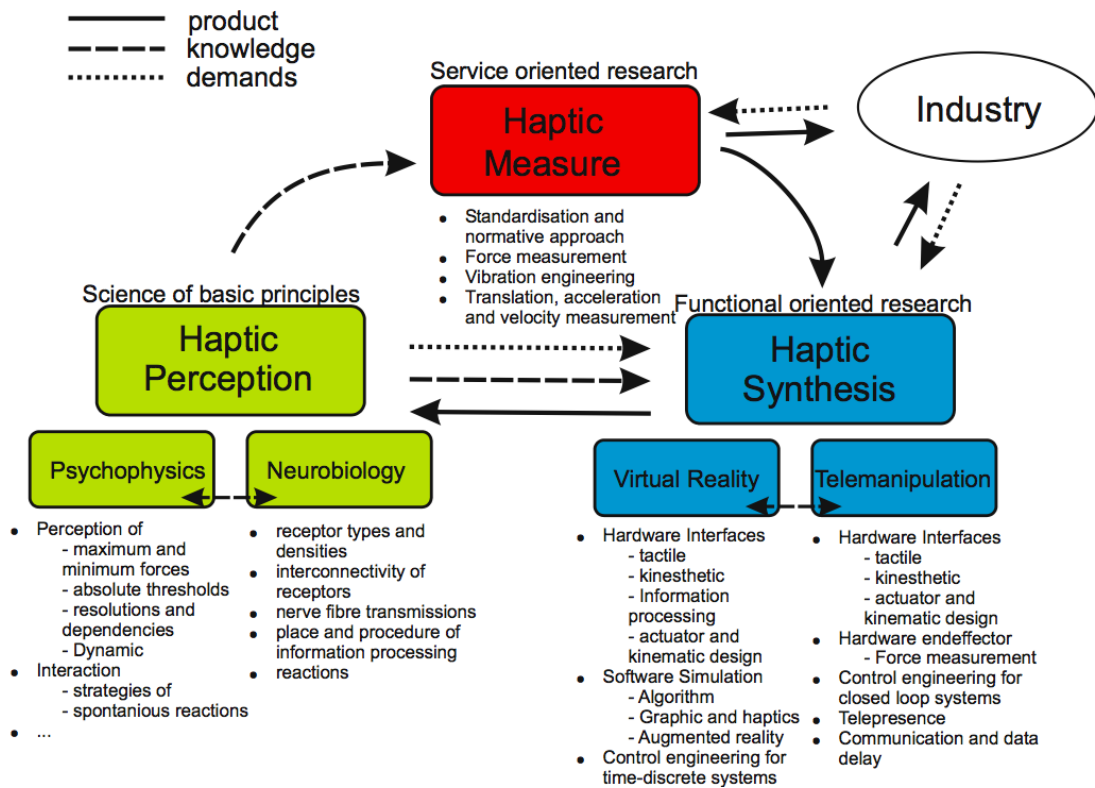


FIGURE 1.6: Overview about the disciplines participatin in haptic research [3].

A validation or a confutation of a scientific hypothesis, which will bring new theories to work with or a revision of the previous ones, requires the interconnection and collaboration of people interested in haptic measure and haptic synthesis. Both these last two groups follow the demands of the industry in order to design products that suits the requests of the market. The research area of haptic measure is oriented to standardize with normative the approach to haptic's world designing products intended to achieve precise measurements in haptic field based on the knowledge gained with scientific research in haptic perception and to provide the necessary technology for the acquisition of haptic object properties satisfying the demands of industry and the necessity for devices' synthesis.

When it comes to design an haptic device, for example to create a tactile display (virtual reality interface) or an end-effector hardware for telemanipulation,

it is necessary to gather information, solutions and knowledge from scientific disciplines (psychophysics and neurobiology) and from engineers working on haptic measurements. The resulting haptic interface may be used to test new hypothesis in human physiology or to answer to a market demand (as underlined in the abstract nowadays researchers are putting the spotlight on medical field). Haptic synthesis' field could be subdivided in virtual reality and telemanipulation that as same as psychophysics and neurobiology are exchanging information and knowledge to improve each other. Telemanipulation devices (manipulators) are intended as mechanical, electromechanical, or hydromechanical systems that enables the teleoperator, directly controlling the device through handles or switches, to perform manual operations while separated from the site of the work. On the other hand, virtual reality system is a computer-simulated environment that wants to simulate the physical presence in places in the real world. Most of the former virtual reality environments were primarily visual experiences, displayed either on a computer screen or through special stereoscopic displays but nowadays some advanced haptic systems are including tactile information. Unlike the telemanipulation these devices do try to control a remote system but wants to reproduce as vivid as possible the reality the operator is working with in order to drive computer-assisted decisions in real environments through an artificial interface, when for various reasons the access or viewing of such information is not entirely easy.

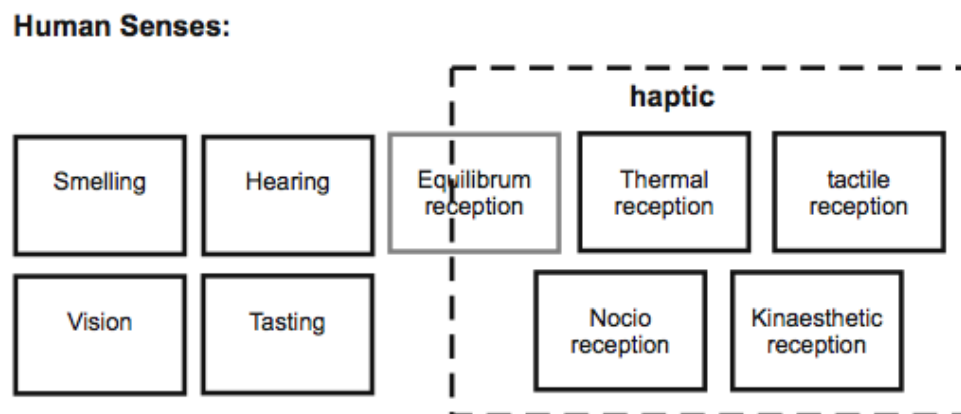


FIGURE 1.7: Human senses with a detail on haptic [3].

This thesis project can be placed in the haptic synthesis as virtual reality device system is requested to be designed. For such devices huge efforts have to be spent on the correct choice of materials for actuation (for the case, how to represent the tactile information) and for the actuator that is driven by a well suited electronics that process and manage the signal transmission.

Of course the project is not standing alone but parallel to the following thesis there are engineers who are working on new solutions for haptic measure: in fact, the display needs a sensor that generates the input signal bringing the mechanical information to characterize the reality. Moreover, another bunch of people are studying the necessary for an optimal design basing their research on the knowledge that comes from the science of basic principles to understand what is the minimum resolution of human perception, how to better maximize the activation of the natural receptors or how it can be recreated the sensations of touch of which humans are used to in everyday-life (rough, smooth, etc.).

1.2.1 Terminology

For a precise definition framework for understanding and communicating various aspects of tactile/haptic interaction the reader should refer to *ISO 9241-910:2011* that provides a correct terminology within the context of haptic systems, defining terms and describing structures and models. Of course the usage of such guidance assure a status of recommendations shared by a large number of researchers, but there is no obligation on its usage so that some papers may differ from the definitions presented in ISO's paper. Here, summarizing, are listed only the most important terms used further to clarify any ambiguity that might arise reading the thesis.

- **Haptics** describes any form of nonverbal communication involving touch, hence tactile reception is only a component of haptic sensory representing a pure mechanical interaction with the skin (fig. 1.7).
- **Haptic device** does for the sense of touch what computer graphics does for vision [19] applying forces, vibrations, or motions to the user. Haptic

system generates an output that is haptically sensed as shown in figure 1.8. When speaking about the most generic system it has to be emphasized that not always a time-variant input signal is necessary. Let's think about the computer's keyboard: the *F* and *J* keys have small slashes to identify the center position of the finger on the keyboard. Those small bars generate through their shape an haptic sensation without any input. In this case, the output response is a time-invariant signal (constant).

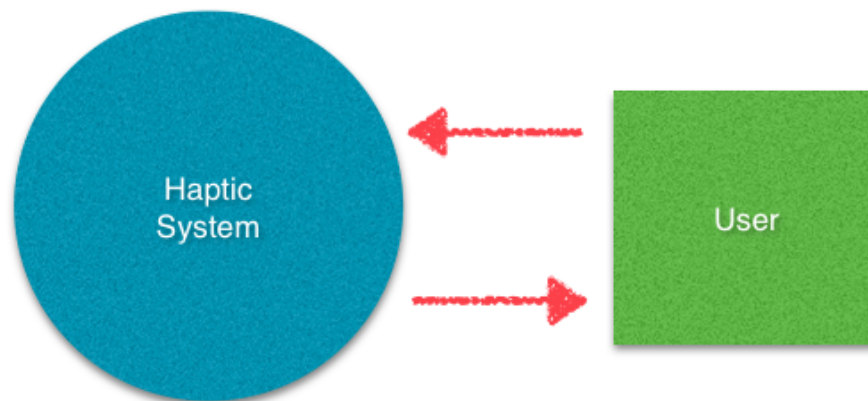


FIGURE 1.8: Haptic device.

- **User** is the human being who uses the information provided by the haptic device regardless the different final purpose such as entertainment, gaming or working. When speaking about work the *user* becomes equivalently operator or teleoperator (in telemanipulation).
- **Haptic interaction** is the exchange of information from the machine to the user, who could use them for different goals. The transmission of information could be mono- or bi-directional as shown in figure 1.8.
- **Haptic interface** is a device that allows haptic interaction since its properties is subjected to changes according to the input signal. It has as final goal allowing the user to acquire an haptic information measuring the device's characteristic.

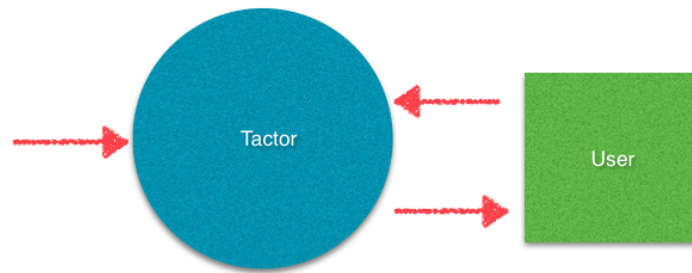


FIGURE 1.9: Tactor device.

- **Haptic display/tactor** is a device intended for a pure tactile interaction with users which is capable of generating a time-variant output according to an input signal. It refers to a sequence of stimuli addressing the tactile sense which can vary in intensity and frequency (figure 1.9).
- **Haptic simulator** as shown in figure 1.10 is a system that recreates virtually the real object's physical properties or is able to generate real environment variables using a computer for their calculation. Simulation is the field where industry is more pushing to develop new technologies since the demands and need are really high.

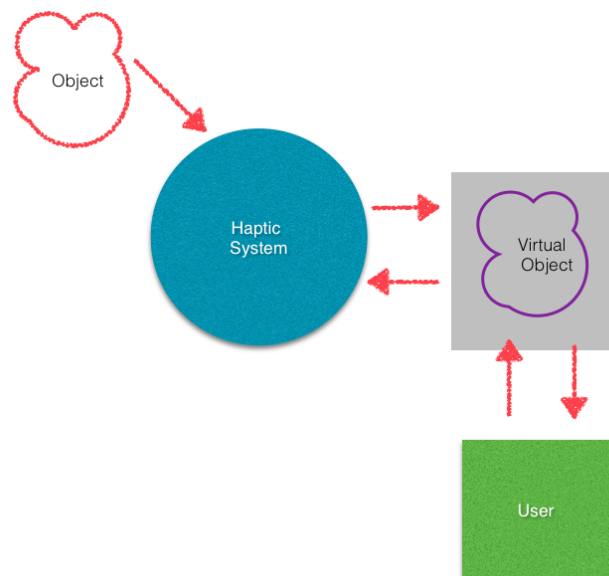


FIGURE 1.10: Haptic simulator.

- **Haptic assistive system** allows to integrate with valuable information the ones obtained naturally by the user (figure 1.11). Those information might be not easily accessible or not accessible at all (for example inside a car's cockpit with critical condition or still during surgery when micro invasive on-tip sensors are used to integrate the doctor's diagnosis).

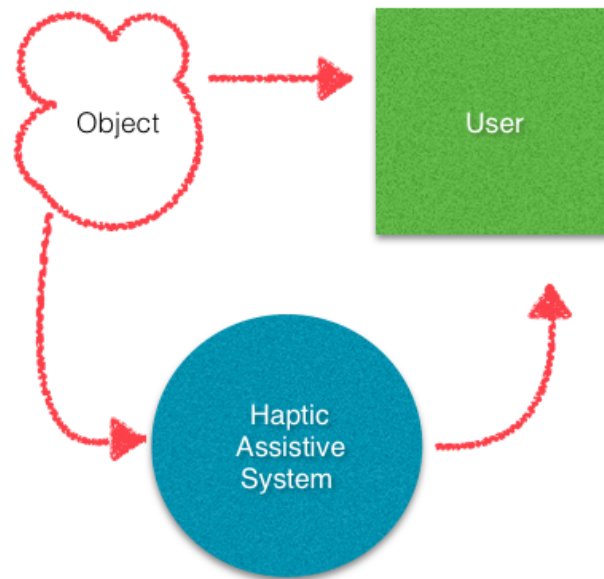


FIGURE 1.11: Haptic assistive system.

Chapter 2

Materials and Technologies

THE following chapter is focused on designing the core component of the tactile display: the so called *haptic interface*. As previously speculated and as shown in figure 2.1 the tactile display is basically composed by two main part: an haptic interface which contain through a case a smart fluid that transmit the information haptically felt by the user and an actuator which allows to vary the characteristic of the display achieving a time variant interface according to an input signal. All the above components have to be assembled inside a unique piece of structure which will be analyzed in chapter 4. More in detail, the present chapter is essentially structured into four sections ranging from the choice of the proper fluid, as it has been chosen the magnetorheological fluid between a wide range of information transducer, to a solution for the proper large displacement membrane and eventually to the choice of a magnetic source.

Since the first steps of the project it has been followed the idea of designing a device as simple as possible. The advantages of having uncomplex displays are immediately observable. Managing a simple design allows the engineers during design phase to create a large number of devices with slightly different characteristic to test and find the best solution for each component. The easiness has to be a common feature of each element and every step in the workflow. According with this concept, choices made in the following sections and chapters – about material and building techniques – try to fulfill the requirement of simplicity, low power consumption and low cost: hence the overall design process and workflow have been adapted to fit that concept.

As already discussed in the introduction haptic devices are hot topic for the modern medicine. Such conclusion is substantially supported by the numerous research project and by the large number of solutions that haptic devices call [20]. A lot of efforts have been spent to find a proper system able to reproduce the most real and vivid *virtual reality* but the dimension of the ones implemented so far is noticeable [21, 22]. The problem of dimension pushed the project to follow MEMS techniques for its fulfillment. Using such technique it has been tried to minimize the dimension but still maintaining reliability, preciseness, effectiveness and of course efficiency of previous solutions. In the following sections will be analyzed and discussed each of the chosen component. For the various topics have been dedicated variable amount of time and efforts, proportional to the toughness encountered during the design, in order to propose novel solutions not already treated in other papers.

An entire chapter about anatomy of skin has been cut out; the reader if interested is suggested to refer to [20] for a brief but detailed introduction on skin and human tactile sensation or could refer to specific book on human physiology.

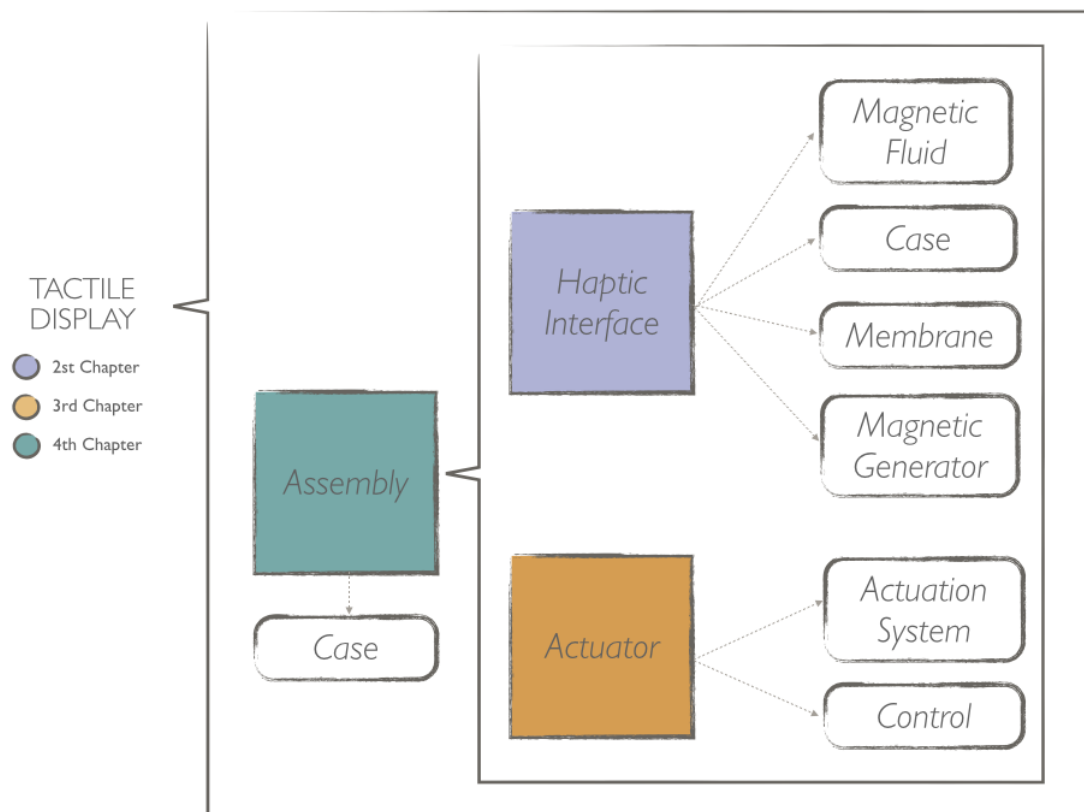


FIGURE 2.1: Main components of the tactile display and correspondent chapters.

2.1 Fluid

Skin's receptors can be stimulated in numerous different ways. The device can directly stimulate the mechanoreceptors by mechanical energy through vibration, pressure or waves. Another category is made of those systems that excite human's tactile feeling using magnetic field directly on the nerves¹ [20]. A third class uses focused ultrasound in order to activate receptors directly or through ultrasound radiation pressure. Thermal flow to add quality characteristics to data presented simulating color in vision [20] looks really attractive and of course a combination of all of them would be an idyllic solution but too complicated and expensive as well. Final goal is to present spatial information through a mechanic transduction.

Within the last two decades a growing interest in the use of Smart Magnetic Composites (SMC) might be noticed. SMCs are part of the well known class of Smart Magnetic Materials (SMM) i.e. those materials whose properties such as viscosity, shape, rigidity, temperature or resistance can be stimulated with a magnetic field. As already mentioned in the introduction medical field is constantly and carefully concerned on developments of such materials: intelligent prostheses, remote surgery, new methods of neoplasm therapy or the magnetic markers [23] are hallmarks of the cutting edge technologies in this field. But also both civil and military fields are stimulated and stimulating for new research on SMCs. Nowadays automotive, train and plane transportation are demanding new technologies and SMCs are widely used for devices such as dampers, brakes and clutches, where controlled energy dissipation is necessary. It is possible to distinguish SMM types and classify them.

¹Miki Laboratory is working on microneedle electrodes that display Braille code.

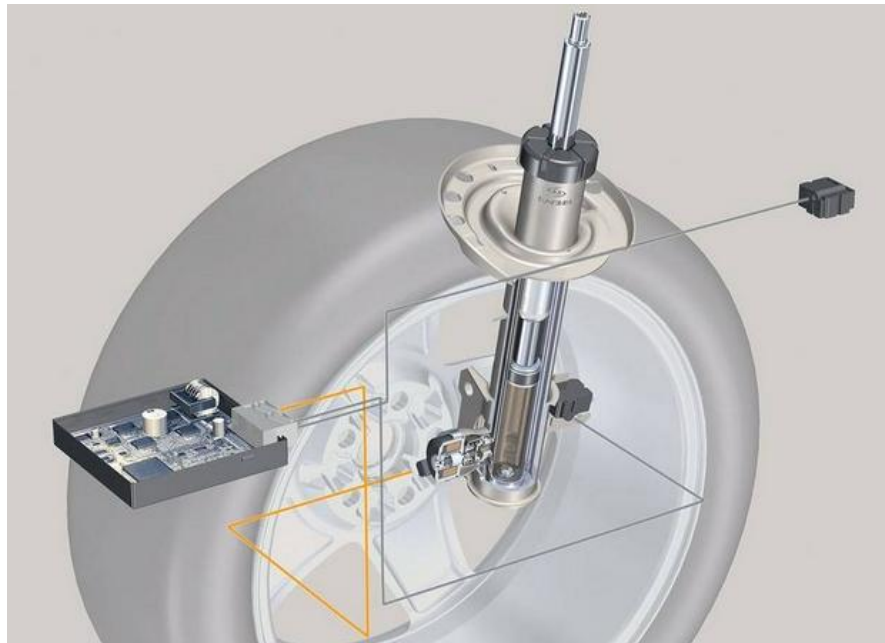


FIGURE 2.2: MR fluid used to control the response of a car suspension.

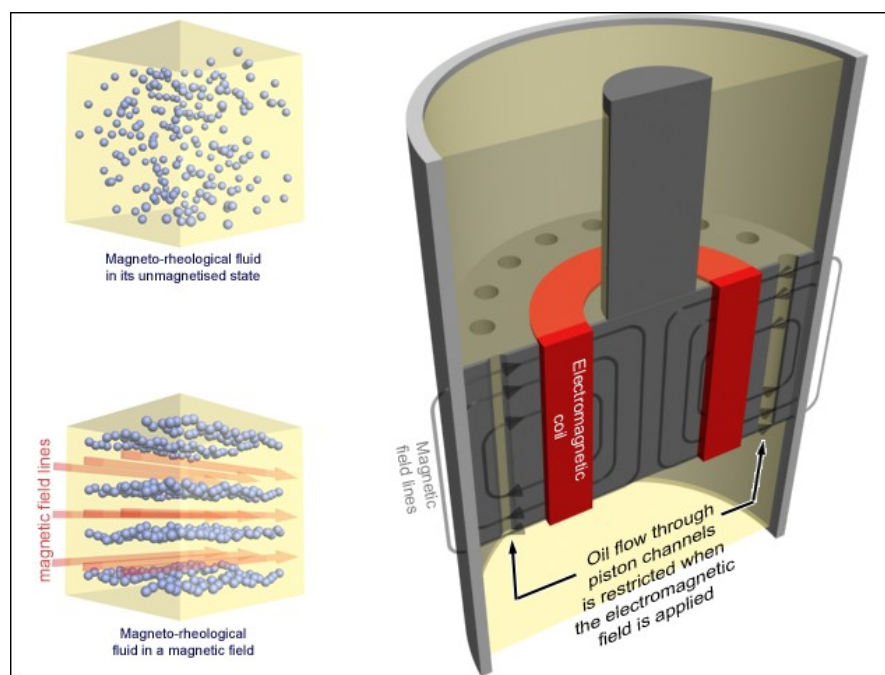


FIGURE 2.3: Physical detail of the electromagnetic control for a piston-like suspension.

- Materials of variable internal structure
 - MagnetoRheological Fluids – MRF or MF.
 - Ferrofluids – FRF or FF.
 - Porous materials saturated with magnetorheological fluids.
 - MagnetoRheological Composite - MRC, gels/greases/... filled with ferromagnetic material powder.
 - Fluids with powdered magnetocaloric materials.

- Materials of fixed internal structure
 - Solid magnetostrictive materials, including those with giant magnetostriction - Giant Magnetostrictive Materials – GMMs.
 - Elastomers filled with ferromagnetic material powders (e.g. carbonyl iron, GMM or their combination), polymers on the epoxy resin base containing powdered ferromagnetic materials.
 - Solid magnetocaloric materials.

The basic idea of a display capable of changing its mechanical behavior in response to an external signal can be achieved in many different ways. As described above, different materials and actuating techniques can be used. Firstly, attention was focused on electrorheological (ER) fluid, a type of SMC sensible to electric current. One of the advantages of using ER fluid is the possibility of constructing a tactile display without any moving components [24]. Nevertheless, high driving voltage is required imposing strong limitation and requirements for the fluid to be free from impurities [21]. Whereas using MR fluid as an alternative actuating fluid, high voltage and bulky electronic can be avoided. When exposed to a magnetic field, the rheology of the fluid reversibly and instantaneously changes from a free-flowing liquid to a semi-solid with controllable yield strength. The phenomenon is consequence of distribution of particles that will be aligned according to distribution of the magnetic field. The alignment of magnetic particles increase the stiffness of the liquid, and by increasing the magnitude of magnetic field it can further enhance the material rigidity by the attraction force of particles [25] as shown in figure 2.5.

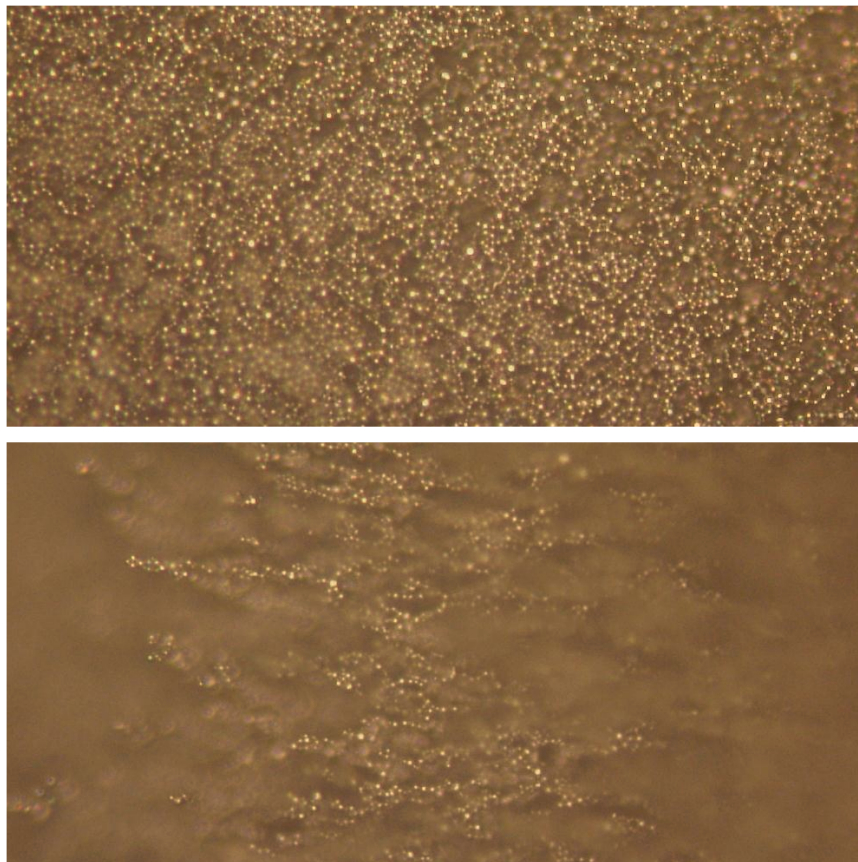


FIGURE 2.4: The figures depicts at the electronic microscope the MR fluid in normal condition (top) and crossed by a magnetic flux (bottom) where all particles are alligned.

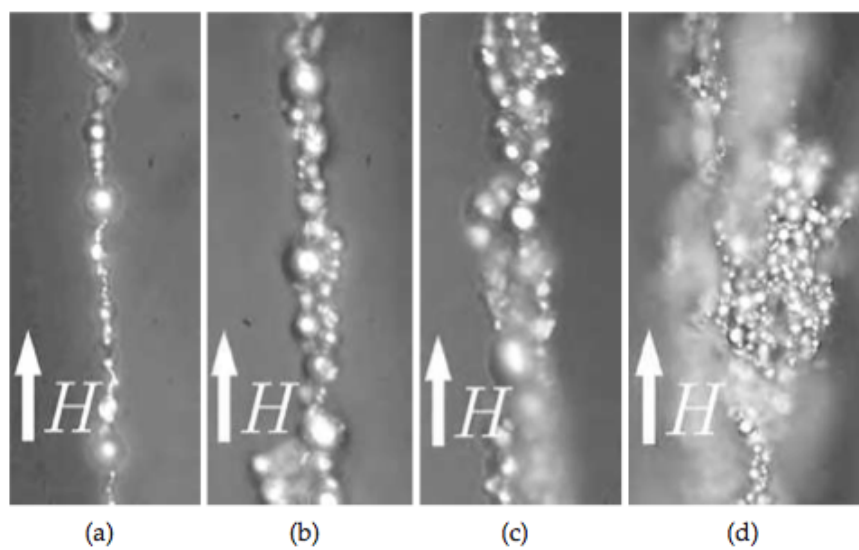


FIGURE 2.5: Detail of the effect of increasing the magnetic flux on the particles' chains [4].

In general, magnetorheological (MR) material is a type of smart fluid composed by micron size magnetically permeable particles ($20 - 50\mu m$) of Fe_3O_4 suspended within a non-magnetic medium, usually a type of oil (glycerol). When subjected to a magnetic field, the rheological properties of these materials are rapidly and reversibly altered, to the point that the fluid becomes a viscoelastic solid. The phenomenon is consequence of distribution of particles that change from isotropic to anisotropic forming chain-like structures after that magnetic field induced polarization in the suspended particles. It has been noted that the stiffness could also be reduced by varying the direction of magnetic field [26]. The Bingham visco-plasticity model can describe the dependence of the fluids with the magnetic field. The shear stress is given by the following equation:

$$\tau = \tau_0(H)sgn(\dot{\gamma}) + \eta\dot{\gamma}$$

where τ_0 is the yield stress caused by the magnetic field, H is the magnitude of the magnetic field, γ is the shear strain rate and η is the plastic viscosity independent of the field. As shown in figure the characteristic of the fluid MRF-122EG of LORD.

Typical Properties*

Appearance	Dark Gray Liquid
Viscosity, Pa-s @ 40°C (104°F) Calculated as slope 500-800 sec ⁻¹	0.042 ± 0.020
Density	
g/cm ³	2.28-2.48
(lb/gal)	(19.0-20.7)
Solids Content by Weight, %	72
Flash Point, °C (°F)	>150 (>302)
Operating Temperature, °C (°F)	-40 to +130 (-40 to +266)

*Data is typical and not to be used for specification purposes.

FIGURE 2.6: Lord™MRF-122EG fluid datasheet.

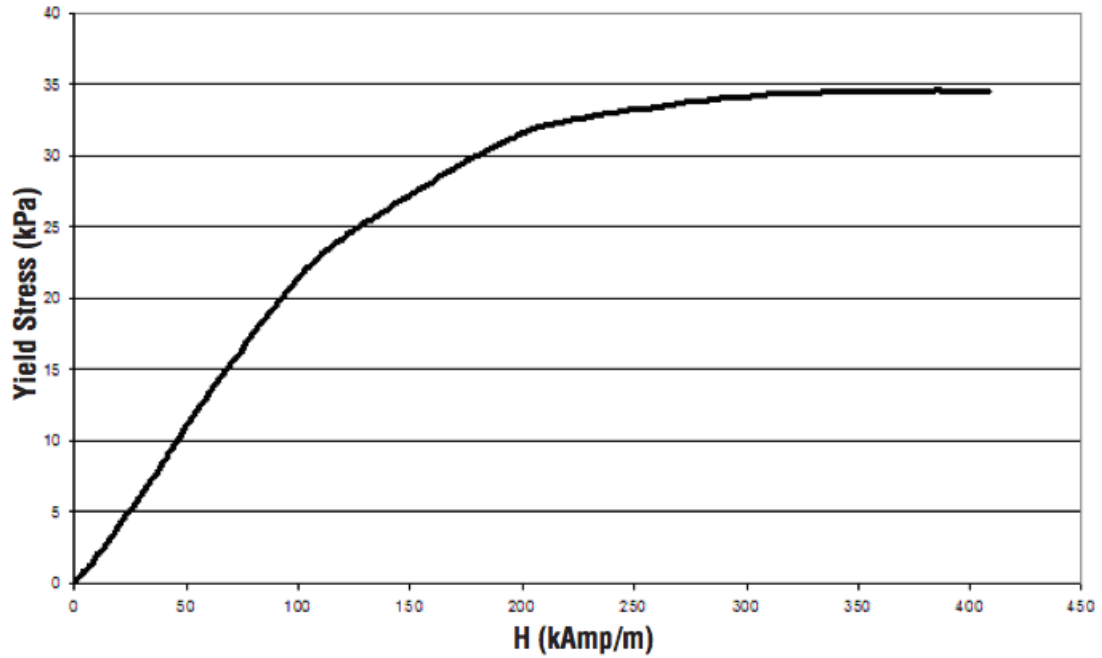


FIGURE 2.7: Yield stress vs. Magnetic Field Strength.

MR fluid is different from a ferrofluid (FF) which has smaller iron elements (figure). MR fluid particles are primarily on the micrometer scale and are too dense for Brownian motion to keep them suspended in the lower density carrier fluid. Under common conditions no separation is observed between particles and the glycerol. However, in static condition could be necessary a shaker to redisperse the particles into a homogeneous state. Ferrofluid particles on the other hand are formed by nanoparticles that are suspended by Brownian motion and generally will not settle under normal conditions. The particles are that small that an analysis with microscope is impossible and because of the particles' dimension these two fluids have very different behavior.

In the present research work, MR or FF fluid based tactile display has to be designed, constructed and tested. Since the basic idea is to design an intelligent composite structure whose magnetorheological response can be actively controlled by an external electrical signal in order that the variation of stiffness could be sensed by human touch. Hence, primarily both MR and FF fluid behaviors has been microscopically analyzed and its responsive force tested. As already mentioned above the behavior due to internal constituents at constant and equivalent magnetic field applied is different. FF fluid generates a repulsive force -that in a second time will be translated as stiffness- lower then MF fluid and not suitable

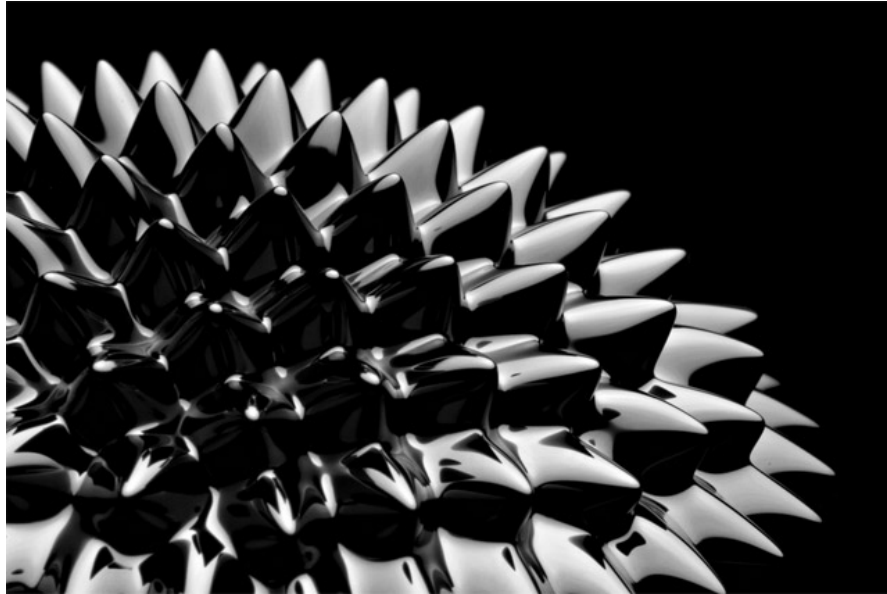


FIGURE 2.8: Ferrofluid when magnetic field is applied.

for intended application of correlating the mechanical properties of the device with human tactile sensations.

2.2 Case

In order to find a material easily constructible, easily feasible and to be bonded with a PDMS membrane as well, polymethylmethacrylate has been considered. The polymethylmethacrylate (PMMA) is a plastic material formed by polymers of methyl methacrylate, ester of the methacrylic acid. It is also known under the trade names of Acrivill, Altuglas, Deglas, Limacryl, Lucite, Orogas, Perclax, Perspex, Plexiglas, Plexiglass, Resartglass, Vitroflex, Trespex and Setacryl. PMMA is often used as an alternative to the glass and is easily bonded to other materials through so-called UV glues, which combine the advantages of practicality and performance of adhesives mono and two-component solvent.

Starting from pre-fabricated plates of different thickness using laser-assisted cut-machine acrylic cases have been created. After designing the .DWG file using CAD software such as Solidworks™ or Autodesk Inventor™ the acrylic plates have been cut according to the desired shape and dimension.

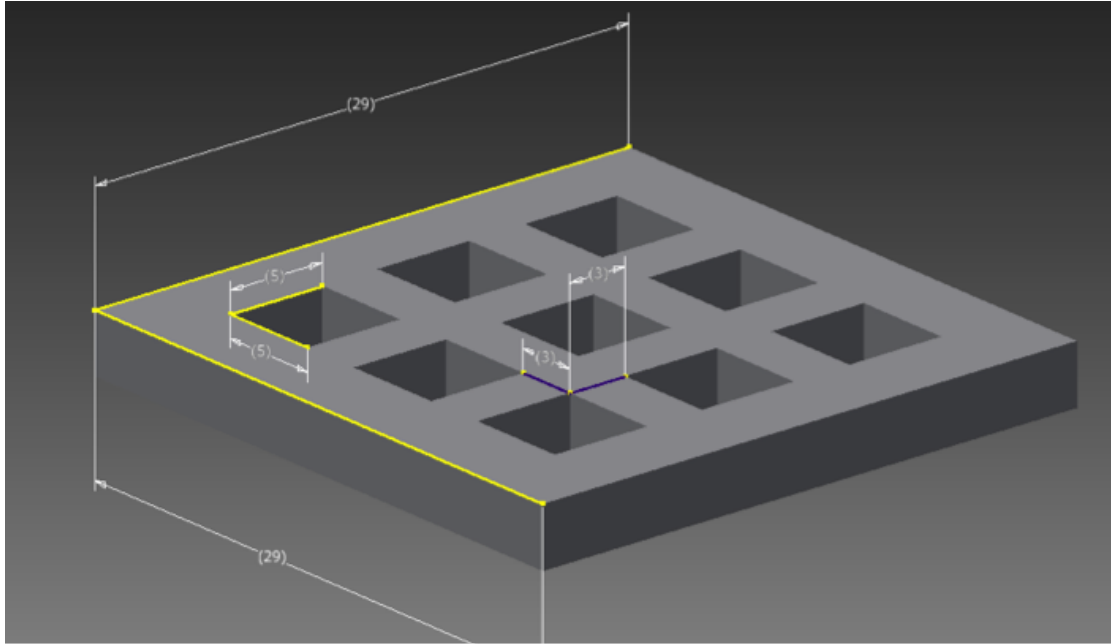


FIGURE 2.9: First type of PMMA case for MR fluid. The dimensions are 30 x 30 mm.

Magnetorheological fluids undergo a change in rheological behavior if an external magnetic field is applied. This significant effect is due to the induced magnetic polarization of particles. The dependence to the magnetic flux of the variation in the viscosity of the fluid allows the display to create an elevated number of stiffness values representing different mechanical properties with the very same device. In other words, one of the major goals is to create a display that when no magnetic field is applied it responds as a neutral matter: the consistency of MR fluid when no magnetic flux goes through it is quite similar to a dense fluid (honey). Whereas when subjected to a magnetic field it behaves as solid gels, typically becoming similar in consistency with dried-up tooth-paste. Without a specific minimum value of stiffness to achieve, when no magnetic field is applied the tactile display has to show a low value of stiffness and behaves as a high viscosity fluid. Varying the magnetic field applied until the desired value the display becomes harder and harder.

In this sense the PMMA containing structure has to fulfill the requirements of “hiding its presence” when the operator touches the device and the one represented in the picture 2.9 does not. It is easy to understand that when the emulsion undergoes into a liquid-to-semi-solid phase changing upon the application of a magnetic field, the bottom acrylic structure is sensed by the human finger limiting him to sense the real change of stiffness in the MR fluid. This is due to the fact

that the considered device change the mechanical behavior through a variation of the internal structure, so no elongation or structural variation are intended as in other previous work [6]. The user has to apply pressure to the display to sense the stiffness variation and such chamber-like solution (fig. 2.9) does not allow him applying any force. Final shape is the one represented in figure 2.10. Of course a fragmentation in smaller chambers allows the engineers to better manage the creation of the pixel's structure thus the chamber's idea has been developed as will be shown in chapter 3.

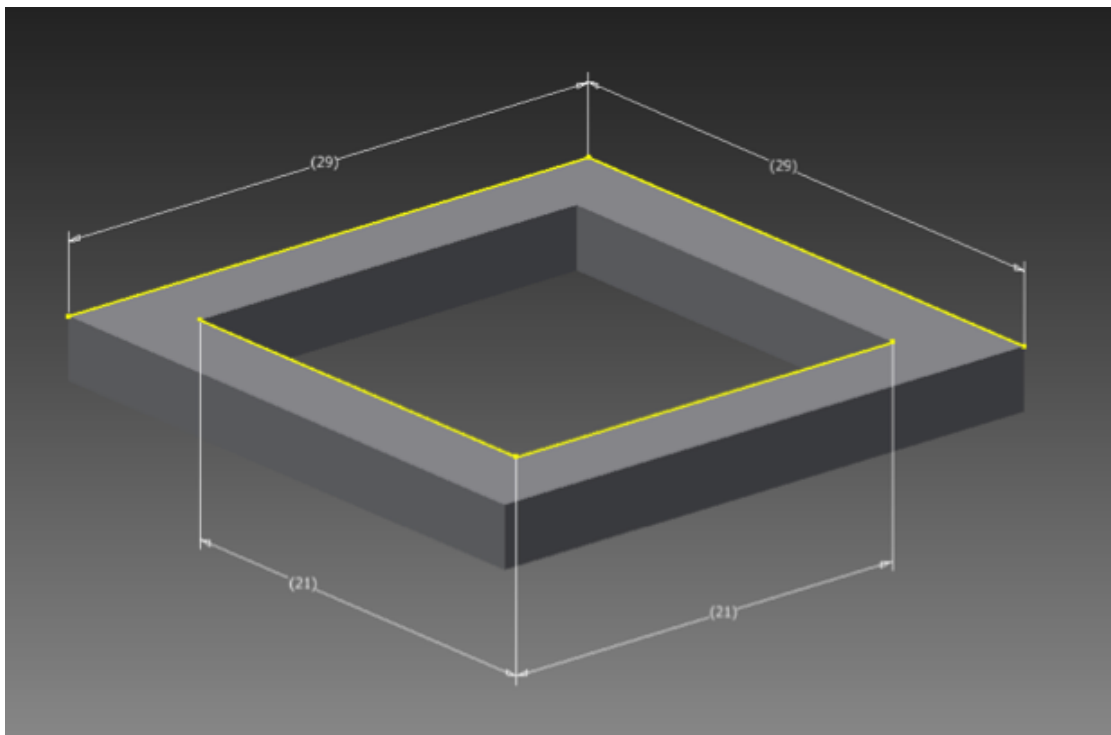
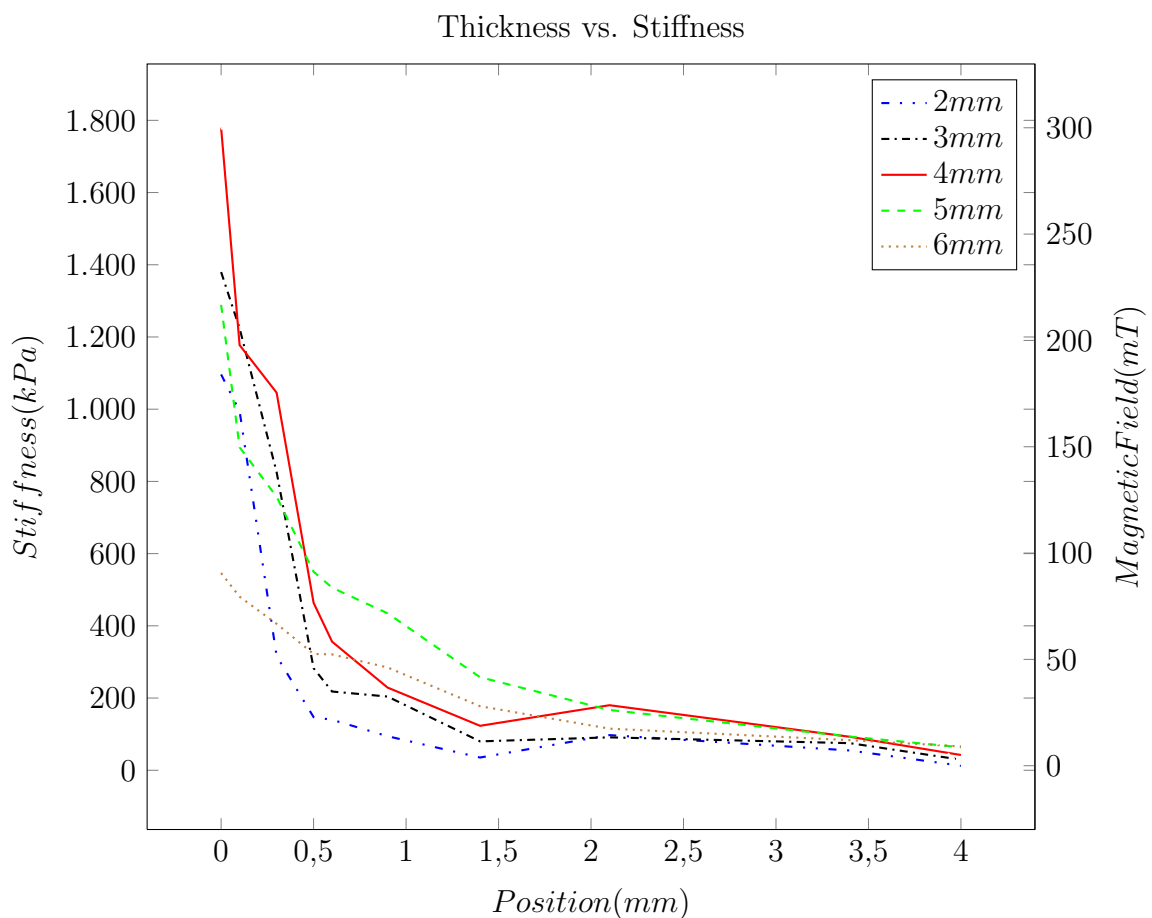


FIGURE 2.10: Single chamber acrylic base for MR fluid.

When the magnetic field is applied it will go through the MR fluid and will be attenuated exponentially with the distance. It comes natural to think that if it is used a 5 mm thick acrylic case instead of a 3 mm the real magnetic field applied to the surface of the device, is lower in the first case than the second one. Since the mechanical variation of the internal structure of SMM material is proportional to the applied magnetic field it comes that the stiffness generated by the first device is lower and changes in viscosity are less detectable. In fact, one of the main issues to face when using such naïf structure is the choice of the thickness.

Using a 3 mm plate instead of a 5 mm plate changes all the final behavior and mechanical properties of the device. In order to choose the proper acrylic case, different devices of different thickness have been tested (2, 3, 4, 5 and 6 mm). First a tactile comparing test had been run in order to have a qualitative evaluation of the five devices, simply moving the magnet up and down at the bottom and with the highest peak value. To validate the “subjective tactile feeling” the maximum value of stiffness of tester devices has been quantitatively calculated as shown in the following thickness vs. stiffness graph. The graph shows maximum stiffness’ value reachable for different thickness of PMMA structure. The values derive from a preload of 0.1 N and a lung of 80% of the acrylic thickness.



To better understand the effect of the thickness on the final stiffness’ value the following example could be clarifying. As extremer the 2 mm thickness display is crossed by the magnetic flux which is slightly attenuated resulting in high value of stiffness but poor tactile sensation: when the user presses on the device reaches easily the bottom plate and the stiffness dynamic range is really low. Whereas using 5mm plate the issue is the opposite. The quantity of MR fluid inside the



FIGURE 2.11: First attempt to create a thin PDMS membrane.

display attenuates excessively the magnetic flux giving a low stiffness value at the user interface but the stiffness can range between a wide range of values.

2.3 Membrane

When it comes to choose a low price and easy to pattern material for membranes, polydimethylsiloxane PDMS wins hands down. Widely used in microfluidics [27], is optically transparent, flexible and cheap enough for students to use in copious quantities without denting lab budgets. These qualities make PDMS an excellent material for intended application such as creating a membrane rapid to prototype: all issues encountered in cell-based studies with PDMS, like absorption of organic solvents and small molecules and its innate hydrophobicity and evaporation of water, are all negligible for intended application. Hence for quick tests of new device's design PDMS fits perfectly the requirements. In the very first step of the membrane design it has been chosen the same workflow used in Miki laboratory in a previous work [28]. Even though the final use of the device is different and different as well is the mechanical behavior of the membrane the fabrication process is equivalent.

Basic fabrication process of PDMS membrane consists of preparing a glass plate coated with CYTOP (Asahi Glass) in advance. CYTOP facilitated the peeling of the largely deformable PDMS membrane when the membrane is transferred to the

PMMA support. CYTOP glass plate preparation consists in curing the glass on a hotplate at 100°C for 20 minutes. When the plate is ready, PDMS is spin-coated on the glass at the proper speed to achieve the indented thickness according to the figure 2.13 since the thickness of the membrane is not linearly proportional to the rpm of the spinner.

Regarding the specific composition of PDMS two solutions have been studied. The preparation process and the components are of course different but both of them require the spin coater and hotplate curing. Firstly a mix of Dow Corning Toray DC 3145 CLEAR and thinner RTV has been used to create a large displacement PDMS (LDPDMS). Whereas the final used solution consists in a harder PDMS (HPDMS) composite made of Sylgrad 184 mixed with Dow Corning with a ratio of 10 to 1. Both solutions require after mixing the composites to use a vacuum machine to get rid of the bubbles (40 minutes). Bubble-free solution is required because if air is spin coated it creates weak parts on the membrane and not a uniform surface distribution. The choice of HPDMS has been made because the LDPDMS was too delicate and its fabrication process was time consuming for quickly testing. So from now on when PDMS is mentioned is referred to HPDMS.

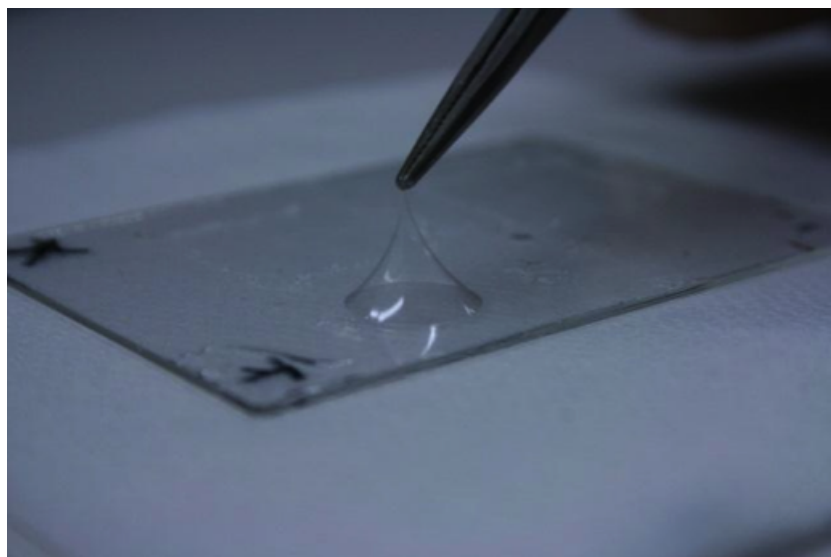


FIGURE 2.12: PDMS membrane on glass substrate cured in advance.

One of the most challenging problems has been found the “right” membrane for the display. A thin largely deformable PDMS if it is thick has a good sealing property

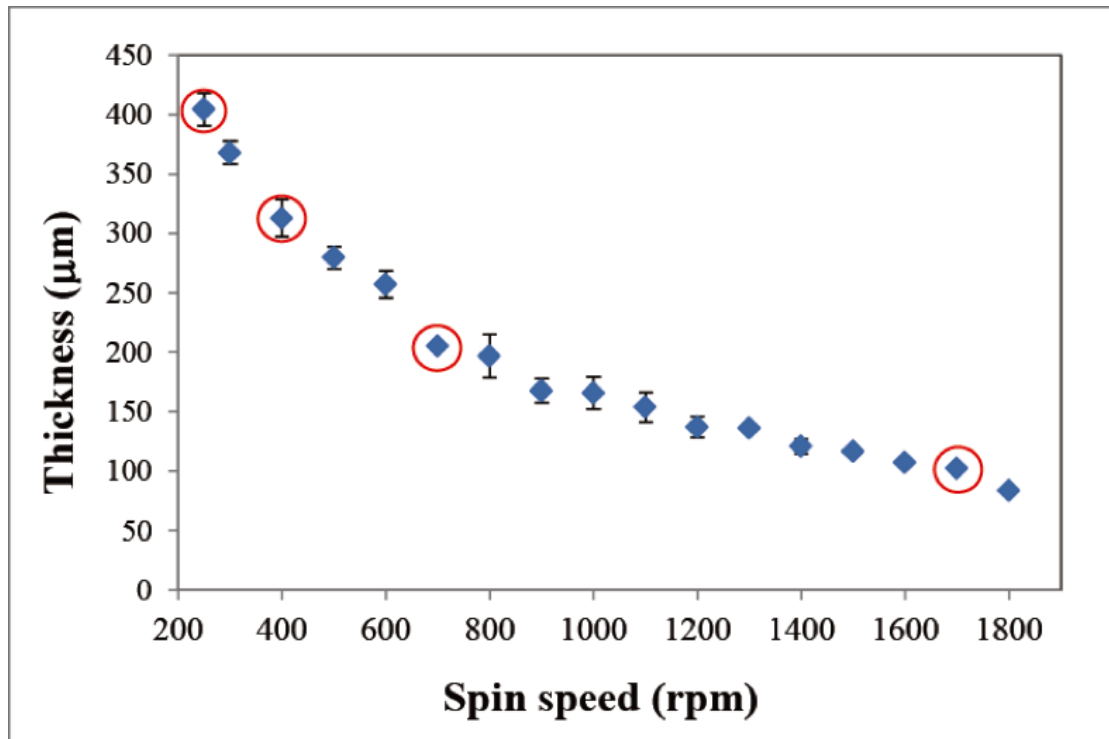


FIGURE 2.13: Relation between spin coater speed and thickness of the resulting membrane [5].

with PMMA structure containing properly the MR fluid. At the same time is less deformable hence its mechanical behavior interferes with the MR fluid varying the natural mechanical response of the entire display. Moreover, the stiffness sensed by the user will be deformed: it will be higher but with less spatial resolution since it has to be applied more force the sense the response of the fluid once magnetic field is applied.

On the other hand when a few micrometer membrane is used the barrier between human finger and MR fluid is noticeably reduced allowing the user to sense the minimal variation of the stiffness generated by the magnetic field on the MR fluid. With this solution fabrication process issues had to be faced. When the membrane is bonded with glue or UV curable resin as well the sealing force is reduced and the membrane struggles to contain the MR fluid when a pressure is applied with the finger. Of course a trade off has to be found: different membranes of different thicknesses have been tested and as final solution 1000-RPM speed has been used. This speed is translated in $100\mu m$ membrane.

2.3.1 Piston-like membrane

An effort had been spent for changing the design of the membrane in order to improve the mechanical response of the display. Basically, the idea was to shape the membrane into a piston-like at the bottom as shown in figure. The concept derives from the widely used technology of dumping system with MR fluids filled in. The cylinder when compressed, the repulsive force generated when a magnetic flux is applied should be higher since higher is the active surface. Moreover, with the piston the spatial resolution should be improved since the high repulsive force is concentrated in the neighborhood of the cylinder. With this kind of structure is like create a display with a button-like mechanical single pixel.

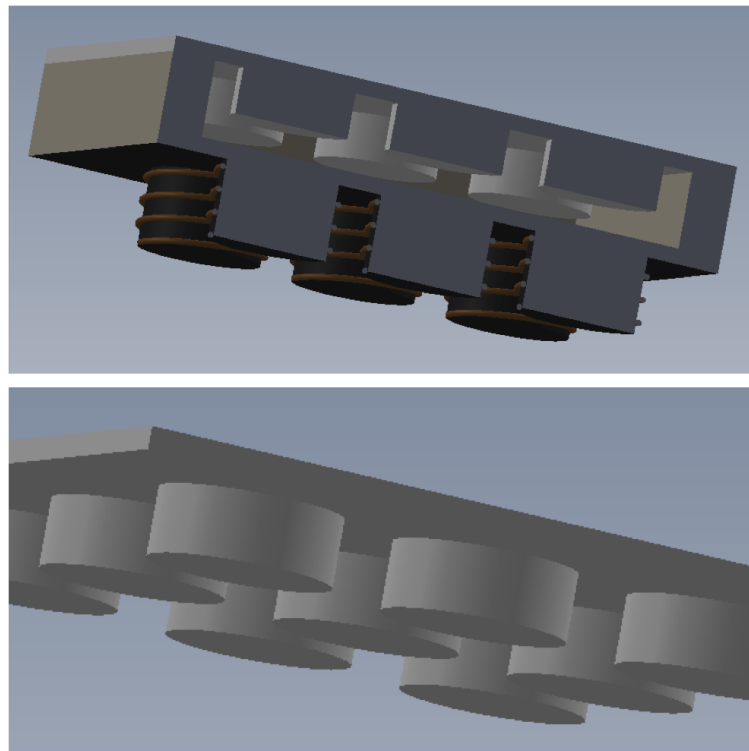


FIGURE 2.14: On the top is represented the section of the device with already the magnetic field generators arrayed at the bottom. The figure above represents the detail of the piston-like membrane.

Firstly, an acrylic base 5 mm thick has been molded with a miller machine as shown in figure 2.15. As first test the membrane has been chosen of 0.5 mm thick

², the cylinder of 3x3 mm and filled with HPMDs. An alternative solution to the mold could be separating the fabrication process of the membrane using the workflow followed before for a thin large-displacement membrane and after that glue the PDMS cylinders on it: PDMS is easily bonded with other PDMS and the connection is quite strong. Another solution is to use SU-8 negative photoresist to create with UV a smaller mold for cylinders as already done for previous work [7].

The limiting factor in this section has been the low resolution of the milling machine: the resulting 0.5 mm membrane is of course too thick and PDMS cylinders are not small enough not to weight on the membrane. Test results are not satisfying at all and the single pixel button-like solution is still an open topic.

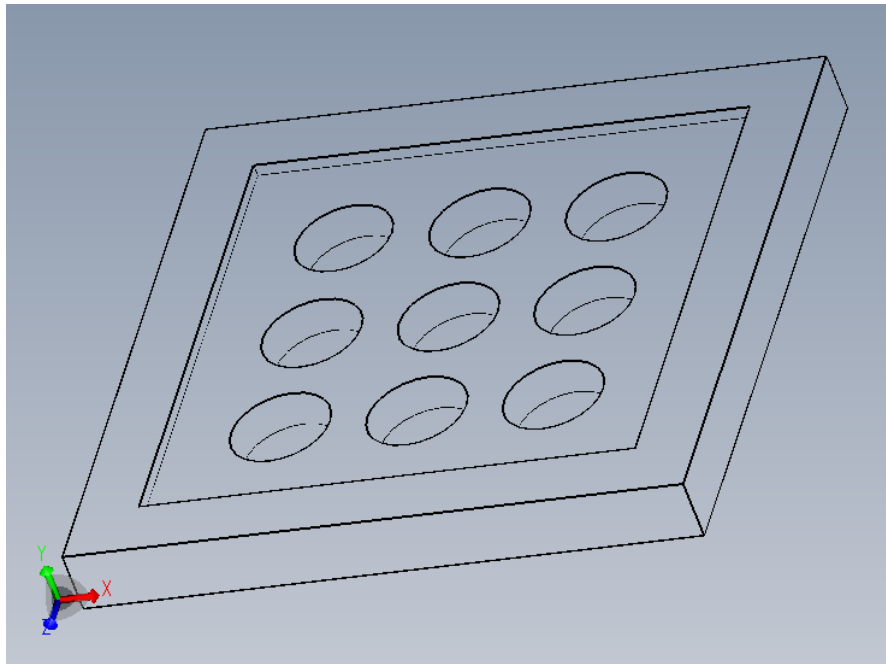


FIGURE 2.15: PMMA mold used to create the cylindrical membrane.

2.3.2 Fluid encapsulation

Figure 2.16 describes the encapsulation process of MR fluid inside the structure and the bondage of the membrane. Summarizing: the PMMA plate was cut using

²0.5 millimeter is the lower resolution of the miller

a laser beam machine. A glass plate was treated with CYTOP to facilitate the peeling of PDMS membrane that was spin coated on it. Another thin acrylic plate (0.5mm) was bonded to the laser-processed PMMA support with glue, applying pressure to eliminate bubbles and cured on hotplate. MR fluid was encapsulated inside the chamber through a syringe. A UV-curable resin (Three Bond 3164) was spin-coated on another glass substrate to obtain a thickness of $100\ \mu\text{m}$ and transferred to the surface of the PMMA plate after pressing the plate onto the resin the largely deformable PDMS membrane on a glass substrate was placed onto the PMMA chamber via the UV-curable resin. After UV irradiation, the membrane was exfoliated from the glass substrate. The resulting device is shown in figure.

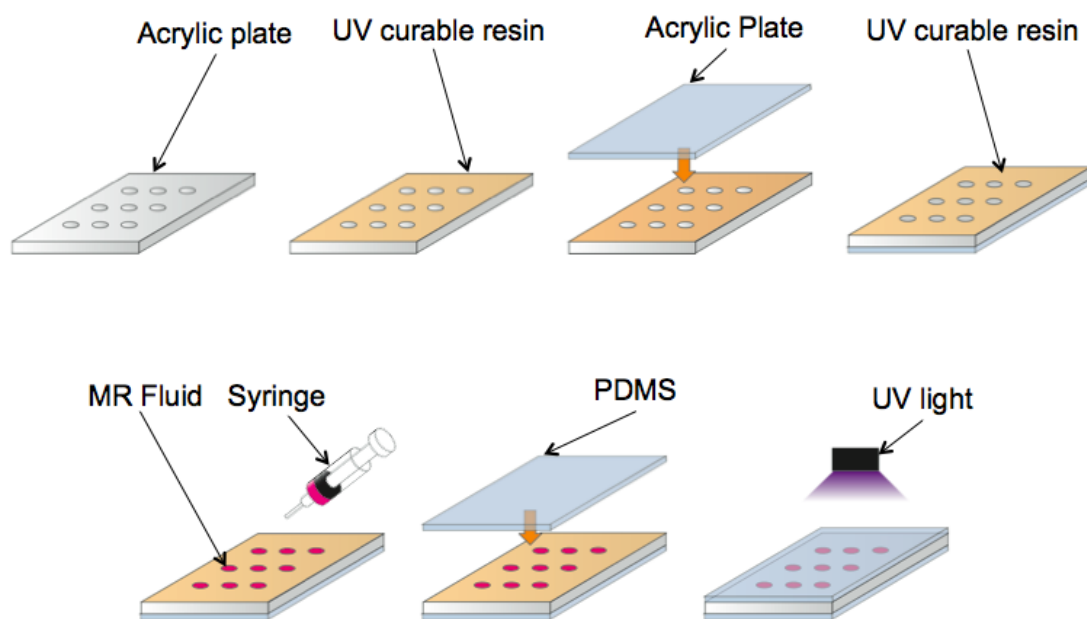


FIGURE 2.16: Process for generic fluid encapsulation.

The previous technique has the main problem of low reliability when encapsulating the MR liquid. After using the syringe there are always few leakages on the border of the PMMA structure, limiting the gluing capability of UV-curable resin. This is due to the fact that no bubbles have to be encapsulated and to achieve that the chamber has to be filled up to the top. When applying the membrane with pressure the glycerin tends to escape on the borders causing the problem explained before.

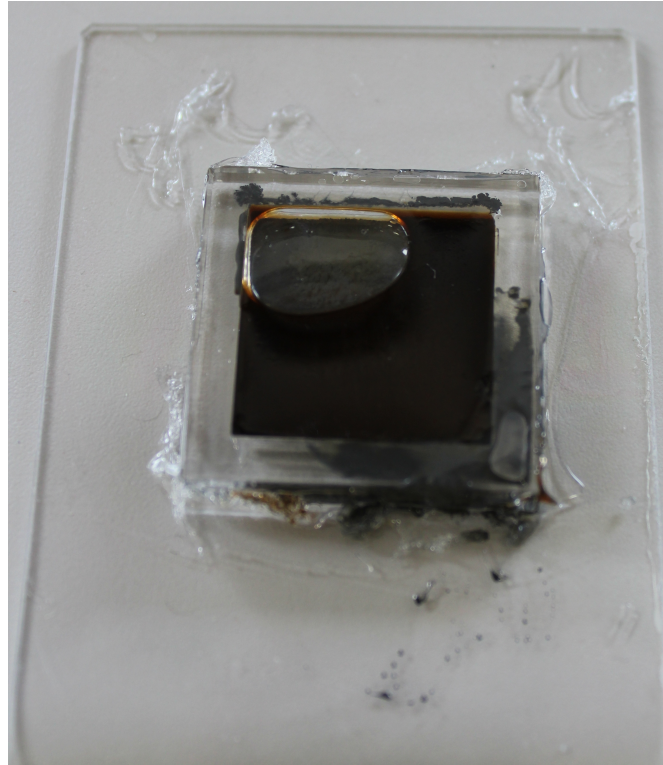


FIGURE 2.17: Result of first encapsulation process.

If bubbles are encapsulated both the mechanical behavior and the resolution of the display are lowered changing the tactile feeling of the user. Moreover, the reliability of the device is noticeably reduced due to the high pressure generated by the compression of the air inside the chamber by the operator's finger. Two alternative solutions have been tested.

2.3.2.1 BILT

BILT technique comes from MEMS solution for wafer bonding for encapsulation. The process treated below fully refers to [29] where is written detailed and with all references. MEMS devices that encapsulate liquid have been proposed to achieve various attractive applications. In optical applications, deformable lenses and scanning micro-mirrors were developed by encapsulating droplets of silicone oil within a parylene film [30]. Encapsulating techniques in MEMS field is a widely diffused and wafer bonding has been frequently used for packaging gas and liquids

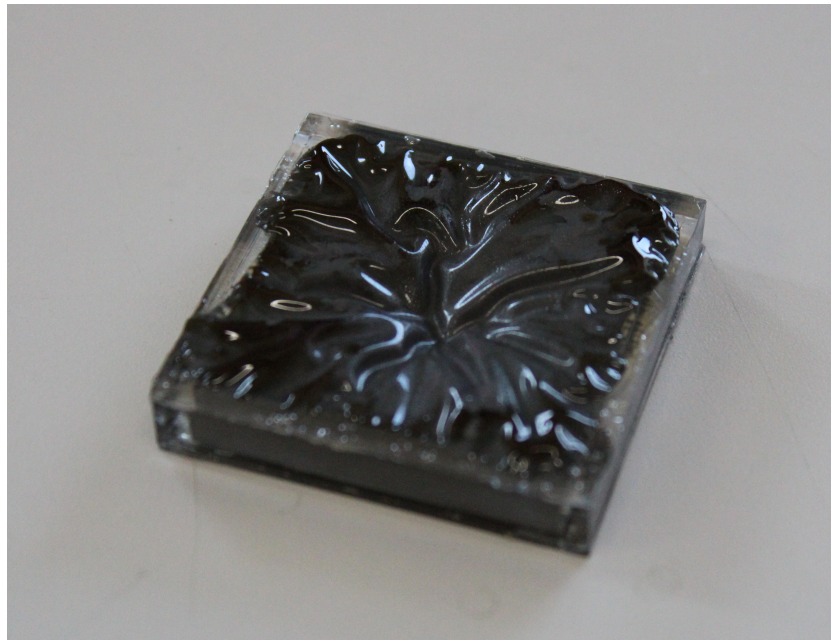


FIGURE 2.18: Result of BiLT encapsulation process.

[31–35] and its precision determine the performance of resulting MEMS devices [36, 37].

The liquid encapsulation method is based on a bonding-in-liquid technique (BiLT). A UV curable resin (3164 Three Bond, Three Bond Chemical Ltd) was used as an intermediate layer and the liquid encapsulation process was conducted in the MR fluid. The advantages are that the resin does not require high temperatures or a vacuum processes but only a UV light for curing. Therefore, thermal expansion of the liquid or device structures and degradation of the materials can be avoided. But the most attractive feature of BiLT is that interdiffusion of bubbles or leakage that deteriorates the devices performance can be avoided. Since the bonding process is completed within the liquid and the sealing membranes do not deform under their own weight as they would in air, no air bubbles are trapped and the liquid quantity can be precisely determined by the substrate design and resin thickness [29]. The BiLT technique is effective for MEMS as much is not for the tactile display. The dimension of the device calls for high quantity of expensive MR fluid and the liquid part of MR fluid is too oily that doesn't allow a proper bonding on large surface compare to MEMS average dimension (fig. 2.18).

2.3.2.2 Syringe encapsulation

A more simple, less time and money consuming fabrication process was used. It has been decided to keep the first bonding and encapsulation technique with a little variation on the PMMA structure and in the process workflow as well. On the side of the laser-cutted plates two holes with a drill have been dig; one for the injection through a syringe of the MR fluid and the other as air-escape's hole and then sealed with glue. Moreover, the process of bonding the membrane on the PMMA has been done before the encapsulation of the liquid: bonding the PDMS with UV-resin on a clean device resulted in a more precise and reliable bonding process. This solution not only eliminates the encapsulation of air bubbles, but also allows faster designing of tactile devices for quickly testing with low wasted materials.

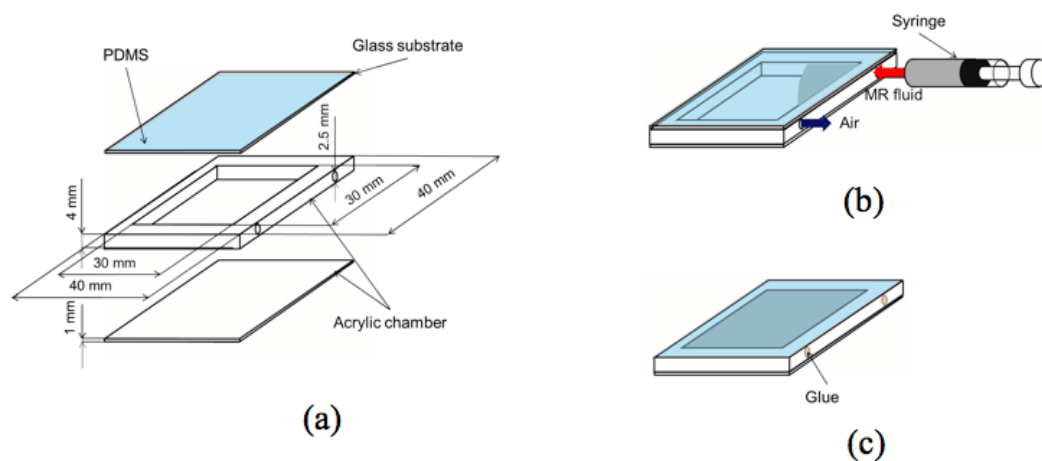
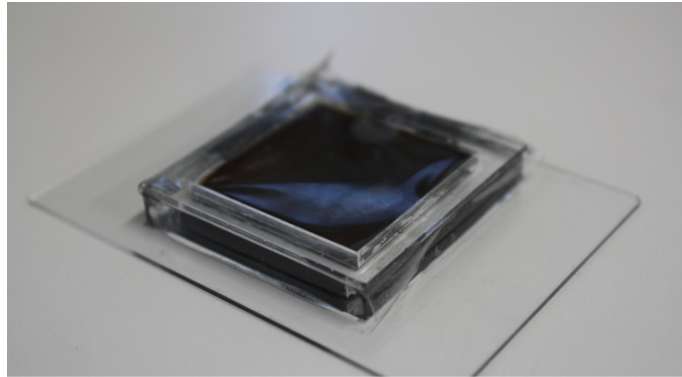
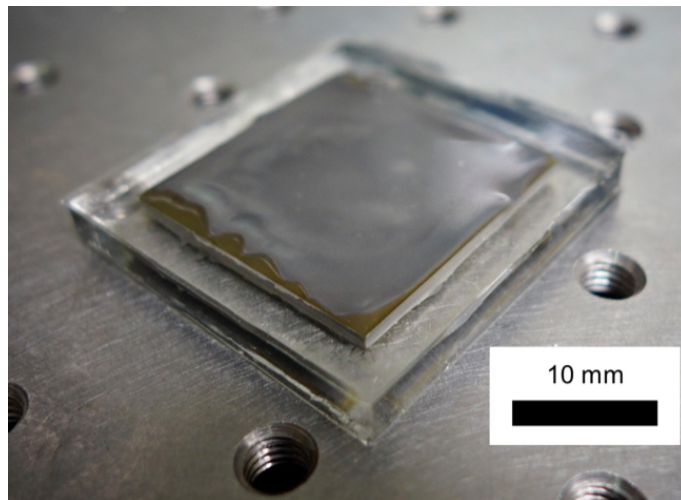


FIGURE 2.19: Fabrication process of the tactile display. (a) Bonding of each layer with glue or UV curable resin. (b) Encapsulation of MR fluid through one channel and removal of air through another one. (c) Sealing of channels with glue and peeling off glass substrate.



(a) In this first case glass plate as bottom sealing structure has been used.



(b) This figure represent the final display obtained according to the process of figure 2.19.

FIGURE 2.20: Display obtained with syringe/two hole encapsulation process.

2.4 Magnetic field generation

A magnetic field, specified by both a direction and a magnitude, expresses the magnetic influence of electric currents or magnetic materials. It can be denoted by the symbols B and H . B refers to magnetic flux density, and H to magnetic field strength. Magnetic fields can be produced by moving electric charges (solenoids/coils) or by the intrinsic magnetic moments of elementary particles associated with a fundamental quantum property, their spin. In other words permanent magnets create an invisible force, which pull on iron objects and attract or repel other magnets.

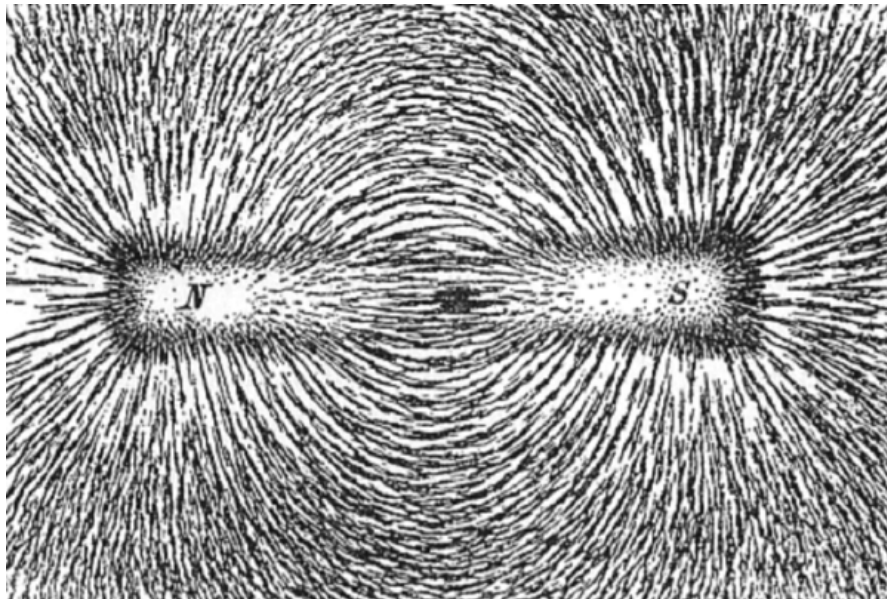


FIGURE 2.21: Magnetic flux lines.

Coils generate magnetic fields noticeably lower than permanent magnet but easily controlled varying the current flowing into them, hence by a potentiometer or by a microcontroller. Whereas, with neodymium permanent magnets the only way to vary the flux is mechanically move the magnet itself where the field's strength is inversely proportional to the cube of the distance from the surface of the magnet. It's easy to understand the numerous advantages of using coils instead of permanent magnets.

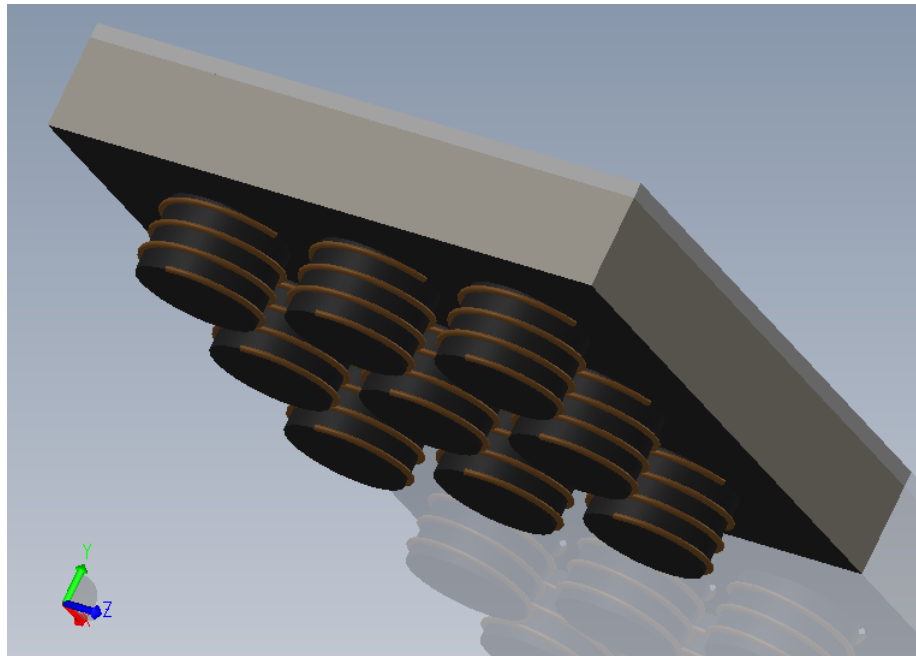
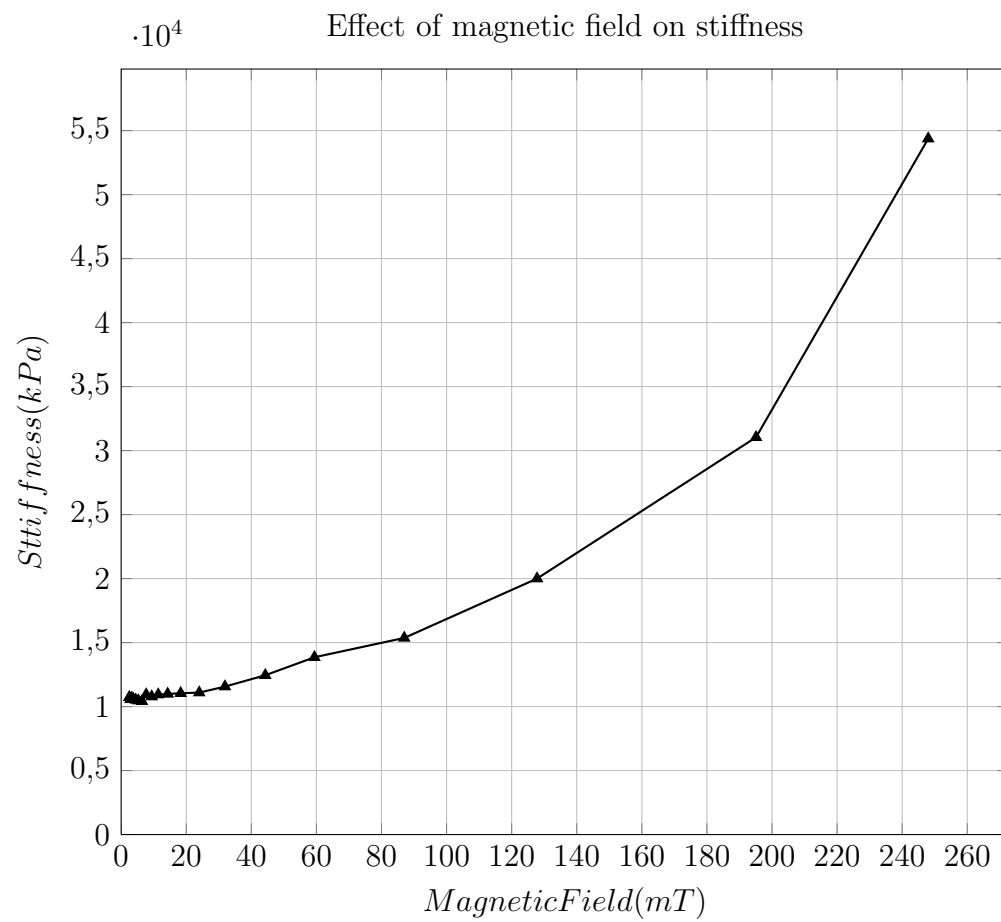


FIGURE 2.22: Coils arrayed under the bottom acrylic plate as actuators for changing magnetic field intensity.

Firstly, as shown in figure 2.22, coils can be arranged as single pixel-actuation at the bottom of the structure and independently controlled. The interference between neighbors is negligible and the basic structure and materials are easy to create and to be supplied at the laboratory. There are no moving mechanical parts; moreover solenoids can be shaped and shrunk as wanted, improving spatial resolution. Permanent magnets on the other side need a precise and feedback controlled actuation technique. Their reciprocal influence and the impossibility of nullify the magnetic flux make their usage as much effective as complicated. In conclusion, the usage of one or the other technology involves different system design and different difficulties. Of course solenoid system is preferred but to make the correct choice it has been tested the magnetic field intensity (mT) generated by both sources. During tactile display designing before considering which magnetic flux source was better a measurement of the stiffness was necessary.



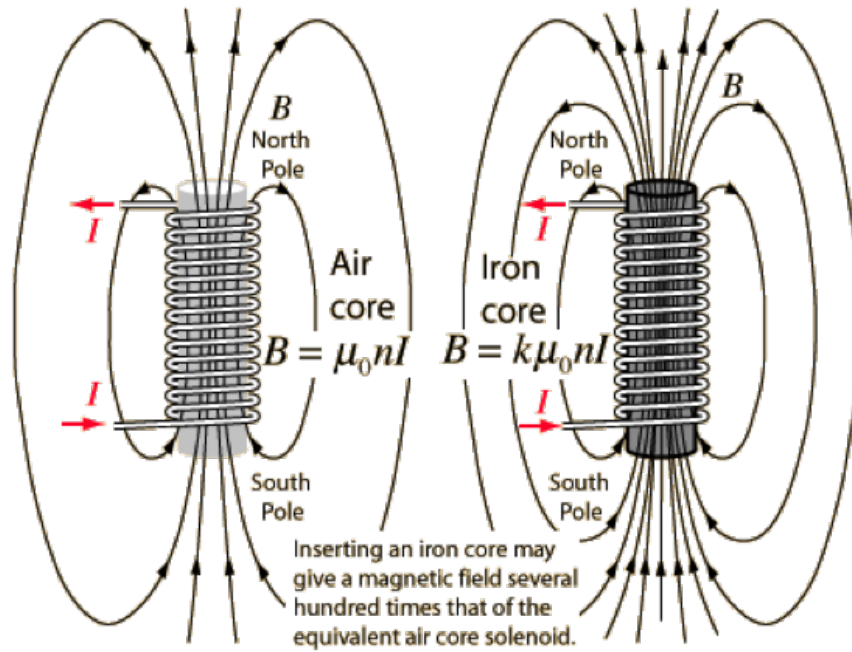


FIGURE 2.23: Physical principle of operation of a solenoid.

2.4.1 Solenoids

The magnitude of magnetic field needed to achieve a proper stiffness for intended tactile application has to be analyzed. The graph above shows that to sense important variation in MR's viscosity magnetic field generated inside has to range from $50mT$ to $250mT$. The values below $50mT$ are due to the summation of membrane mechanical property and glycerin compression. It means that below that value magnetic flux is not strong enough to ally the iron particles and consequently generates the variation of display mechanical property. The concept is quite similar to $\frac{S}{N}$ ratio for electronics: glycerin and membrane's stiffnesses are the noise and iron nanoparticles' stiffness is the signal. Under $50mT$ $\frac{S}{N}$ ratio is minor than 1 and not satisfying.



FIGURE 2.24: Coils of different dimension used for tests.

The figure 2.24 shows the three different types of coils used for intended application (the dimension ranges from 5 mm to 12 mm in diameter) and the basic structure is shown in figure 2.23. Bigger solenoids of course exist and generate higher magnetic field but if the trade off between dimension for spatial resolution and magnetic field intensity for a proper stiffness is considered, the maximum value is 12 mm diameter. If we analyze the magnetic field generated by the coils with a teslameter using a current of 1.2 A it is clear that the field is not high enough. Not even with the biggest solenoids generates a variation necessary to overcome the noise of the glycerin and membrane of 10 kPa. Even though their usage is really attractive and design process could have been easier, coils have been rejected.

2.4.2 Permanent magnets

The solution of using permanent neodymium magnet is the one left. The numerous disadvantages that derives from this solution have to be overcome. In fact as shown in the following graph the highest value of magnetic field reached with this technique perfectly fits the range required for the MR fluid to vary its rheological properties. So upon application of a magnetic field generated by neodymium magnets, the particles become magnetized and align themselves roughly parallel to the imposed magnetic field.

All the analysis and tests of the device have been done using permanent neodymium magnets as it will be analyzed in the result's chapter. The direction is now to have a magnet to generate the variation in the magnetorheological properties of the fluid and find a proper actuation system for the correct positioning of the magnet. In fact, the problem as already mentioned above is to move precisely the magnet: the final idea is to create a relation between the magnet position expressed by electrical signal and the stiffness displayed on the surface for that magnet's position. In the next chapter will be analyzed different solutions to move the magnet. Each actuator has to be strong enough to manage the magnetic field generated, fast for real time application and precise to suits the relation between input signal and output position.

Effect of distance on Magnetic field intensity in permanent magnets and coils

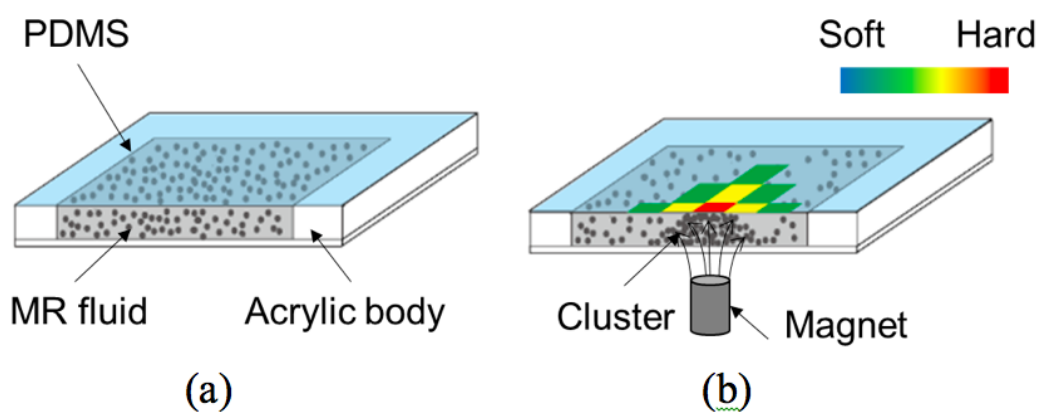
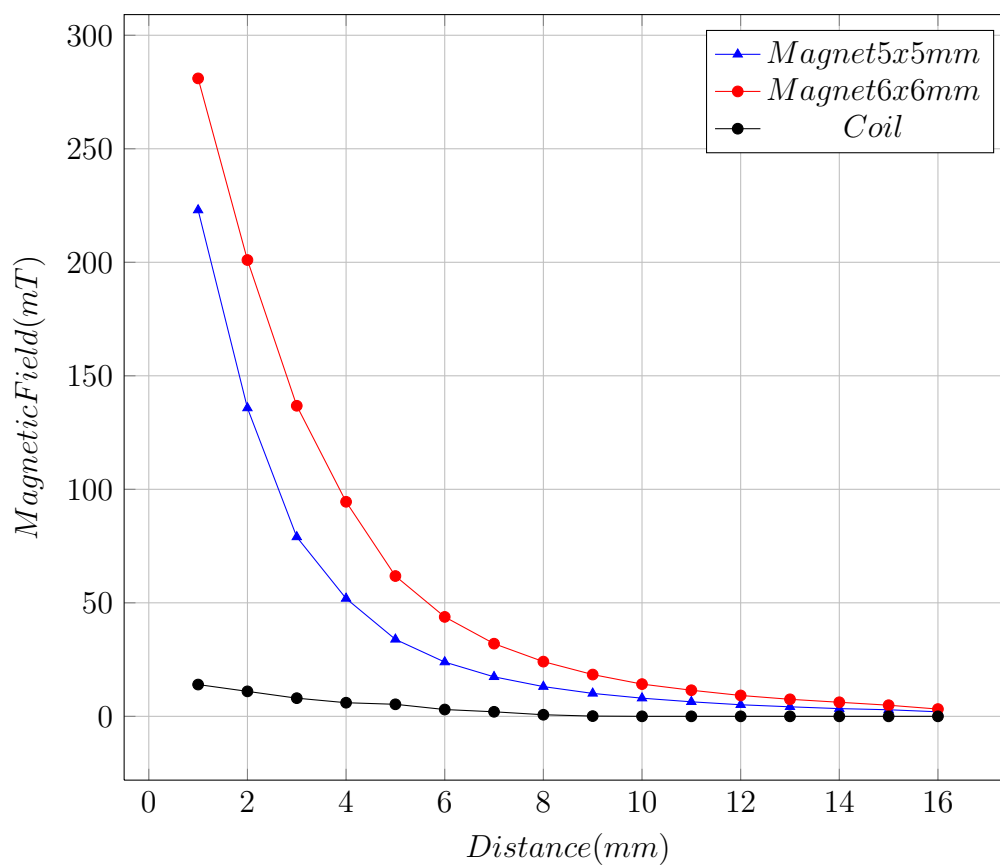


FIGURE 2.25: Effect on iron particles when magnetic flux is applied.

Chapter 3

Actuators

As already preannounced in the previous chapter, here the emphasis of the discussion is on designing an actuator capable of moving and placing the neodymium magnet in the right position to generate high variation in the rheological properties of the MR fluid in order to be sensed by the user through the large displacement PDMS membrane. Of course different ways allow achieving that but each one has its own pros and cons.

In order to classify the actuators it can be distinguished the type of energy mediating in the activation of the end effector, intended as the final part of the actuator in direct contact with the magnet. Of the three major categories mechanical, electrical and thermal during the design of the display have been considered the first two. While the electrical devices use current's flow or electric field, the mechanical actuators include actuators based on piezoelectricity, electrically controlled pneumatic valves or electromagnetic forces [38]. Many key-factors such as design flexibility, reliability, resolution and difficulties in fabrication and integration, drove the design.

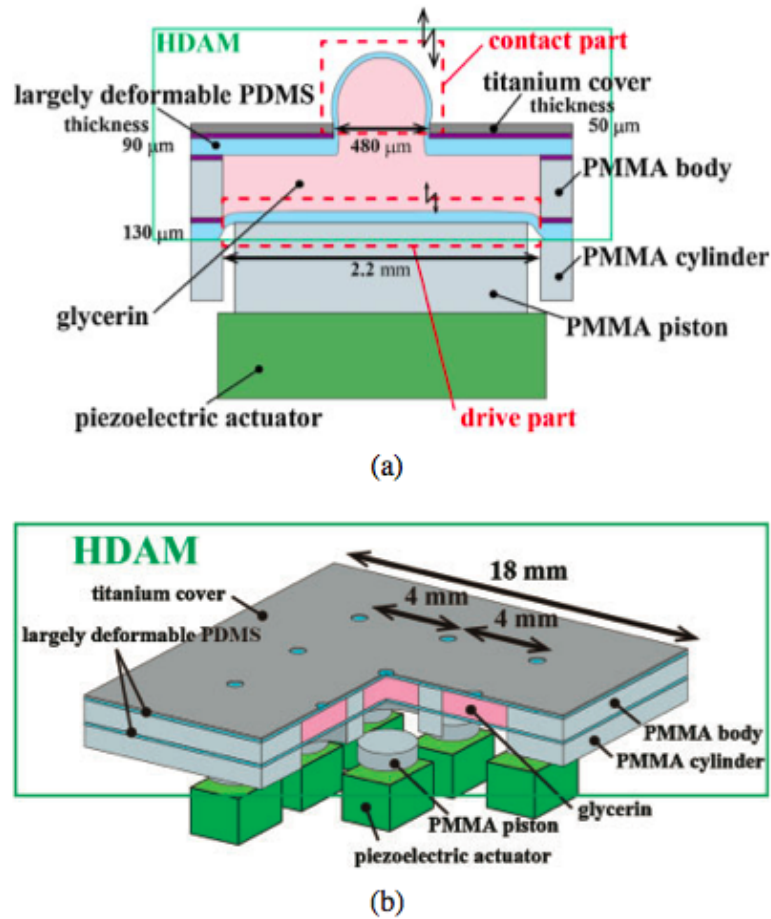


FIGURE 3.1: Schematic cross-sectional views of (a) HDAM and (b) vibrational Braille code display [6].

To have a clearer idea of which device more suits this study-case the stroke's range of the end effector has to be analyzed and has to be found the minimum necessary to change significantly the stiffness of the display. As already analyzed the magnetic intensity decreases inversely proportional with the cube of the distance. In the tactile device is required to range from absence of magnetic flux to the maximum intensity when the magnet touches the bottom PMMA plate. Subsequently it has been evaluated the intensity of the magnetic field for 15 measurements up to lean against the acrylic plate that corresponds to a distance of 1mm from the fluid. This has been evaluated for both the 5x5 mm and for the 6x6 mm. Eventually, has been analyzed the relation between the distance of the magnet from bottom plate and stiffness' change in order to compare the values with real tissues (fig. 3.2). The protocol was: 0.01 N of preload, 15 measurements were performed at step of 1 mm. The device is an acrylic plate with 4 mm, membrane made with 1000-RPM HPDMS with a base plate of 1 mm.

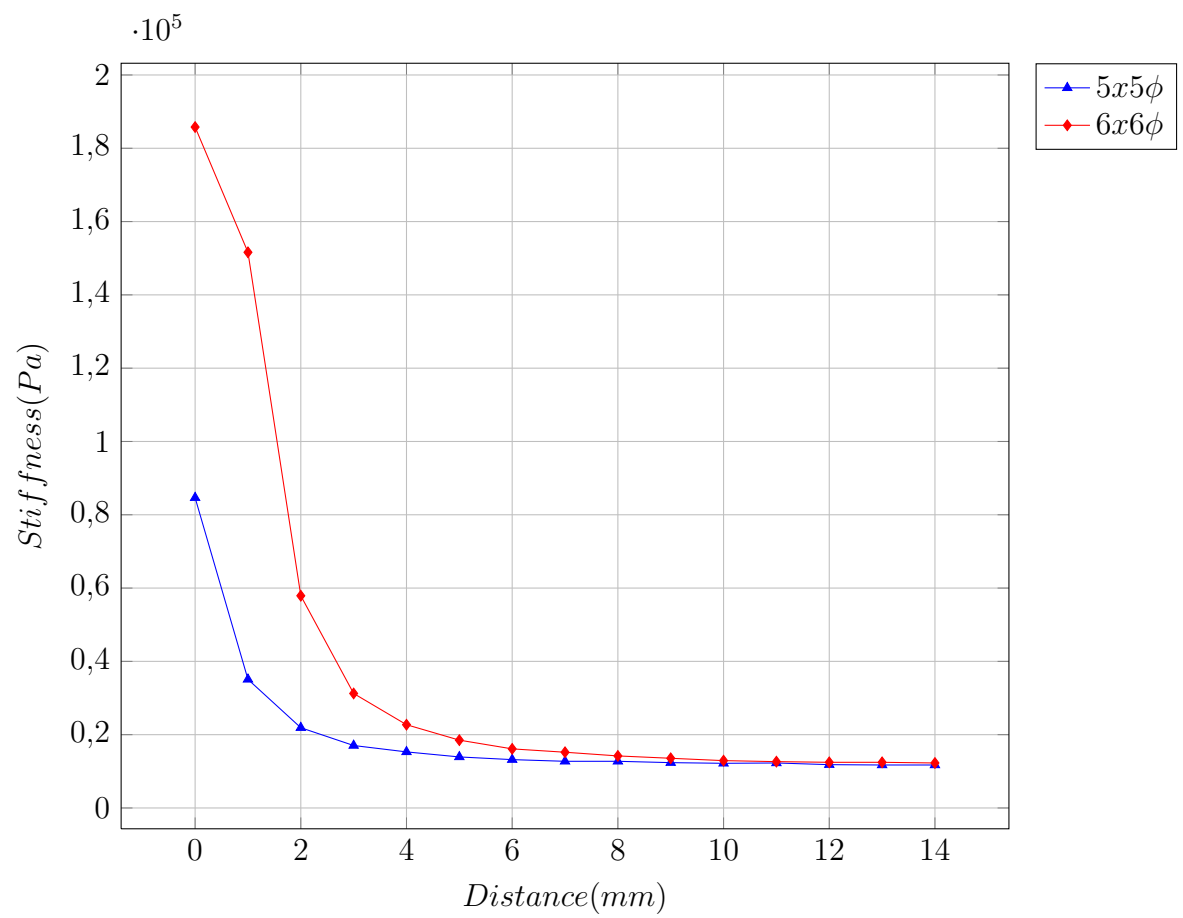
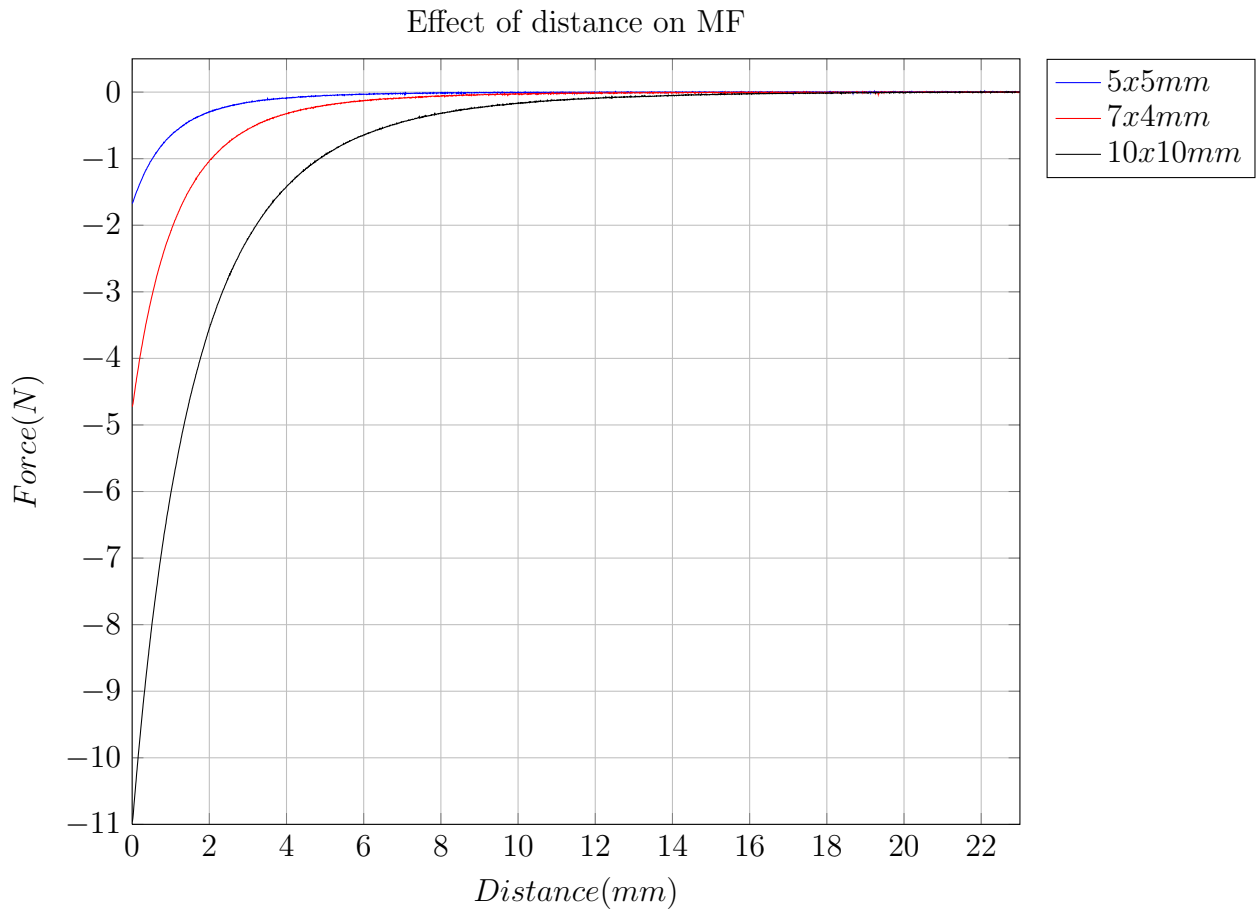


FIGURE 3.2: Stiffness vs distance distribution.



As shown in figure 3.2 it can be considered that the magnetic field effect is absent when the measured stiffness is due to the mechanical response of the combination of the membrane and the MR fluid. So the interval ranging from a distance of 3 mm between the top of the magnet and the bottom acrylic plate up to the point where the magnet reaches the bottom plate the effect of magnetic flux intensity is of interest, neglecting the rest. Hence, from 0 to 3 millimeters a wide range of stiffness can be displayed. Now it is clearer why an actuator with a smaller range than 3 mm can't fit the project. Moreover, it has to be found an actuator strong enough to generate a repulsive force to move the magnet. As shown in the following figure the MR fluid generates an attractive force that the actuator has to work with. Hence, in the 5 mm neodymium magnet case when the magnet is touching the bottom plate of the device it has to face almost 2 N attractive force. It is easily understandable that for a "huge" actuation system is not a problem, but with a scaled actuator as the considered ones is a big deal and usually the force generated is not strong enough to fight the attraction force generated at the interface.

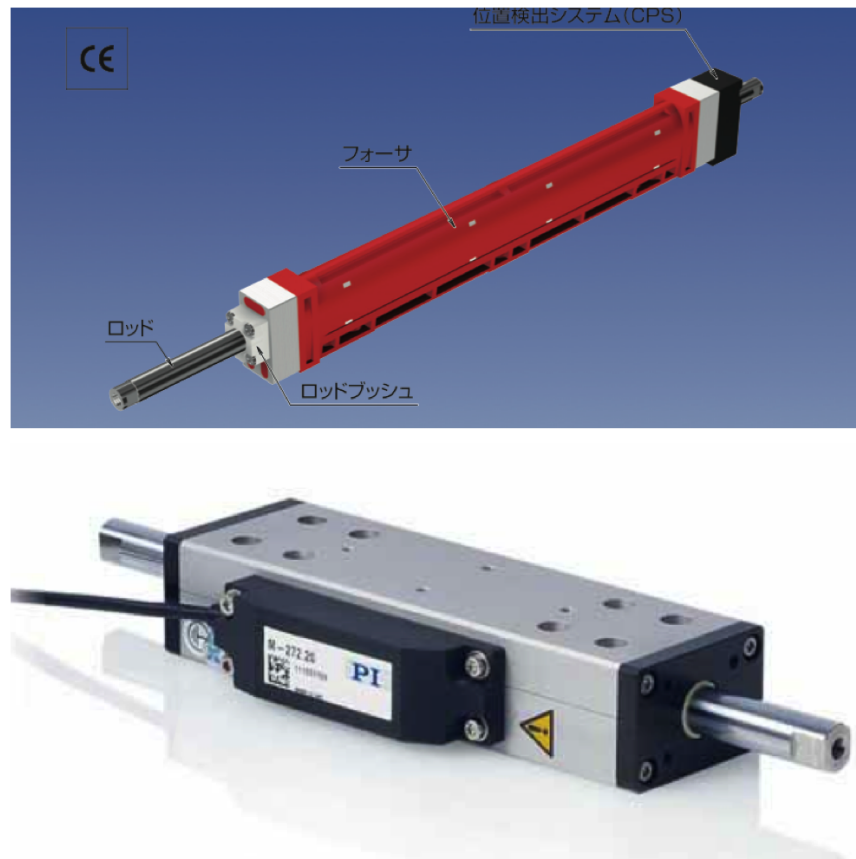


FIGURE 3.3: The first study-case is linear actuators. Usually this kind of devices calls for huge space inside the system hence, usually work standing alone.

3.1 Actuation systems

Compact standard-class linear drives are widely used in automation engineering for application such as handling, micromanipulation, metrology, etc. The basic ideas are common and consist in having a fast device, maintenance-free and easy to integrate. The previous features also have to be combined with a reliable position control, repeatable accuracy and cost effective solutions. In this direction ranging from the conventional combination of electric motor and spindle to piezoelectric, different systems have been studied and the idea of direct drive, self-locking at rest with no heat generation system has been found in different device on the market.

In order to reduce the dimension of the actuator it has to be neglected the integrated linear scale encoder and look for devices with less stroke: the ultrasonic actuators, piezoelectric actuator and air actuator can be considered. All these

	M-272.20	Tolerance
Active axes	X	
Motion and positioning		
Travel range	50 mm	
Integrated sensor	Linear encoder	
Sensor resolution	0.6 μm	
Min. incremental motion	1.8 μm	typ.
Unidirectional repeatability	2 μm	typ.
Bidirectional repeatability	3 μm	typ.
Velocity	150 mm/s	max.
Mechanical properties		
Guiding	Ball bearings	
Push/pull force	8 N	max.
Holding force	8 N	max.
Lateral force	10 N	max.
Drive properties		
Motor type	U-164 PLine® ultrasonic piezo drive	
Current consumption	800 mA*	
Reference point switch	Optical	
Miscellaneous		
Operating temperature range	-20 to +50 °C	
Material	Aluminum	
Mass	0.47 kg	$\pm 5\%$
Cable length	1.5 m	$\pm 10\text{ mm}$
Connector	MDR, 14-pin	

Recommended controller/driver: C-867.OE
 Power for the motor is supplied by the drive electronics, which requires 24 V DC.
 * For drive electronics

FIGURE 3.4: The data sheet refers to the bottom device in figure 3.3. Even though the stroke of the end effector is a strong feature and attractive as shown in the data sheet the dimension is not suitable for intended application. Other strengths are velocity up to 150 mm/s, self-locking at rest, integrated linear encoder and integrated linear guiding system so the device is really attractive.



FIGURE 3.5: Pen cylinder above allows reducing the dimension of the end effector and the structure as well. It's “pen-like” easily to be arrayed. The main issue is the actuation control: controlling air with a pump and compressed air is suitable for on-off application but when a precise positioning is required, generate a precise signal could be challenging.

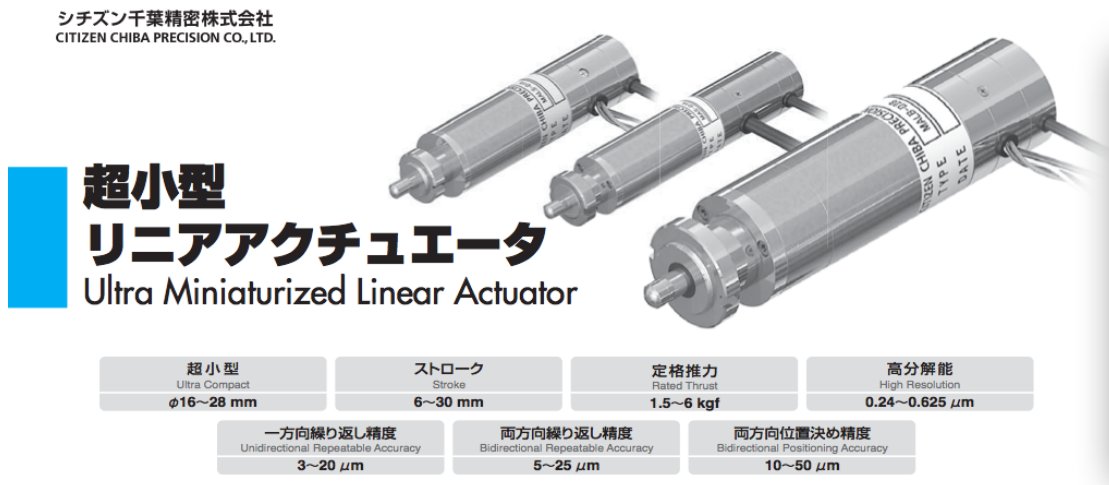


FIGURE 3.6: This linear actuator is ultra miniaturized but still compared to “usual” linear actuator as the ones pictured in figure 3.3. For the case in object 16 mm diameter is still too big.

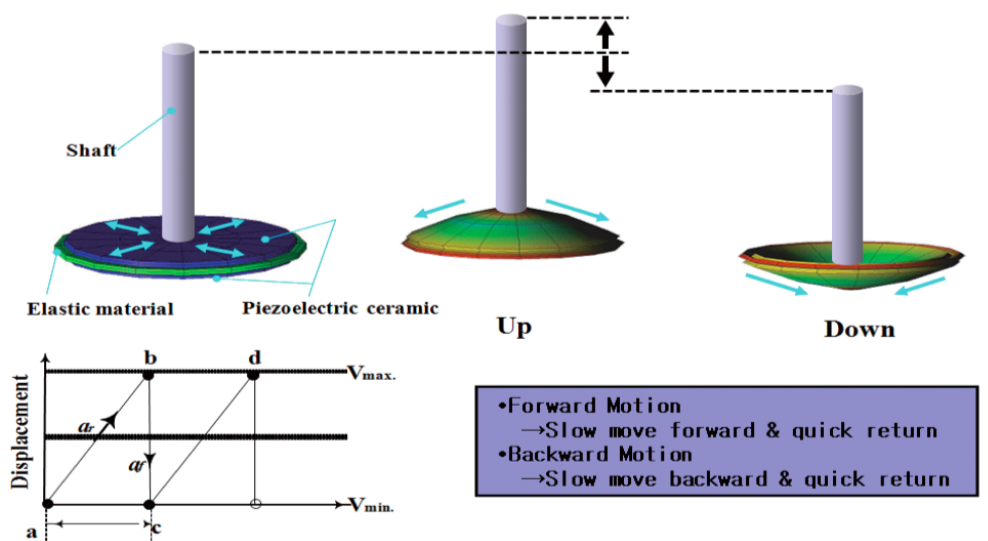


FIGURE 3.7: TULA Ultrasonic actuators allow moving the end effector really fast and precisely. Moreover, the device is shrunk to a likely dimension suitable for but the stroke module is too low. This kind of devices is widely used for precision positioning such as cameras but when it comes to move a 5x5 mm magnet is not suitable anymore.

systems present a good dimension feature and can be easily arrayed under the display losing of course some others interesting features that characterized previous devices.

After analyzing systems with different features the attention moved to voice coils. Widely used in mechanical ventilation they generate force proportional to the current that flows through the motor coil, a force almost constant in the specified



FIGURE 3.8: C2946 Voice coil actuator.

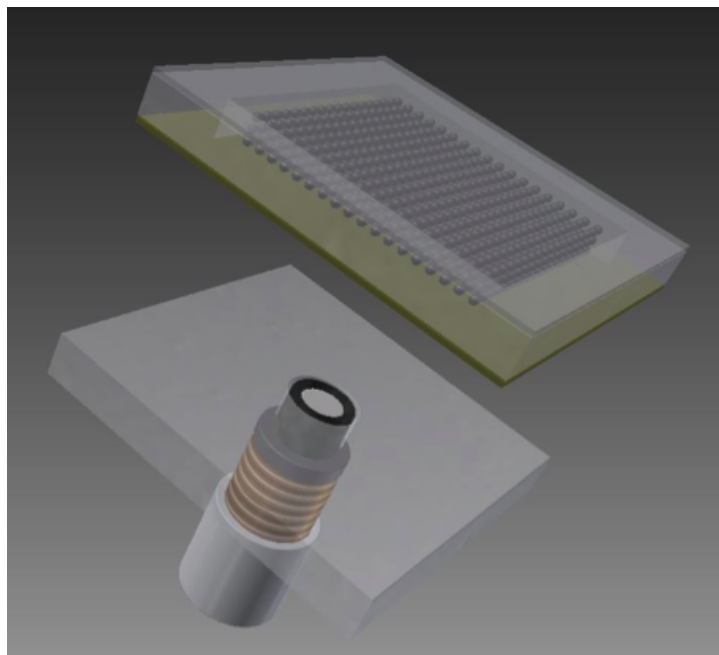


FIGURE 3.9: The idea of how integrating the device under the display is shown in figure and the dimension are scaled.

stroke range and all that at very high speeds and accelerations. On the other hand there is no positioning system ¹ but the speed and the intensity of the stroke can be easily controlled modulating the shape and the module of the current through a microcontroller as it will be analyzed in the next chapter.

¹Voice coils actuator with positioning system exist but are massive and too expensive so not considered in this project

3.1.1 Voice coil actuation (VCA)

Voice coil actuators mainly consist of a conductor wrapped around a cylinder and placed in a magnetic field: according to Lorentz's law a force is generated as:

$$\mathbf{F}_{Lorentz} = \mathbf{i} \cdot \mathbf{l} \times \mathbf{B}$$

The formula above says that as results of moving charges as a current \mathbf{i} in a magnetic field \mathbf{B} with a length l of the conductor the resulting Lorentz-force is \mathbf{F} .

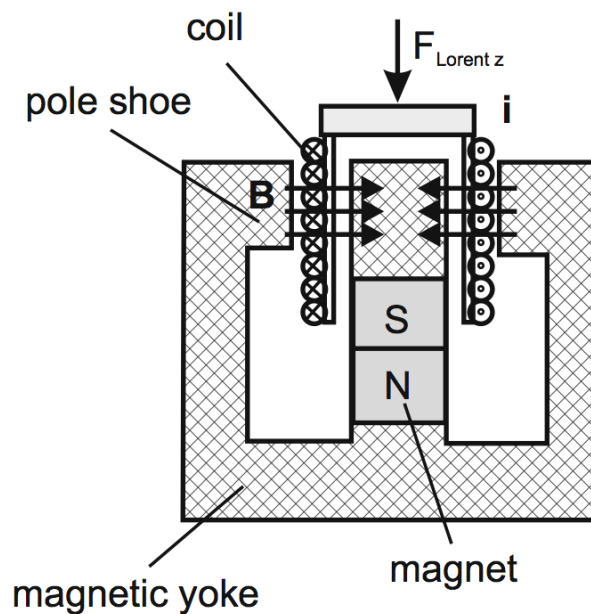


FIGURE 3.10: Moving-coil actuator [3].

To have an idea of the magnitude of the force \mathbf{F} the following example might be clarifying. A plausible resistance of the conductor could be 3.5Ω and the current flowing in it varies between 0.75 A and 1.2 A . Taking as example a value of 0.78 A the total power dissipated is:

$$P_{el} = R_{coil} \cdot i^2 = 3.5\Omega \cdot 0.78A^2 = 2.13W$$

Then, with a magnetic flux intensity of $\mathbf{B} = 1.2T$, easily achievable with a neodymium magnet, and a conductor length $l = 1.58m$ wrapped up on the plastic cylinder, the force generated is:

$$F_{Lorentz} = ilB = 0.78A \cdot 1.58m \cdot 1.2T = 1.48N$$

To understand how fast this system is the analysis of the acceleration should be of interest. Starting from idle mode and supposing that the coil's own mass is $m = 8.8g$, to perform a displacement of $x = 10mm$ it takes:

$$t = \sqrt{2\frac{x}{a}} = \sqrt{2\frac{xm}{F}} = 0.011 s$$

that calls for an electric energy loss of:

$$W_{el} = P_{el} \cdot t = 23.4 mJ$$

There are two types of VCAs: with a moving magnet where the coil is attached to a stationary soft magnetic housing and with a moving coil that consists of the usually stationary field (a magnet) assembly and the moving coil assembly. Applying a voltage or a current across the terminals causes the VCAs' moving part to travel in a given direction and reversing the polarity it will change the direction. The generated force is proportional to the flux crossing the coil and the current that flows through this coil. Voice coil actuators perfectly suit applications where precise control is needed, primarily because they can be supplied with position feed-back device and also because they can generate more force than solenoids for a given size, stroke and input power. The fast acceleration capability by moving small mass allows real time application and can also be improved by designing a light moving part.

The physical characteristics of a VCA also make it a preferred choice in medical, aerospace and military applications in which size and weight are as important as its functionality. Many medical equipment applications are required to have high

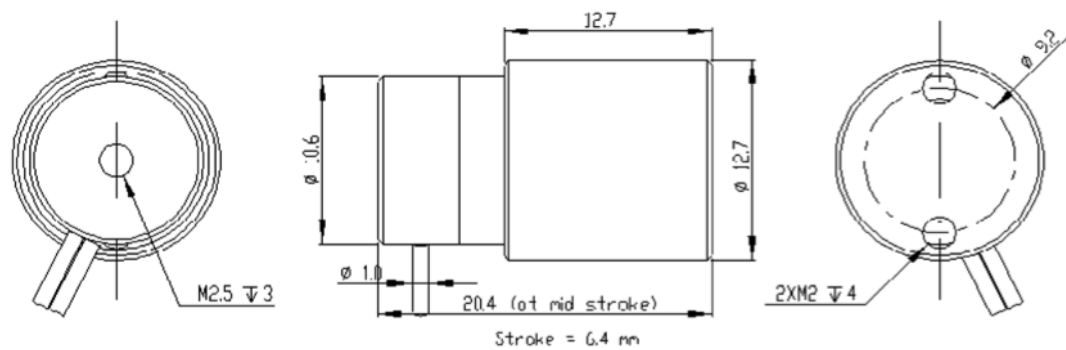
AVM12-6.4

FIGURE 3.11: Technical specification of VCA used for tactile display.



FIGURE 3.12: VCAs.

mobility, and every component is required to meet a specified dimension. Voice coil actuators have been selected for their technologies and performance. They are high power density devices, so in applications with a short stroke or excursion angle, a voice coil actuator can do the job where other technologies such as motors or gear motors, will be too big and heavy. According to what explained up to this point VCAs have been the obvious choice to control force, speed, travel, and acceleration/deceleration for continuous performance and accurate positioning.

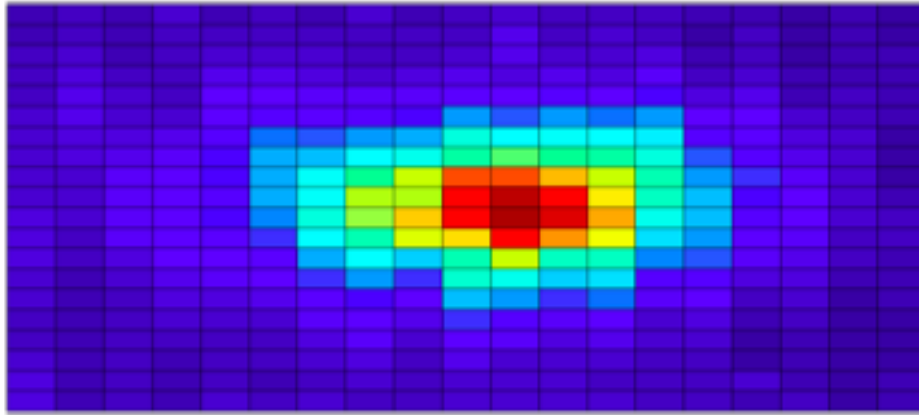


FIGURE 3.13: Stiffness distribution generated on the display using a neodymium magnet.

3.2 Solution for the magnetic field confinement

The basic idea of this section has been to find a solution for magnetic field containment. Since the final goal is to create a single pixel-unit made of voice coil actuator and a small neodymium magnet on top of it, the spot of stiffness on the display generated by that pixel should be well defined and as small as possible. If the magnetic flux density spread wider and wider the display will lose in spatial resolution and the single spot, aka pixel, will be too way big for intended application.

So different solutions have been studied for magnetic flux containment: the improvement can be achieved acting on different part of the device. The main issue has been that magnetic field can pass through anything. There is no known material that totally blocks or contains magnetic field. It can only be redirected away from the objects you want to protect providing an alternative path for the magnetic field lines.

3.2.1 Re-routing for shielding

Firstly shielding materials have been analyzed. They offer a high-permeability path for magnetic field lines to travel through forcing them to pass through a specific path. Nowadays shielding materials are made of high-permeability alloys that contain about 80% nickel fabricated as foils and baked at 2000 °F in a dry

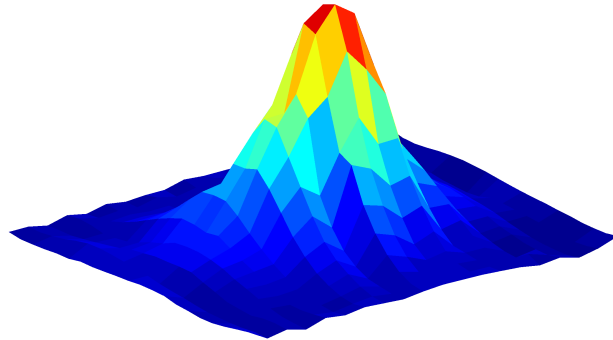


FIGURE 3.14: 3D stiffness distribution generated on the display using a neodymium magnet.

hydrogen-rich atmosphere to anneal them: annealing improves the material's attenuation and its capability of redirect magnetic flux density. To be effective and efficient the shielding shape should be a loop. It is important that the shield offers a complete path for the field lines, so that they do not exit the material.

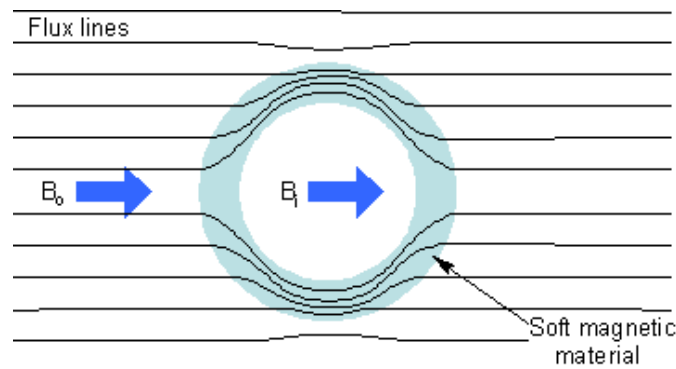


FIGURE 3.15: Sheets of Permalloy, Mu-Metal™ or soft ferromagnetic metal coatings. The permeability of Mumax 350000/500000 $\frac{H}{m}$ versus 3000 $\frac{H}{m}$ of iron.

The best actuating solution would be a magnetic system able to create a single pole field well confined in order to reach a pixel-like shape in stiffness distribution for example by placing the magnet in a multilayered high permeability container and only exposing one pole surface of it. This multilayer system could be made of soft iron sheets separated from each other by a non-conducting material, like plastic

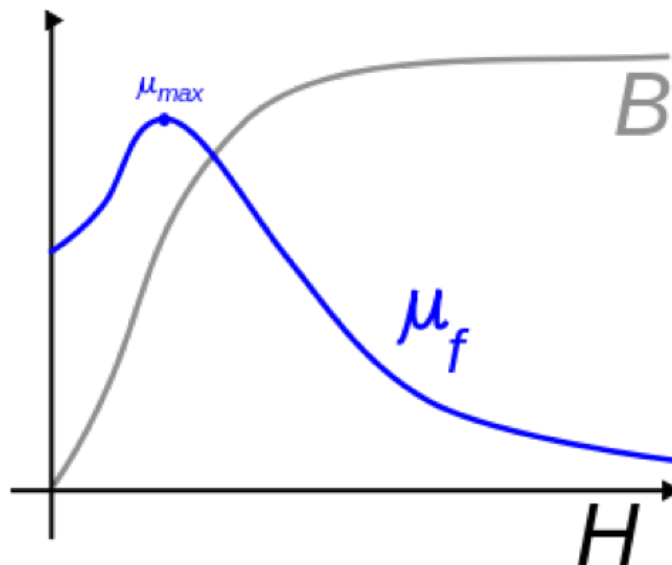


FIGURE 3.16: Saturation induction: Mumetal™ is a very good magnetic shielding in certain applications where very low fields ($\leq 1\text{Gauss}$) are required but it saturates at about 0.2 to 0.4 T, while soft iron saturates at about 1.4 T which is a better choice for the intended application

² or epoxy. Iron sheets are an excellent shielding material, since is somewhat like short-circuiting the magnetic field geometry by encapsulating it behind these layers. The type of shielding exemplified incorporates a fully closed loop: it's all about the reshaping of the magnetic geometry, leading the field into a current-like propagation through the ferrous multilayer.

This technology of altering a magnetic field by bending it into a constricted path is common orthodox scientific knowledge. The trick here is not really shielding off one of the poles from the other, but instead by leading this field into a narrow path hidden behind the shielding properties. In this way the magnetic field it is just confined in to a narrower path and the exposed pole is still actively relating to the other pole but just altered the geometry of the field structure, so that the electromagnetic visibility of one pole outside the shielding circuit is inhibited. MU-metal is just a multilayered system on ferrous material, preferably simply soft iron that does shield by diverting the magnetic field and re-routing in a desired direction. The magnetic field from each magnet pole enters normally (along the axis) into the soft iron, travels outwards in the iron radially and exits. The result is that when checking the shielded surface with a Gauss-meter, it does not register

²Electrical insulating tape.

anything, which is the very concept of a magnetic shield. Thus re-routing and shielding are equivalent concept.

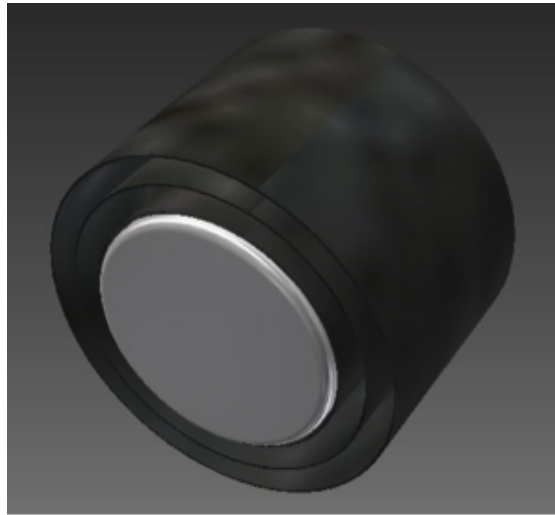


FIGURE 3.17: By only exposing one pole end area of the magnet to the surrounding, it still have a complete field interaction between north and south poles, but this north-south interaction is executed inside the shielded volume.

3.2.2 Septa

Another solution to improve the spatial resolution has been creating septa at the bottom of the device. Due to the no-Brownian motion of the particles they tend to precipitate at the bottom separating from the liquid part of the MR fluid (glycerin). The iron particles' layer is uniformly distributed at the bottom of the plate with no interruption or boundaries between each part. Thus, the idea of improving tactile feeling by confining the particles into a spot-like septa with no connection between each part, similar to waffles showed in figure 3.18.

With this technique the quantity of iron particles doesn't change but its spatial distribution is varied. Focusing the concentration inside a specific spots the tactile feeling is much more close to a pixel-like. Moreover, if the material which compose the septa has low rigidity mechanical properties (close to the ones of the MR fluid) is not only containing particles but also not sensed by the user's finger. An interesting material could be the photocurable perfluoropolyethers (PFPEs):

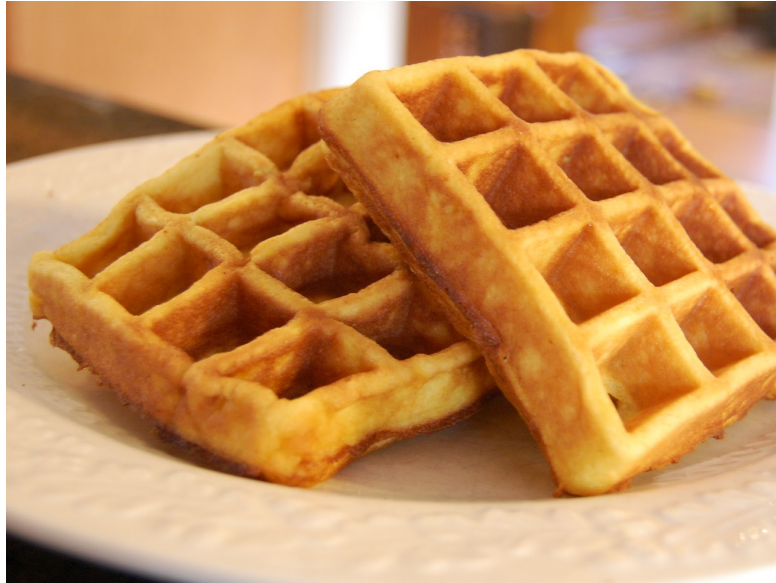


FIGURE 3.18: Waffles.

liquids at room temperature and can be photo-cured into micro-fabricated devices. It exhibits low surface energy, low modulus and low toxicity. Ideally, the septa should also contain high permeability material, likely made with a small iron cable running through the structure in order to confine more the magnetic field to avoid interference between each pixel. This last topic and low-density material as well are still open arguments.

For the time being PDMS solution has been used. Firstly a mold has been designed and after pouring the PDMS into the mold and baking for curing, the PDMS structure is pilled off and glued at the bottom of the plate. Two different solutions for mold's designing have been studied. Firstly made of SU-8 UV negative photoresin and after cutting a PMMA plate with a miller. Soft lithography with SU-8 has been widely used as MEMS technique for molding. Already used by Miki Laboratory for formation of polymer microneedle arrays [39], what written and represented below fully refers to it [39].

Septa structure was molded using a negative photoresist containing sharp hollows. The mold was formed by the diffraction of exposure light, creating tapered structures after development. When channel-like structure (fig. 3.21) used as a photomask, a sharp hollows was formed, as shown in Fig. 2(a). After exposure, the orange parts of SU-8 became stiff as shown in Fig. 2(b), and only the yellow parts were removed after development. Longer exposures led to stiffer, thicker SU-8 layers as shown in Figs. 2(c) (shorter exposure time) and 2(d) (longer exposure

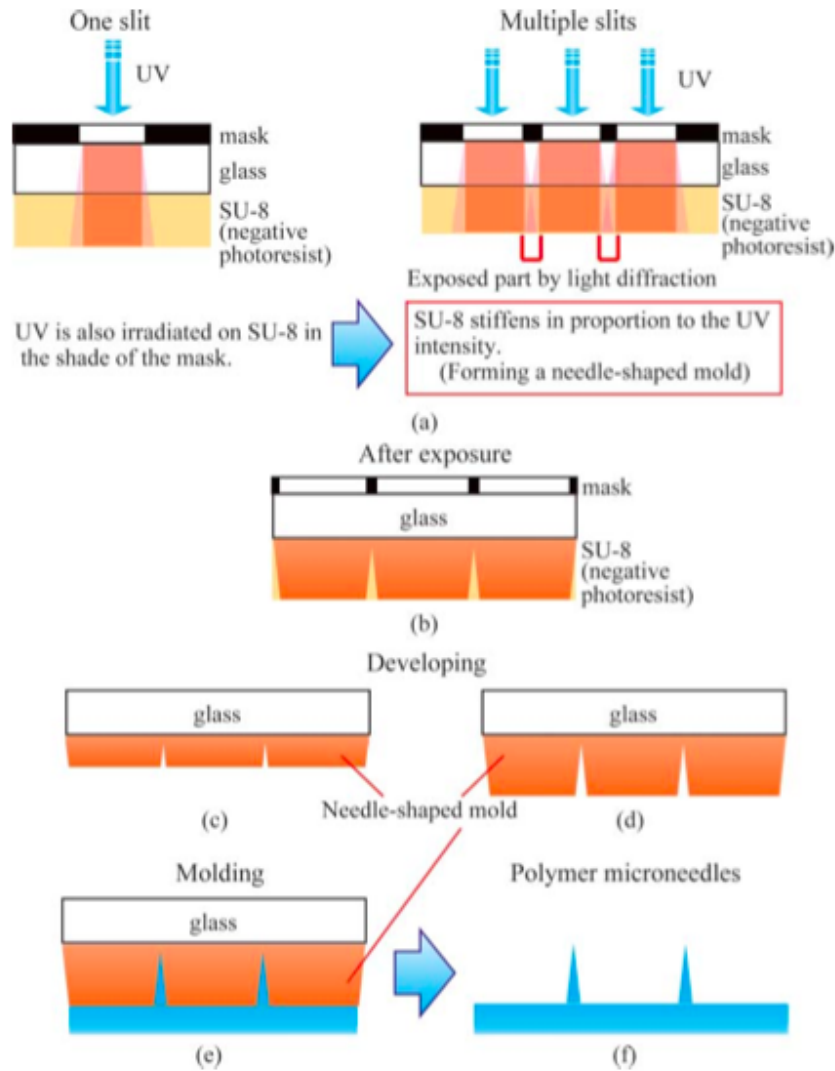


FIGURE 3.19: Manufacturing of polymer microneedles: (a) Exposure with one slit and multiple slits, (b) after exposure, (c) developing after short-term exposure, (d) developing after long-term exposure, (e) molding, and (f) formation of polymer microneedles [7].

time). After development, PDMS septa has been molded as shown in Figs. 2(e) and 2(f).

Even though this technique is fascinating for the preciseness and repeatability the major problems faced using SU-8 is create a structure deep enough to contain iron nanoparticles. This technique was born to built structure of about $300\mu m$. Thus, molding the SU-8 until 1 mm or more become challenginga and piling up various layers until the desired thickness is not possible. Moreover the operation of peeling

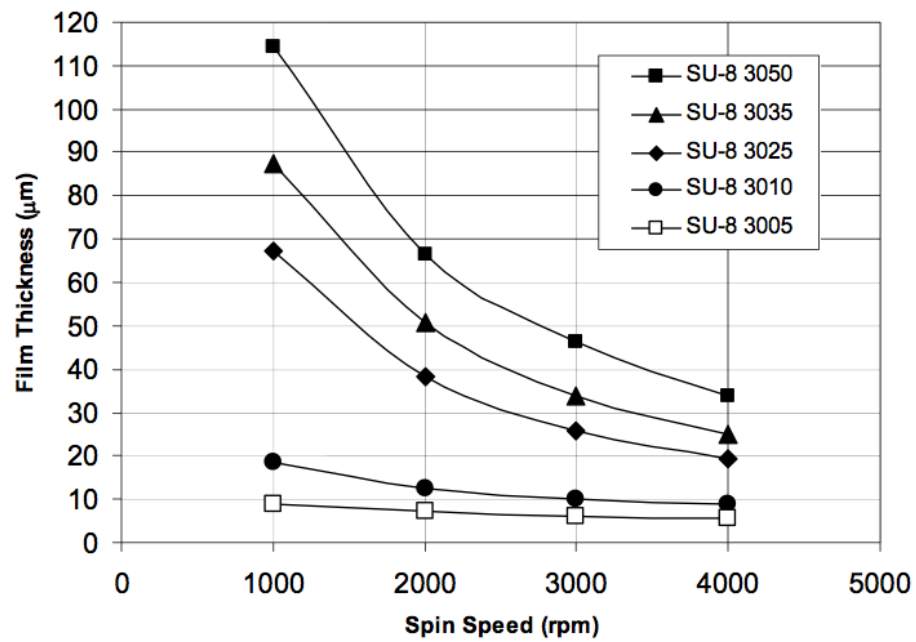


FIGURE 3.20: SU-8 thickness relation with spincoater's RPM speed.

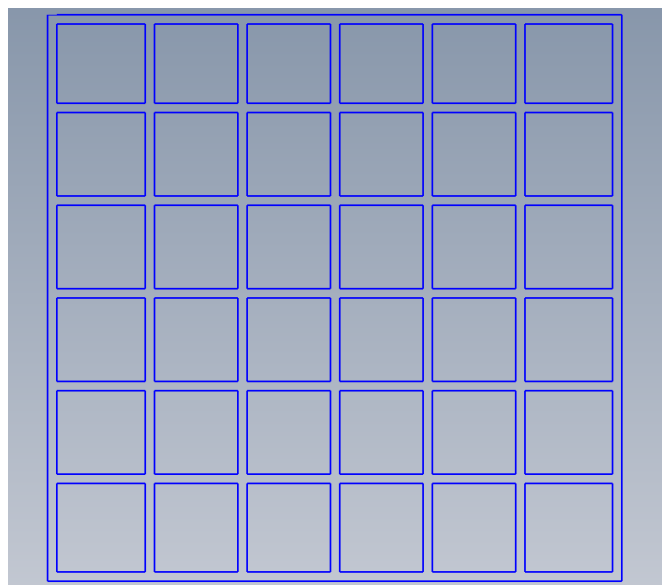


FIGURE 3.21: Mask used for creating septa.

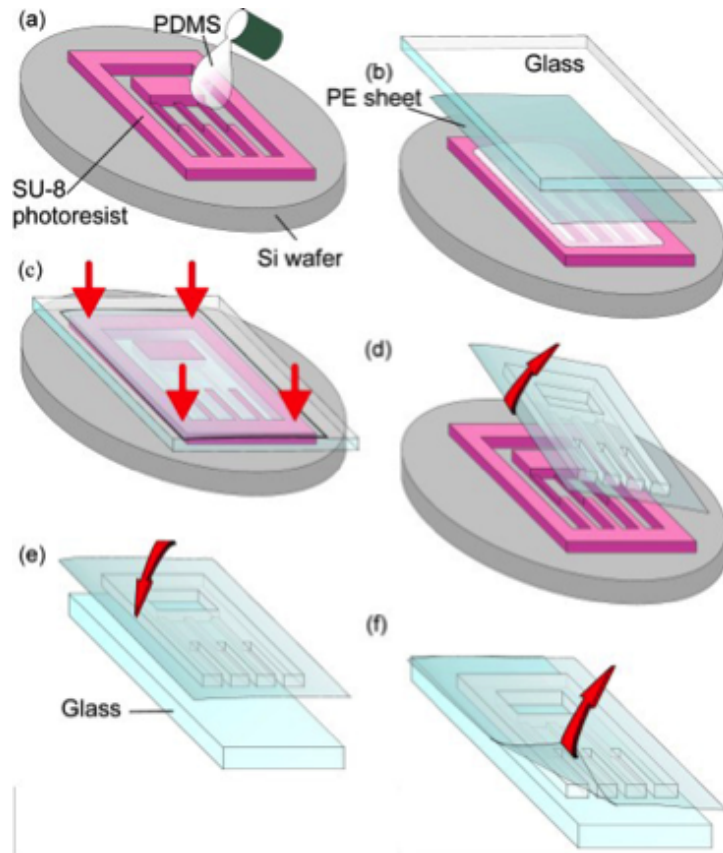


FIGURE 3.22: FolchLab's solution for PDMS peeling off.

off the PDMS structure from the mold is really delicate. Peeling operation generates a bonding force that is troublesome. *FolchLab*³ for 3D micro fluidic devices proposes an easy solution to solve this problem as shown in figure 3.22. When the polymer is PDMS, the sheets are micromolded by pressing a polyethylene (PE) sheet between the master wafer (covered with a few droplets of PDMS prepolymer) and a glass plate. The goal of applying pressure is to fully exclude PDMS from the areas where the master contacts the PE sheet. Conveniently, when the PDMS is cured and the PE sheet is peeled off, the PDMS microstructures trapped between the PE sheet and the master prefer to stick to the PE sheet. The PDMS microstructures then are exposed to oxygen plasma, which activates the PDMS surface; when this PDMS surface is contacted with clean glass (or PDMS), the PDMS binds to the glass (or PDMS) surface. The PE can then be peeled off, leaving the PDMS layer on the surface. The PE sheet allows for precise alignment and visualization of the PDMS pattern during alignment.

More rude and naive method is using the miller. With a drill of 0.5 mm diameter

³<http://faculty.washington.edu/afolch/FolchLabResearchProjects.htm>

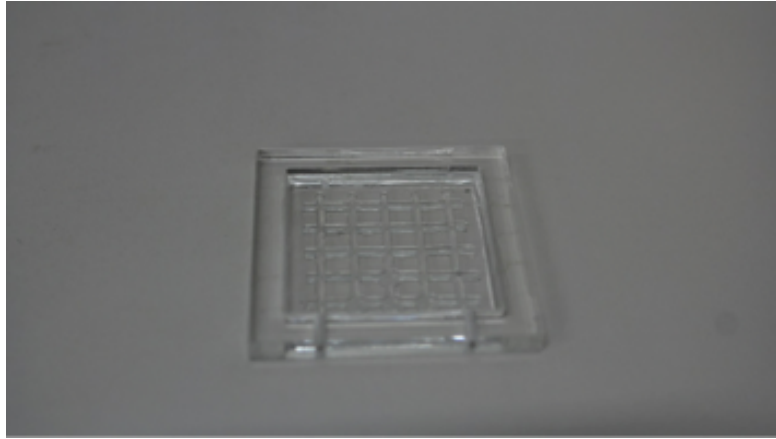


FIGURE 3.23: 1 mm deep and thick PDMS septa, bonded with UV-curable resin at the bottom PMMA plate.

of course the dimension of the septa become thicker than using SU-8: nevertheless the containment capability is the same the tactile transparency of the structure disappears. The miller is not precise enough for such small structure and it is physically impossible to design a mold with septa's thickness under 1 mm. After that simply pouring PDMS solution, leveling and baking⁴ the septa are obtained as shown in figure 3.23. 1, 2 and 3 millimeter deep structure have been molded, bonded using UV curable resin and tested for tactile feeling inside a 4mm thick PMMA structure. The 3 mm solution in addition to the already mentioned problem of the dimension of the drill, when it comes to go deeper to mold the PMMA plate the shape of the drill enlarge the already large channels because the drill is not design to go deeper than 2mm. If the septa's structure is too thick, is almost impossible to apply a pressure with the fingers and bend it loosing the capability to sense the stiffness variation caused by the MR fluid.

3.2.3 Iron nanoparticles

Taking advantage of creating a septa-like bottom structure it is possible to fill the holes with more iron nanoparticles increasing the stiffness generated by the fluid and consequently the stiffness that a single pixel could generate. Before the operation of filling the MR fluid a small quantity of iron particles are poured inside the septa. Since the MR fluid is quite dense, the particles are not small enough for Brownian motion they tend to deposit at the bottom of the plate staying confined

⁴The PDMS' composition is the same of the membrane and also the baking process is almost the same.

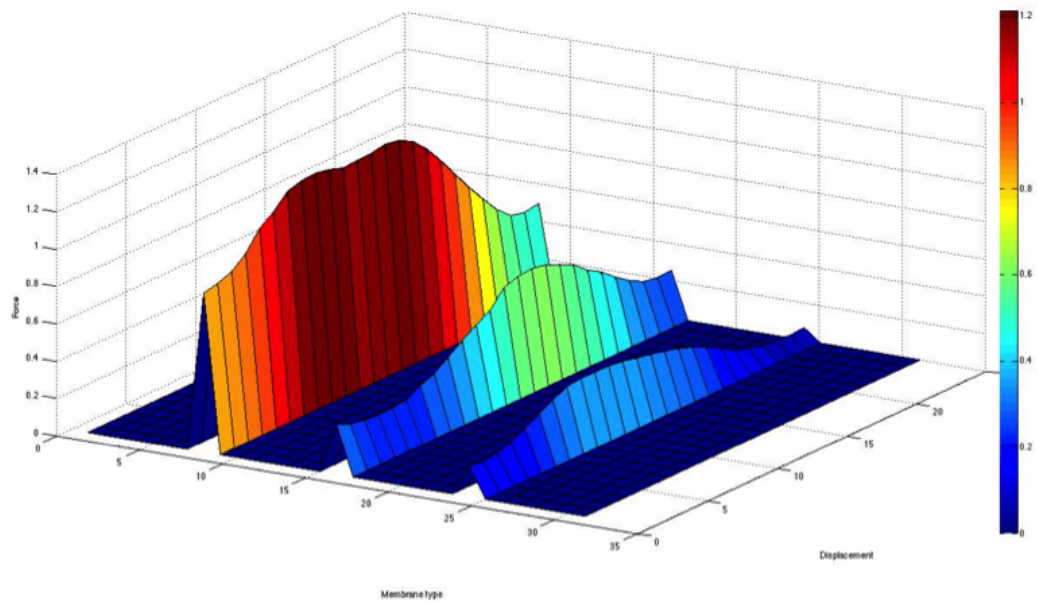


FIGURE 3.24: Effect of using extra iron particles. Three different quantities have been studied and repulsive force has been analyzed along the display's axis.

inside the septa. As shown in figure 3.24 the stiffness generated by increasing iron particles is noticeable and fascinating for intended application. In the last chapter will be analyzed how this solution could be improved.

3.2.4 Magnet's polarities

An additional tool for the measuring is the one depicted in figure 3.26. Projecting the idea to array the entire number of magnet under the bottom of the tactile display it has been analyzed how does the polarity of the magnets affect the resolution of the system. It has been studied how to confine as much as possible the area influenced by a single magnet to avoid interference between each spot and the another one. As shown in figure 3.25:

When two magnets are placed closed to each other the resulting magnetic field is influenced by the reciprocal position of the poles. As shows figure x if the poles are arrayed parallel to each others the magnetic flux spreads wider related with the case when poles' direction is alternated. To test the effect of this hypothesis on the MR fluid has been design a board that allows placing the magnets according to different polarities at different distances to validate it. As shows figure below the spot generated by two different magnets is different. The first case with parallel

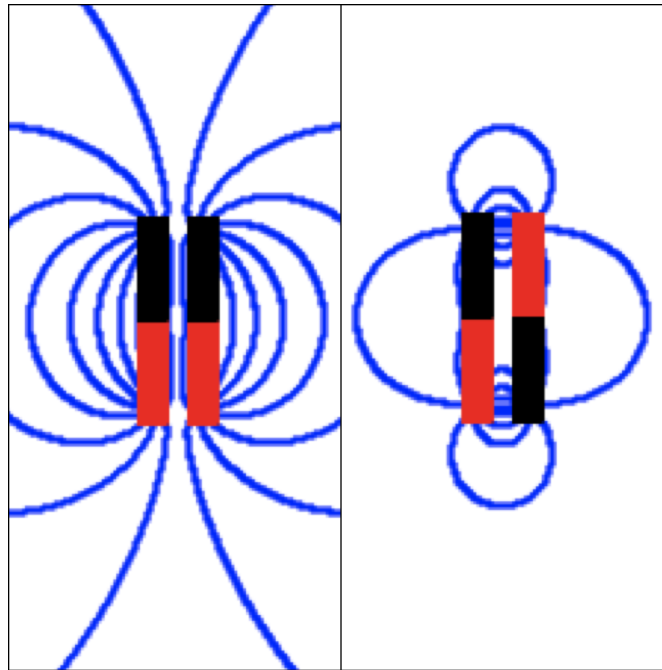


FIGURE 3.25: Through a simulator is possible to distinguish the difference in the combined magnetic field by changing the magnet's polarity.

poles allows to better distinguishing the two spots generated by the magnets under it.

Once the polarity is decided with the tool above is possible to recognize the minimum distance at which two magnets are recognized as separated and not as single spot as will be analyzed in the result's chapter.

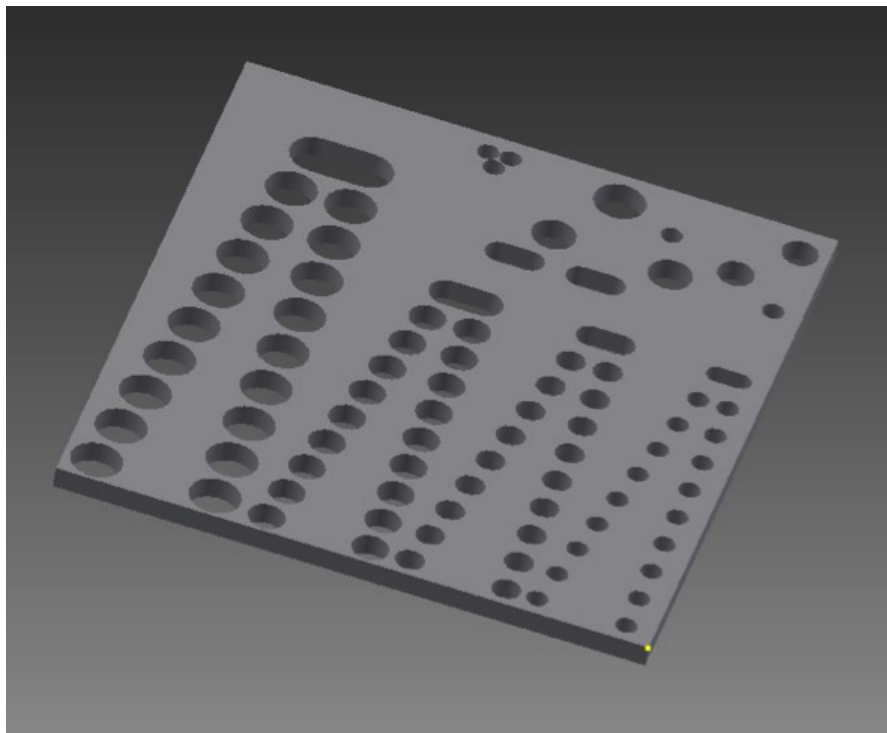
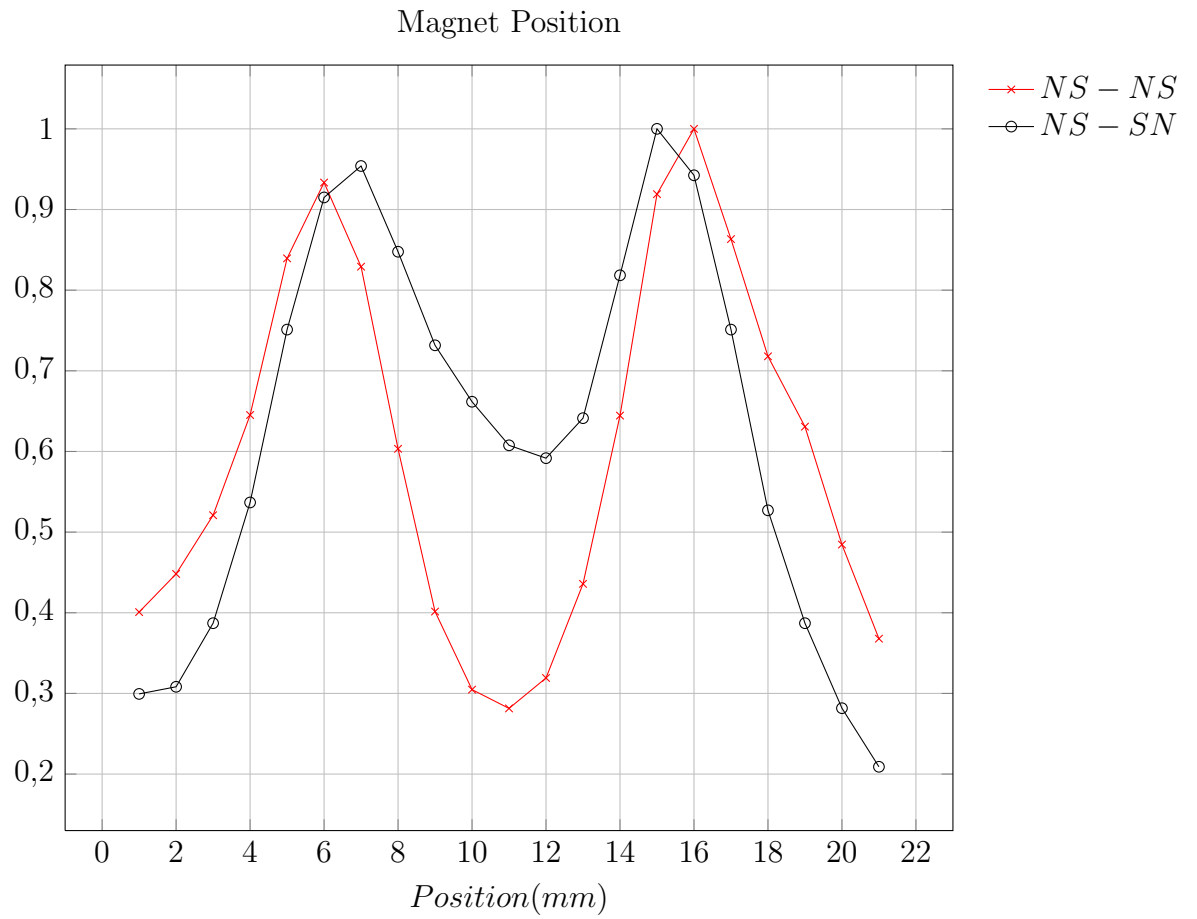


FIGURE 3.26: Tool for magnet's polarity test. It's shaped using a PMMA plate and cut by a laser-assisted machine.

Chapter 4

Assembly

IN the preceding chapters has been analyzed the workflow that developed the idea of the device. The idea of the tactile display is represented in picture below with the three main components: large displacement PDMS membrane, PMMA body with MR fluid filled in and the bottom acrylic base to close the device. Moreover it has been choose a neodymium magnet as element that changes the mechanical properties of the fluid. After that in order to move the magnet have been analyzed different solutions to put the magnet close or away of the display for stiffness variation. After the comparison of various actuators the voice coils reached the expectation of velocity for real time application and dimension to array them in series under the display.

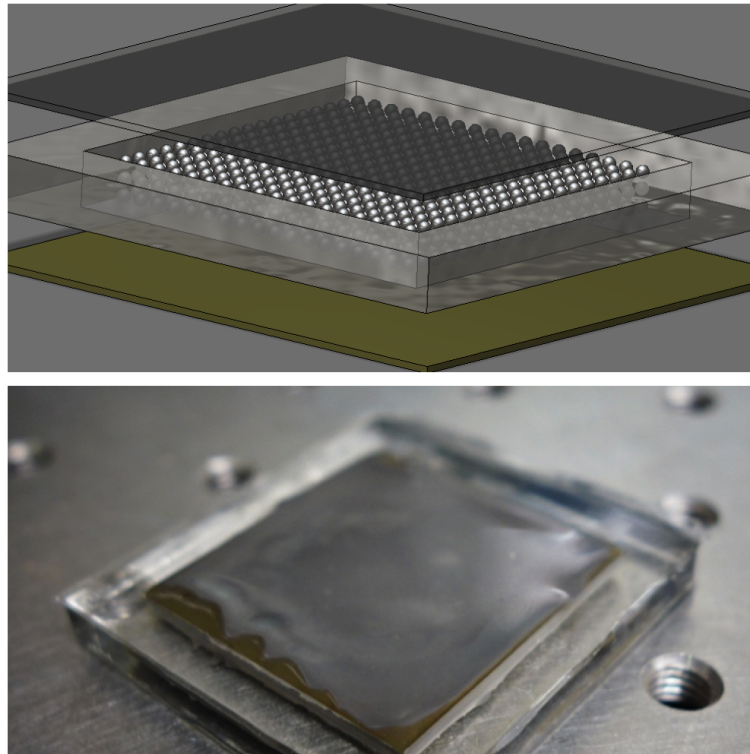


FIGURE 4.1: Tactile display.

Now that the display and actuator has been choose it's time to integrate them inside a system that allows tests on different devices with the same voice coil actuator. As shown below in figure 4.2:

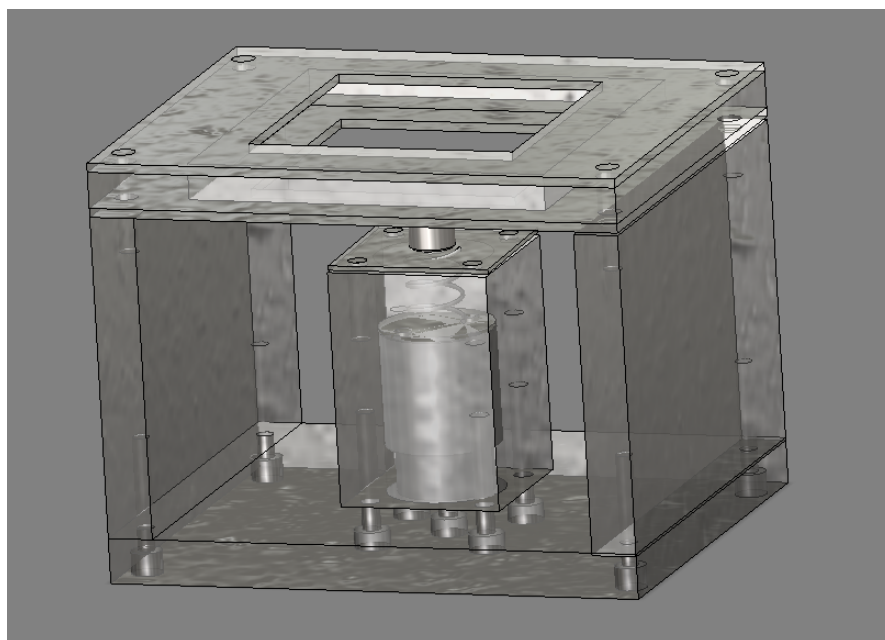


FIGURE 4.2: PMMA structure to test the tactile display.

The support for the display is realized with pieces of PMMA of different thicknesses, shaped with laser cut machine and assembled with screws. The structure is quite simple and easily repeatable. The top of the system is realized with three different pieces in order to “sandwich” the display of figure 4.1. Detailed structure is represented below (fig. 4.3).

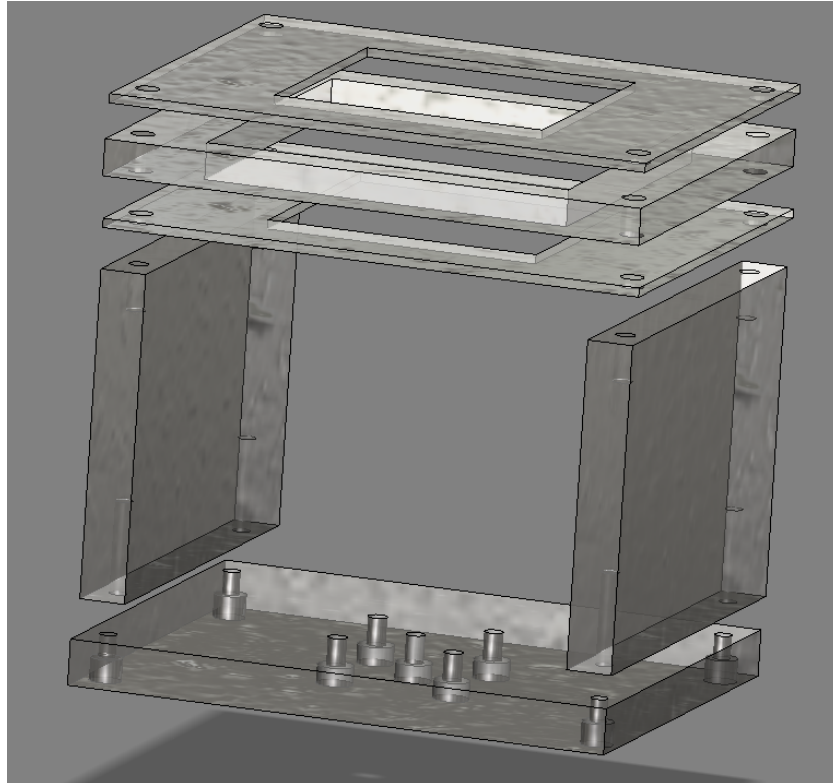


FIGURE 4.3: Extrusion of structure’s components.

The most challenging component is the container for the voice coil. As solution has been taken the idea of the cylinder of a motor. Shaping a unique piece of PMMA with a 3D miller machine the result is shown below:

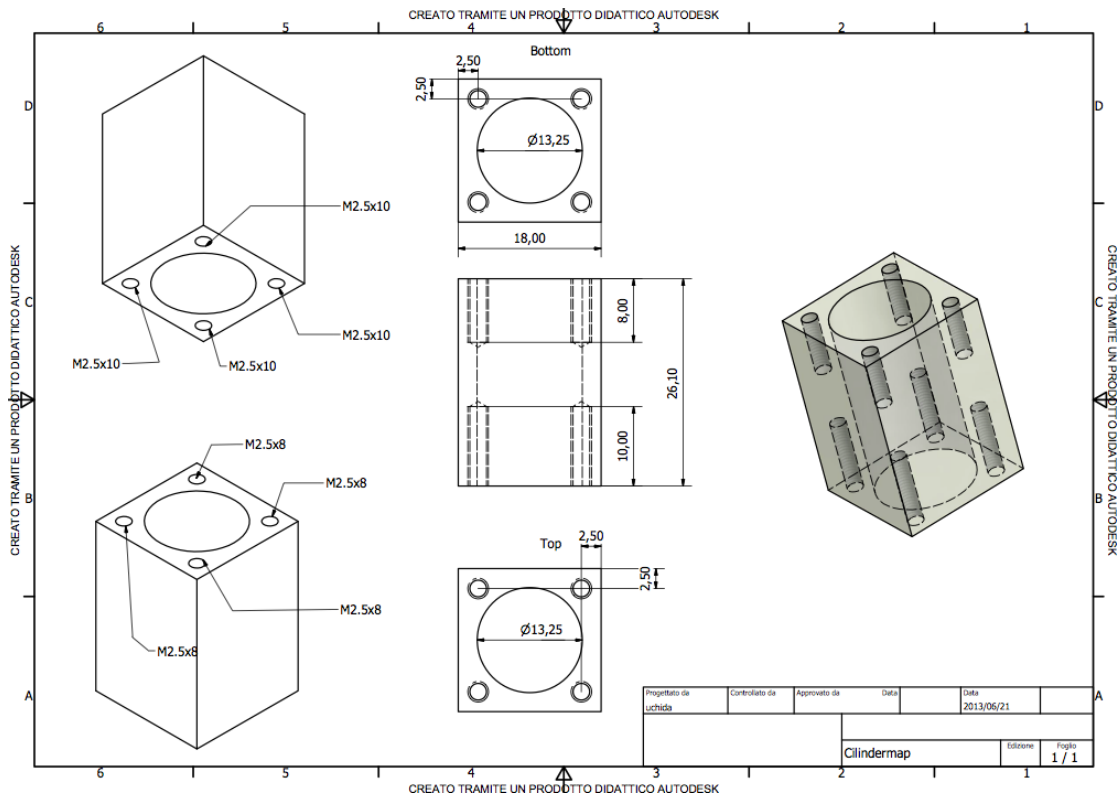


FIGURE 4.4: Technical sheet for the desing of the VCA's container. The shape recalls a motor cylinder.

More in detail on top of the cylinder has been created a stopper system since the two parts of the voice coil (in this case the magnetic part) are not tied each other. Moreover, on top of the voice coil through a disk shaped with the proper dimension and bonded with two small screws is used as support for the spring. The choice of the spring is necessary since as already mentioned above the two parts of the voice coil are independent. In fact, when the magnet is moved closer to the bottom plate also the iron particles' effect of the MR fluid gets stronger and calls the magnet attracting it. Is easily understandable that when a current is flowing through the coil the final effect on the magnet is like on-off button. In fact, due to the weight of the system there is a minimum current to move it up: when the current is progressively increased nothing is moving until the coil generates enough force to push the system up. The effect is impulsive and the magnet is pushed up to the bottom plate of the device losing the current controlled positioning system. For this reason a force that pushes back the neodymium magnet is necessary. In this sense the spring helps to better control relation between the current applied and the position of the magnet since it contrasts the attracting force of the iron particles when the magnet is moved closer to the bottom and eliminate the "big bang" effect of the voice coil. So when it's time for a precise positioning inside the

range of movement of the voice coil a spring becomes necessary¹. All the analysis above is necessary since has been chosen a simple voice coil actuator without a pre-incorporated feedback-controlled positioning system. Of course this kind of devices are on the market but quite expensive. Not represented in figure 4.5 there is a piston-like PMMA cylinder, laser-cut and glued to the disk support on top of the voice coil. This is the element that moves up and down, with reverse current, the magnet and passes through the hole created in the middle of the stopper.

¹In the present chapter has not been presented the long study that drove to the choice of the spring. The parameters necessary to define a spring are the dimension of the section, length, width and repulsive force generated at half compression: thus, the spring has to fit the cylinder and at half of its compression has to generate a proper repulsive force to compensate MR fluid's magnet attraction. The repulsive force is correlated with the section and is lowered by the length. Hence, the perfect trade off had to be found and not always the perfect spring is commercialized.

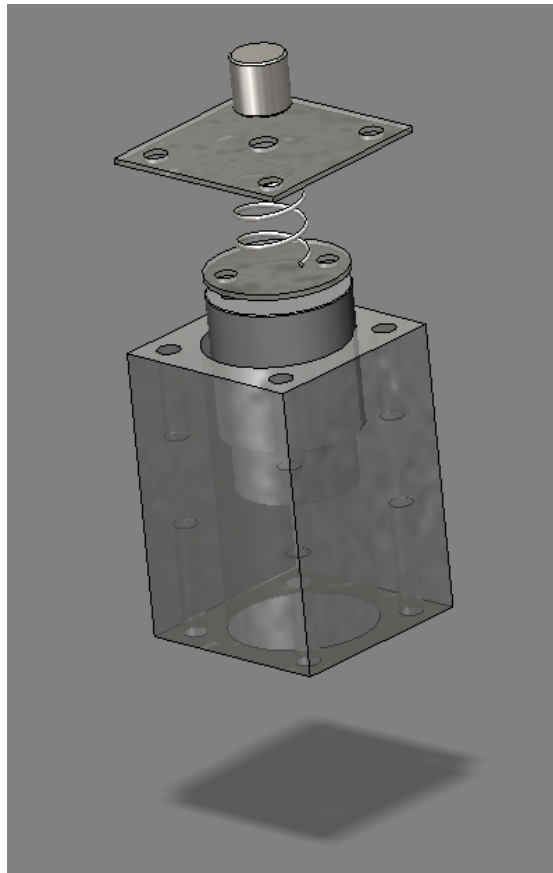


FIGURE 4.5: Detail of the VCA's container.

4.1 Control of the actuator

Even though for the spring the relation between the force applied and the compression is linear with k in the voice coil the magnet and the iron particles generate a non linear relation between the current flowing through the coil and the final position of the magnet, in other words the stroke of the voice coil. In fact is not possible to apply a current and linearly move for positioning the magnet under the display.

As first solution studied to solve this problem came the neural networks. With a supervised learning the nodes are trained to follow the non-linear relation: as input there is the current generated that flow in the coil and as output the final position intended as the distance between the magnet and the bottom plate of the tactile display. Using the appropriate toolbox in Matlab inserting the value obtained experimentally the network can be trained.

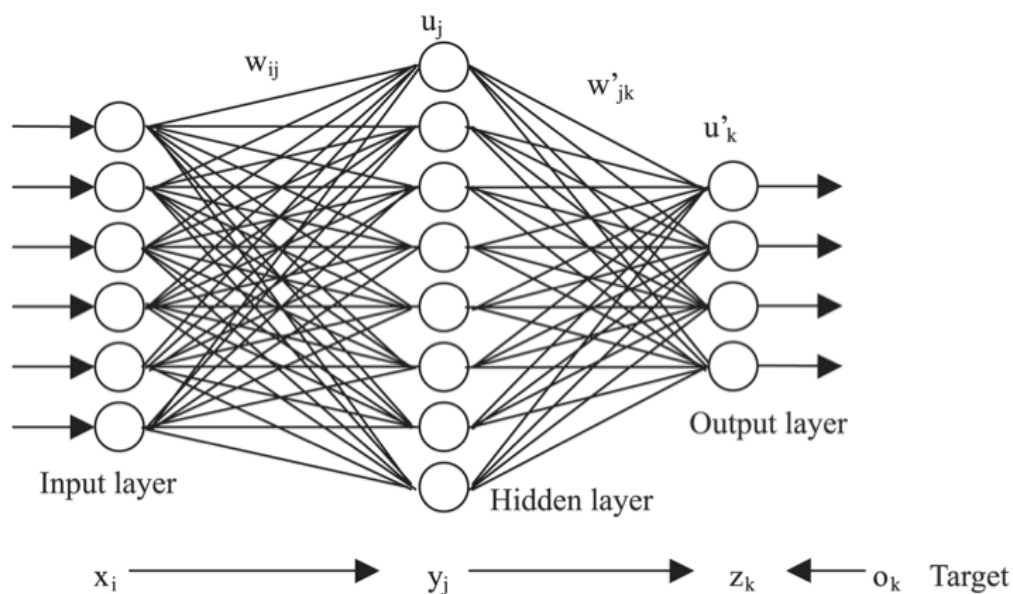


FIGURE 4.6: Basic structure of a neural network.

Another solution analyzed is with the principle of equivalent area (PEA) that drives the system with pulse width modulation (PWM). As reference has been analyzed [8] which fully explain the basic theory of PCA and proposes new solution of different orders and complexity.

PWM has been widely used in control systems and when the frequency of pulses can be chosen to be very high compared with the bandwidth of the system to be controlled, according to the PEA, two continuous-time signals are considered equivalent if the areas under these signals are identical during a certain time interval (fig. 4.7). When applied to the system with the same dynamics, PEA-equivalent signals will produce, at the end of each time period, the output signals whose values are different with an error of the second order of this period.

From this relation:

$$\int_{kT}^{kT+T} u(t)dt = u_p\sigma$$

where $u(t)$ is the servo signal, u_p is the pulse-amplitude, and σ is the pulse-width. The PWM signal that exactly satisfies the PEA cannot be generated on-line thus the pulse-width σ is determined such that the integral in the left-hand side of the equation is approximated by V_a and the digital PEA is given by:

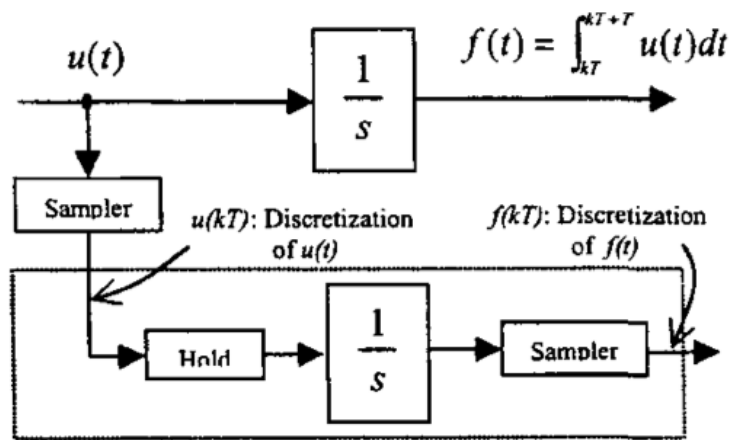
$$V_a = u_p\sigma$$

where

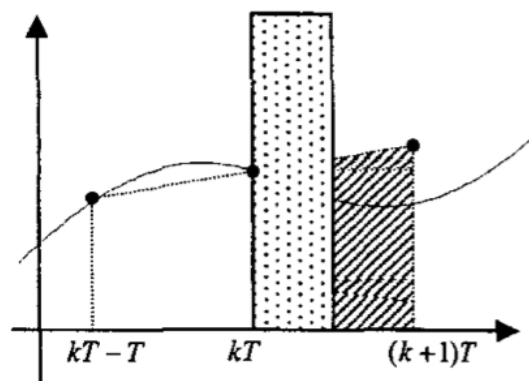
$$\int_{kT}^{kT+T} u(t)dt \approx V_a$$

This V_a must be calculated on-line for the pulse-width determination.

As example the easiest form of PCA is described. The first method corresponds to the use of the zero-order-hold and requires only one sample at the present time $t = kT$ and assumes that this value holds until the next sample instant $t = (k+1)T$. The product of this sampled value and the period T is the projected area V_a , in the next pulse period and this value is used to determine the pulse-width (fig. 4.8).



(a) The concept of the analog and digital [8].



(b) An example of PEA-equivalent signals [8].

FIGURE 4.7: PCA's basic concept.

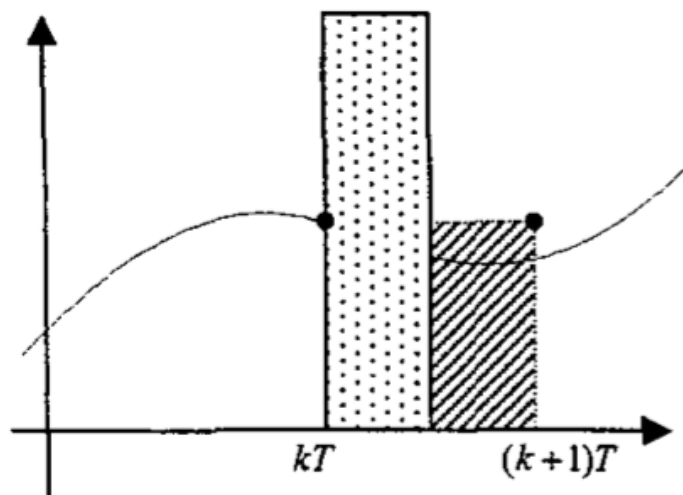


FIGURE 4.8: First PCA's method [8].

It can be used the value sampled at the past time instant $t = (k-1)T$, in addition to the one at the present time (fig. 4.9) or even three samples at $(k-1)T$, $(k-\frac{1}{2})T$ and kT (fig. 4.10).

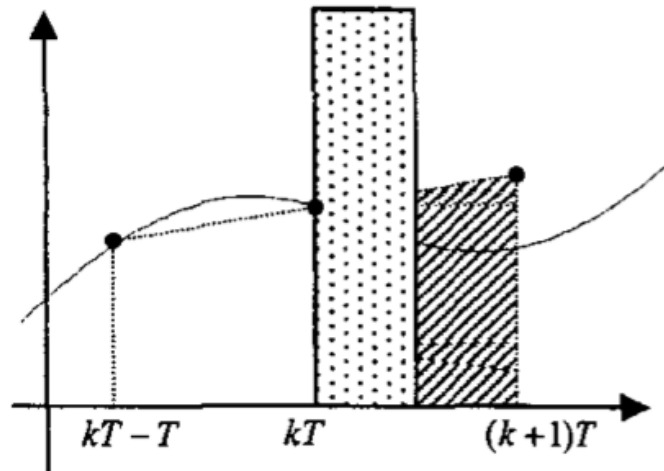


FIGURE 4.9: Second PCA's method [8].

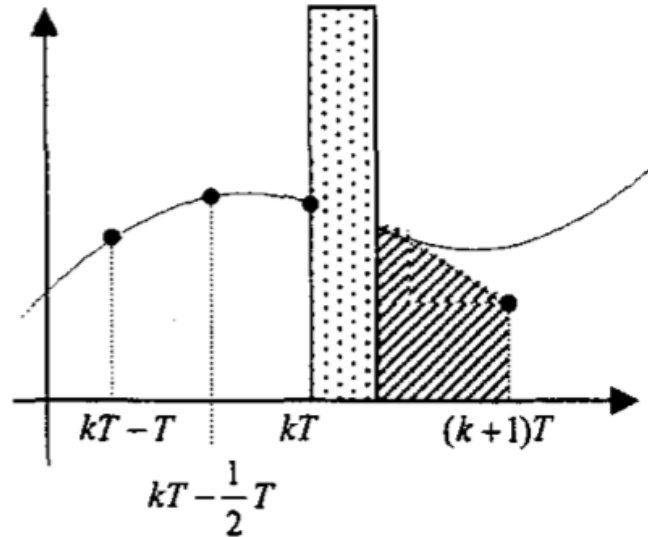


FIGURE 4.10: Third PCA's method [8].

Both neural network method and PCA can be implemented on Arduino™ board. On the other hand Arduino™ is not able to produce a current higher than 15 mA per pin. Thus, is necessary an electronic driver transforming low power signal into an appropriate level to drive the actuator. Between a wide variety of solutions offered by the market a good solution has been found in a dual full bridge drivers that from 15 mA can generate enough current (up to 1.2A peak value) to fulfill the requirements of moving the voice coil.

Dual bridge because when the magnet is touching the bottom plate of the display the iron particles as already mentioned generate a force that keep the magnet there. Hence, it has to be generated an opposite force that calls the magnet back, since simply turning off the current inside the coil doesn't change anything. The situation is similar to a stepping motor. Dual bridge is necessary since while turning a motor on and off requires only one switch (or transistor) controlling the direction is deceptively difficult. It requires no fewer than four switches (or transistors) arranged in a clever way. These four switches (or transistors) are arranged in a shape that resembles an *H* and thus called an H-Bridge. Each side of the motor has two transistors; one is responsible for pushing that side HIGH the other for pulling it LOW. The advantage of this technique is that there is no need of training and the implementation is really simple, allowing to easily controlling non-linear system since the control signal is converted in PWM.

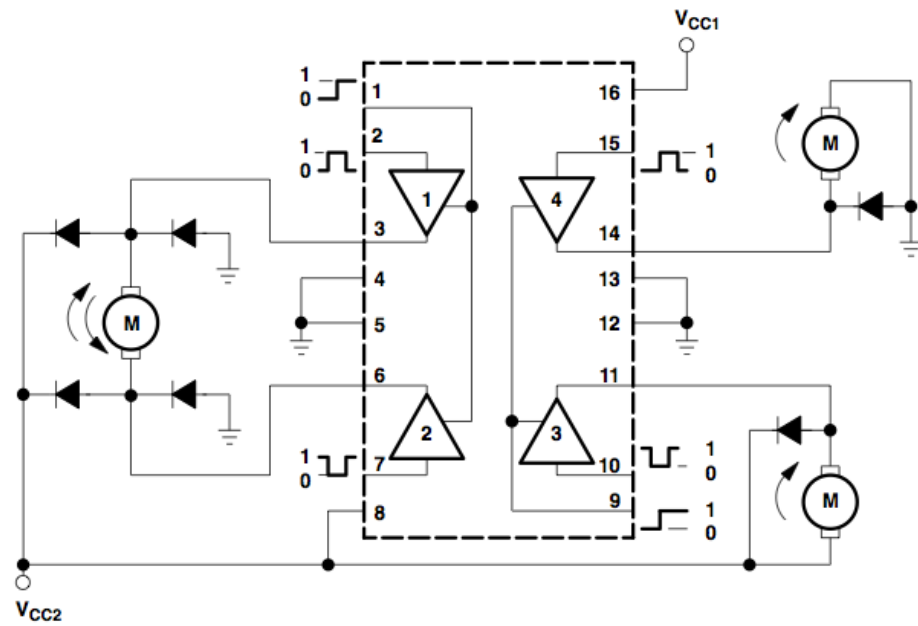


FIGURE 4.11: Internal schematic of L293D

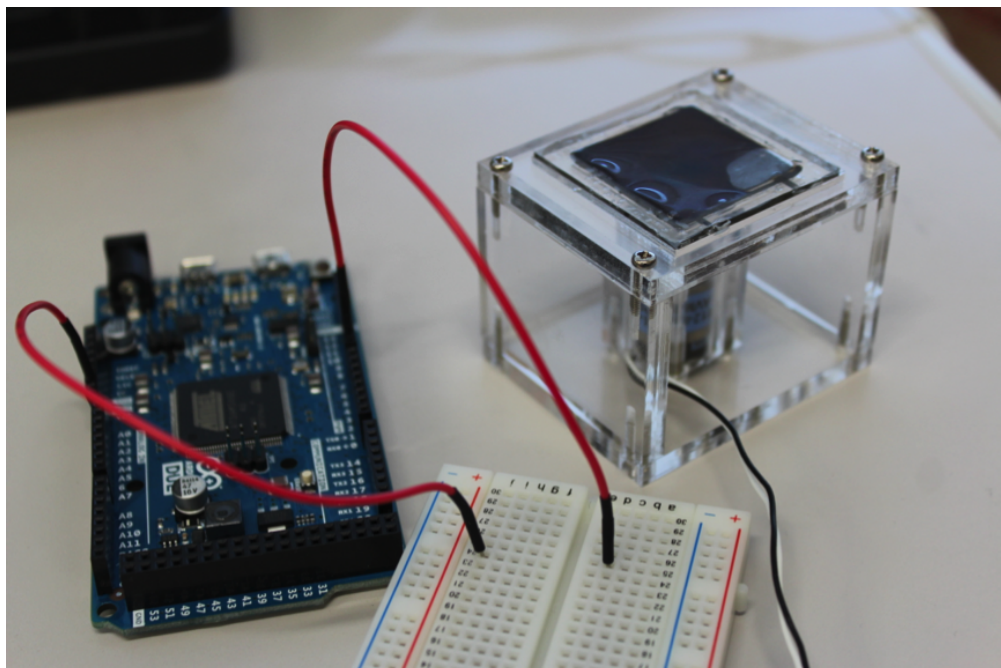


FIGURE 4.12: Picture shows final device assembled and connected to the Arduino board.



FIGURE 4.13: Tools for measurements.

4.2 Tools for measurements

To measure the value of the magnetic field it has been used a teslameter, which is a practical handy type Gaussmeter having a digital display and precise until 0.1 mT (fig. 4.13 (a)). On the tip of the small probe there is a sensor and simply getting closer to the source of the magnetic flux the value is displayed on the digital screen. The main measuring machine is the strain gauge as shown in figure (fig. 4.13 (b)). The testing machines can control and measure displacement and test forces on micro samples in the several μm or several mN micro regions and that can evaluate strength to high precision. A high-precision linear sensor ensures high displacement measurement precision (displacement display resolution of 0.02 μm and displacement measurement precision of $\pm 0.2 \mu m$ up to 5 mm displacement). The range of load cells is from 0.5 N to 2 kN assures a testing force measurement precision of $\pm 1\%$ from a minimum load of 2 mN. The machine is controlled via PC using the Trapezium2™ software: it allows visual operating environment, ultra-high speed sampling, navigation function and net upload function.

The native end effector of the strain machine has been substituted by a cylinder-like PMMA piece with a smaller area² for a more precise testing of the stiffness. It's easily understandable that knowing the area that provide the pressure on the tactile device, the module of the force feedback generated by the device and the strain is possible to calculate the Young's Modulus, also known as the Tensile Modulus or elastic modulus, which is a measure of the stiffness of an elastic material and is a quantity used to characterize materials. Young's Modulus is the ratio of tensile or compressive stress to corresponding strain below the proportional limit.

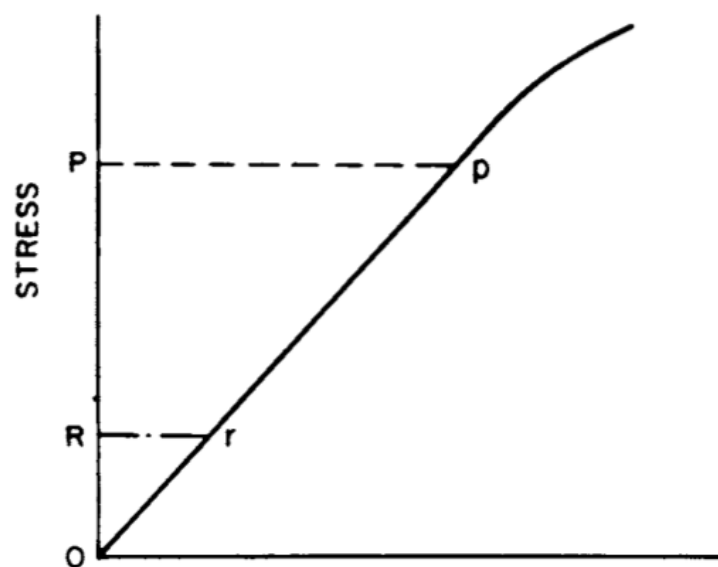


FIGURE 4.14: Young's Modulus between stress P, below proportional limit and R or preload.

If a plot of load-versus-extension (force versus elongation) is obtained by means of an autographic recorder (fig. 4.13 (b)), the value for Young's modulus is obtained by determining the slope of the line for forces less than the force corresponding to the proportional limit. Choice of the lower force point depends on the limitations set³ and in any case for most loading systems and test specimens, effects of backlash, specimen curvature, initial grip alignment, etc., introduce significant errors in the extensometer output when applying a small force to the tested specimen.

²Cylinder's base is $4,66\text{mm}^2$

³In this case is the point where the response is no more generated by the membrane and by the MR fluid but only by iron particles.

Measurements shall therefore be made from a small force or preload, known to be high enough to minimize these effects. Young's modulus is thus calculated from the force increment and corresponding extension increment, between two points on the line as far apart as possible, by use of the following equation:

$$E = \left(\frac{\Delta_p}{A_o} \right) / \left(\frac{\Delta_c}{L_o} \right)$$

Where Δ_p is the force increment, A_o is the cross-sectional area, Δ_c is the extension increment and L_o is the original gage length.

In addition it has been used a stepper for a precise positioning of the magnet at the proper distance from the bottom acrylic plate (fig. 4.15) and then measured the relation between the distance and the magnetic flux intensity.

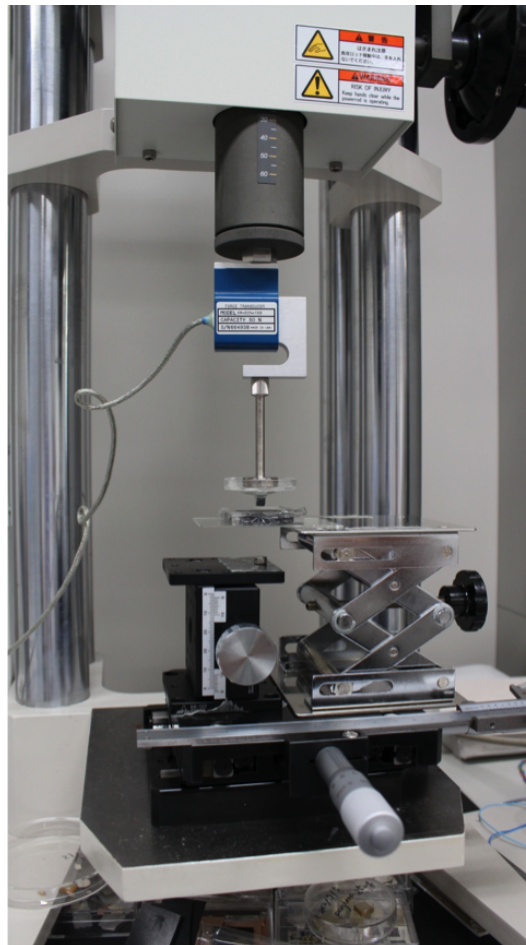


FIGURE 4.15: Experimental setup for measuring the relation between magnetic flux and stiffness.

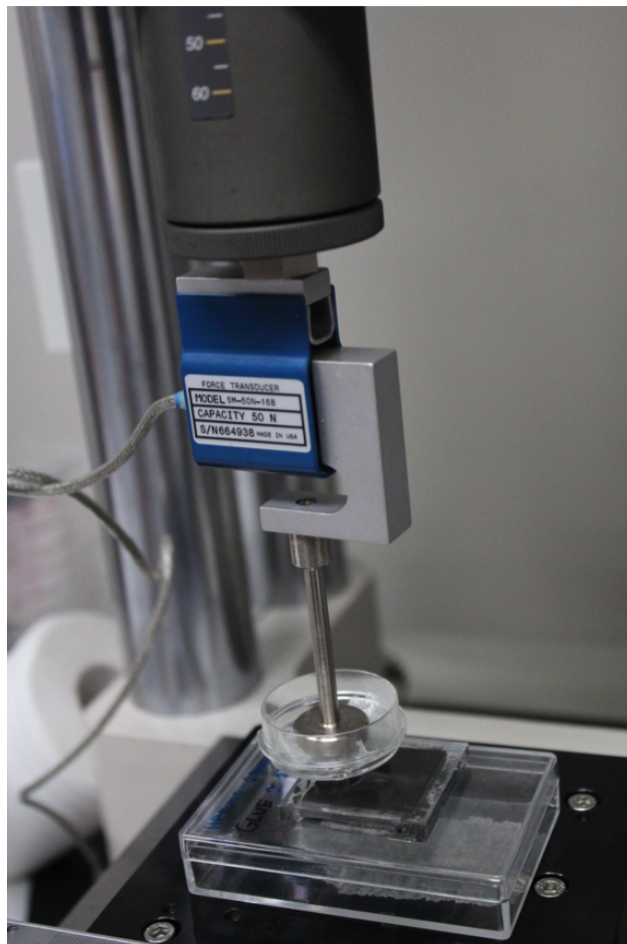


FIGURE 4.16: Detail of the loading cell, tactile display and strain machine.

Chapter 5

Experimental results

THIS chapter is focused on the graphs of the experimental results where are presented and analyzed.

As already presented the following first graph represents the relation between the distance and the magnetic field generated by the neodymium magnets. Once more it has to be underline the capability to generate high field intensity with small magnets, impossible to achieve with a simple solenoids with a current flowing in it. With the probe of the teslameter bonded to a PMMA support designed for the test (fig. 5.4), the magnet is moved precisely with 1 mm step towards to the probe. The values take into account the thickness of the bottom acrylic plate hence the module of the magnetic field is the one that is sensed by the iron particle inside the chamber.

Later on, using the experimental setup depicted in figure 5.2 moving the positioning stepper 1 mm each step and measuring the stiffness generated in the point above the magnet, it's possible to write down the relation between the distance of the magnet from the bottom acrylic plate and the stiffness simply calculated as a ratio between the repulsive force generated by the display and the active area of the cylinder that pushes on the membrane (4.66mm^2). It has been used an acrylic base structure of 4 mm with 0.5 mm bottom PMMA plate, a PDMS membrane obtained with a spin coating speed of 1000-RPM. The stroke of the machine is 3 mm with a preload of 0.1N for the reasons mentioned in chapter 4.

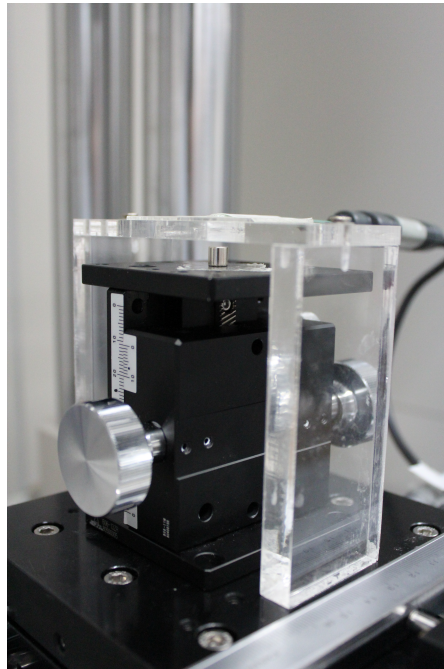
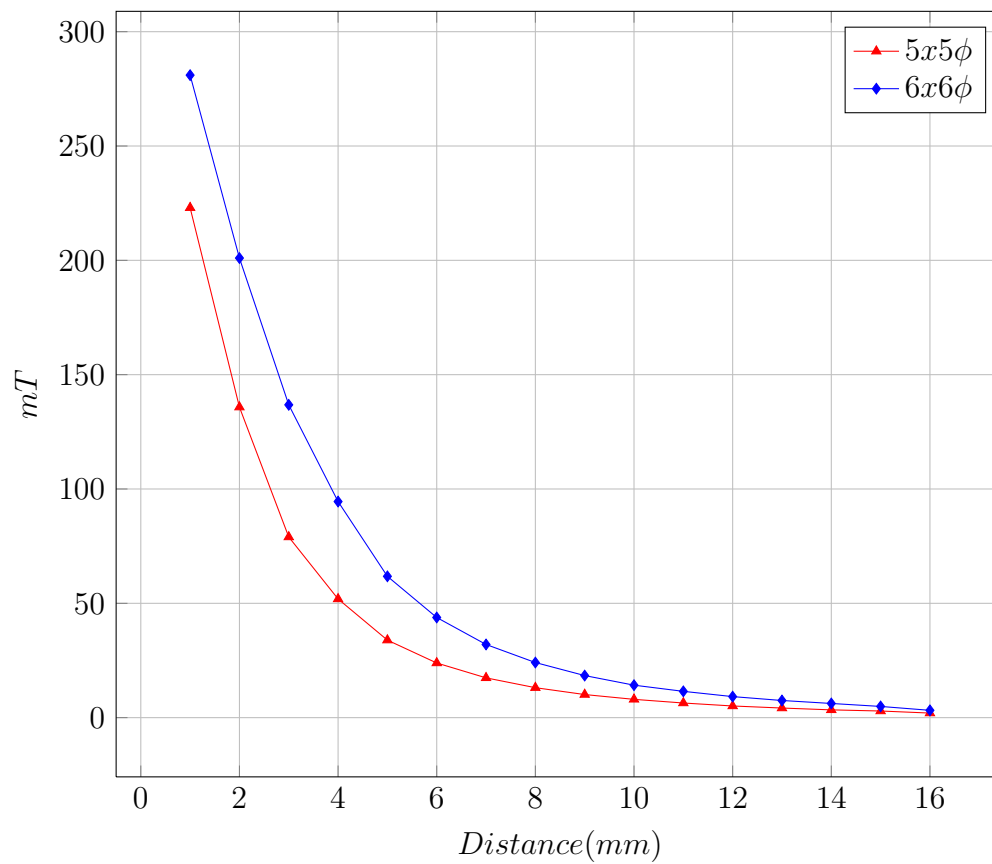


FIGURE 5.1: Experimental setup for measuring the relation between magnetic flux intensity and distance from bottom acrylic plate.

Magnetic Field Intensity of Neodymium Magnets



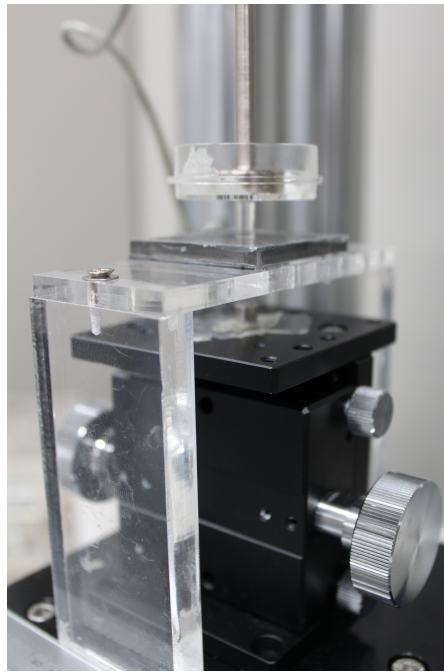
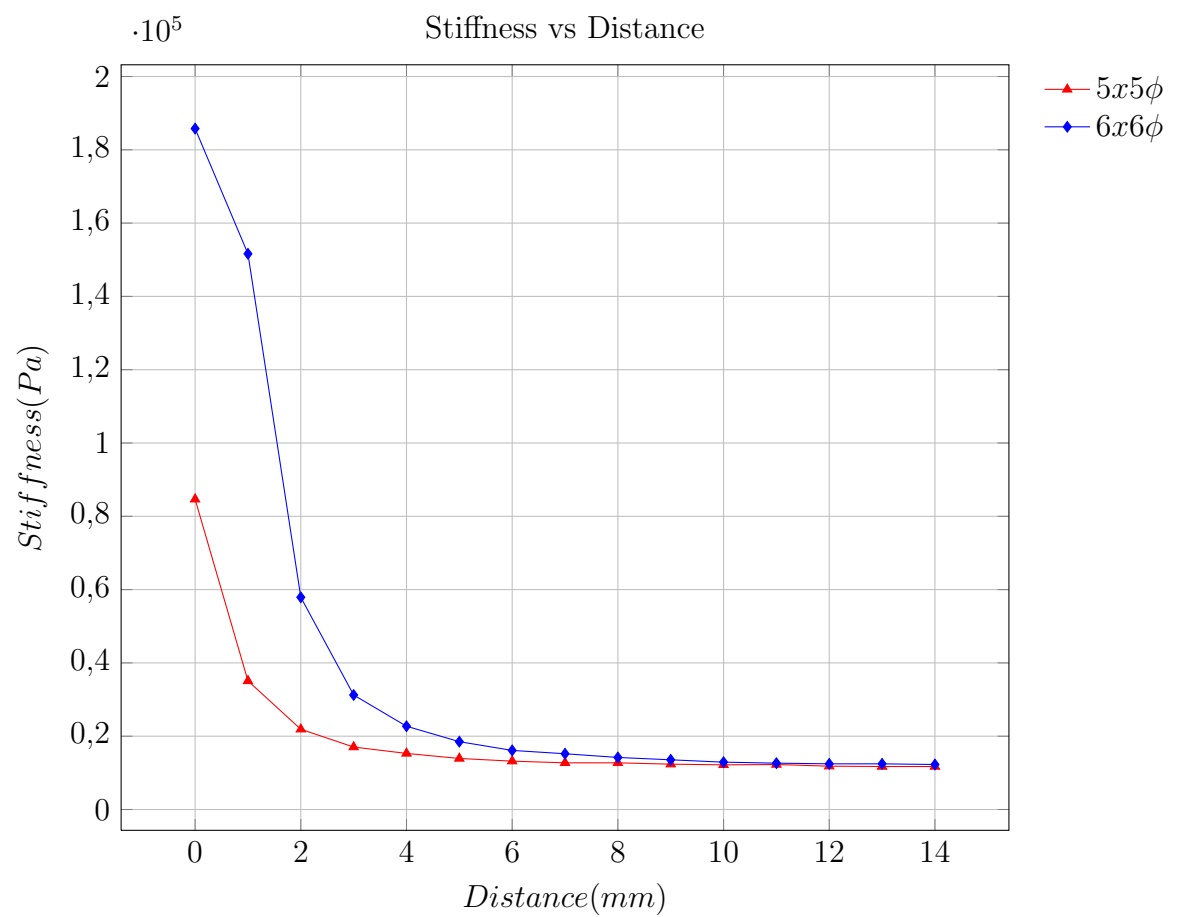


FIGURE 5.2: Experimental setup for measuring the relation between stiffness and distance from bottom acrylic plate.



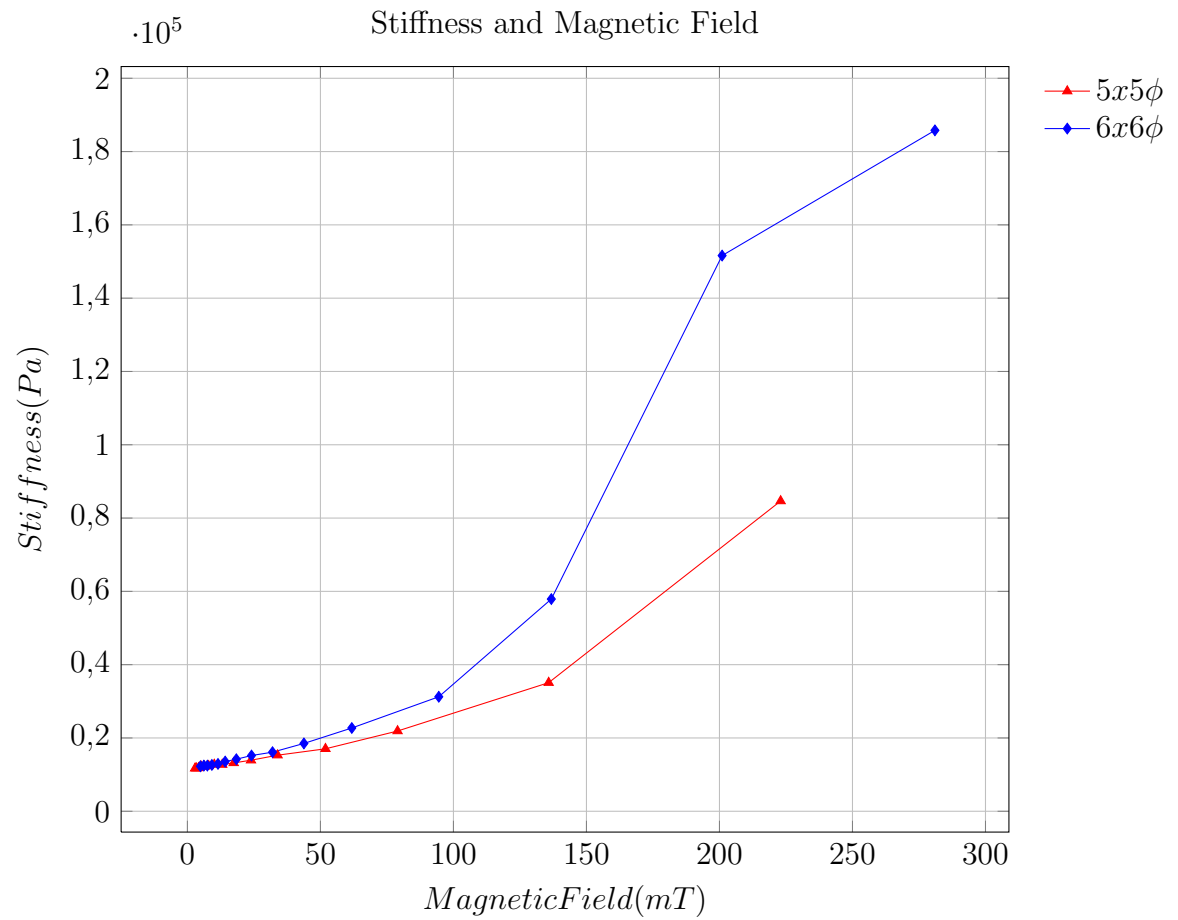


FIGURE 5.3: The figure represents the relation between the stiffness and the correspondent magnetic flux intensity. The graph is obtained as combination of the two previous ones.

The speed of testing shall be low enough to avoid creating unwanted effect for an accurate determination of the stiffness, yet shall be high enough to speed up the testing phase. In order to study such effect for a prefixed spot on the display and for the same stroke has been calculated the standard deviation of the measured force. As shown in the graph the speed doesn't affect the value of the force displayed, thus for the following testes has been always used the maximum speed of the machine.

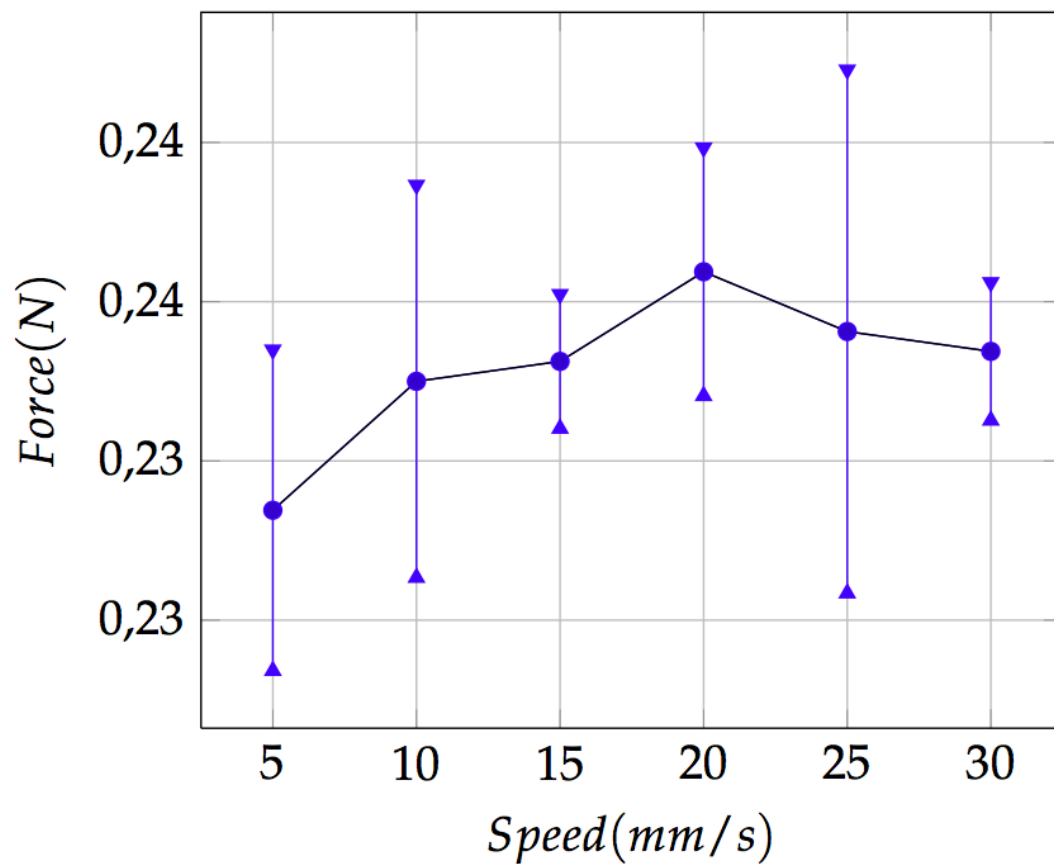
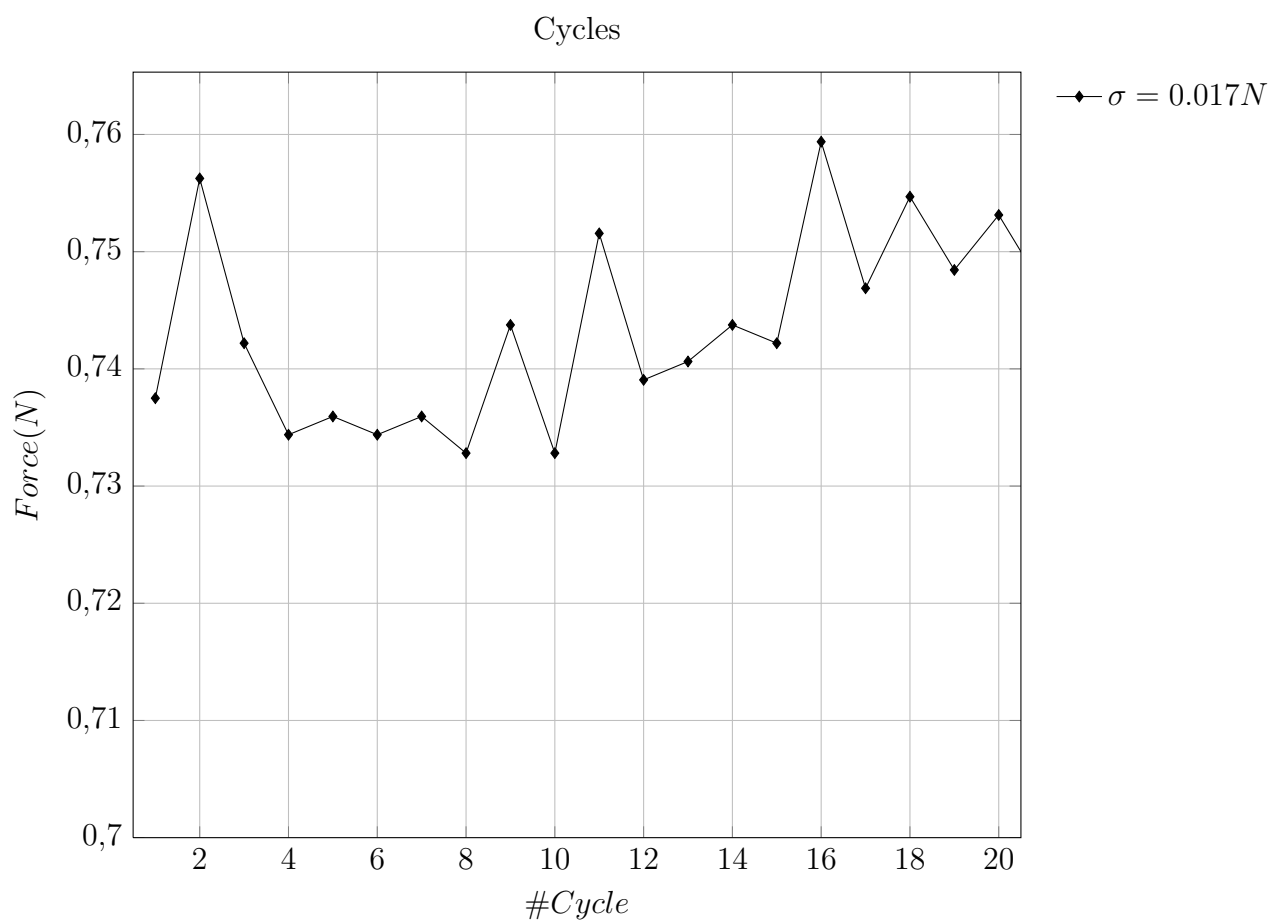


FIGURE 5.4: Speed test.

To simulate the value's stability of stiffness displayed by the MR fluid a cycle test has been conducted. Applying the same force cyclically in the same spot has been analyzed the standard deviation of the value displayed. As demonstrated by the graph the human touch cannot distinguish the variation in the repulsive force caused by the repositioning of the iron particles after they are compressed by human finger.



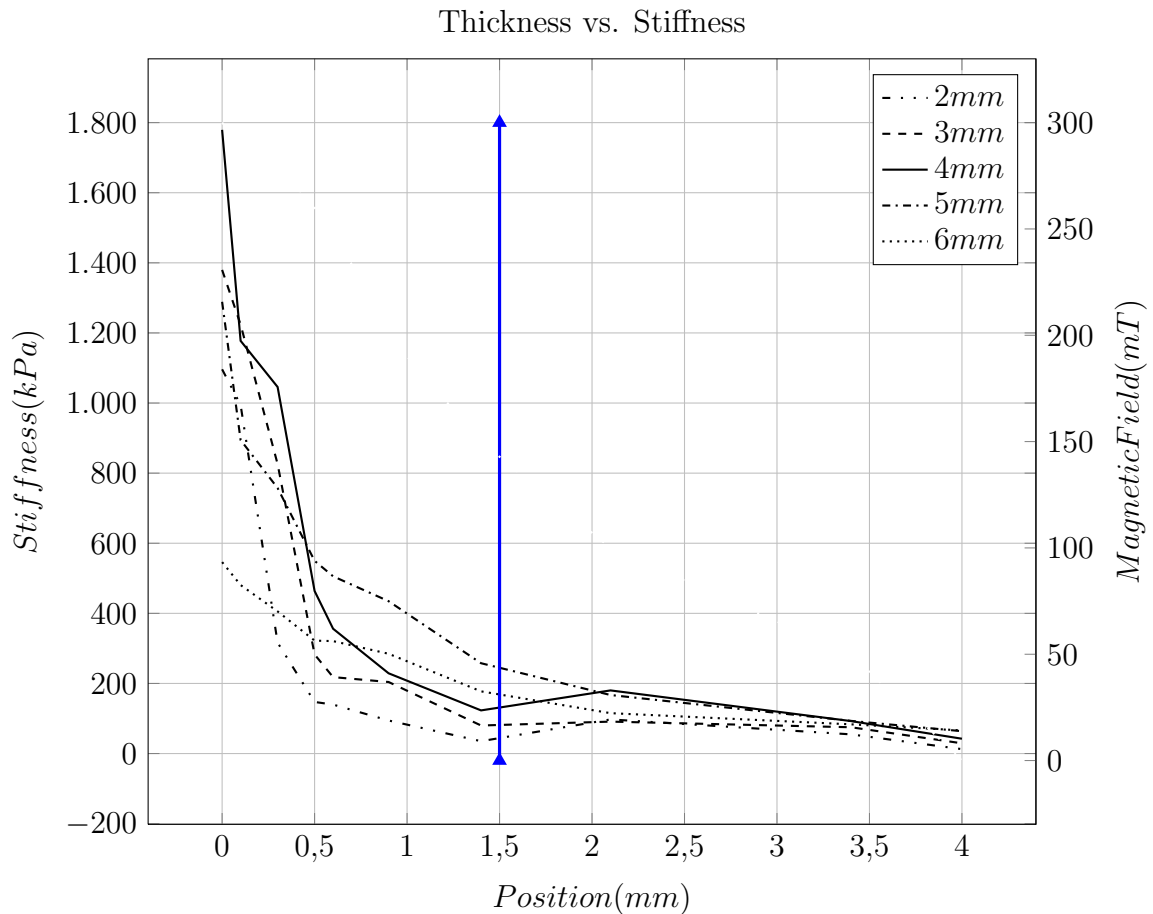
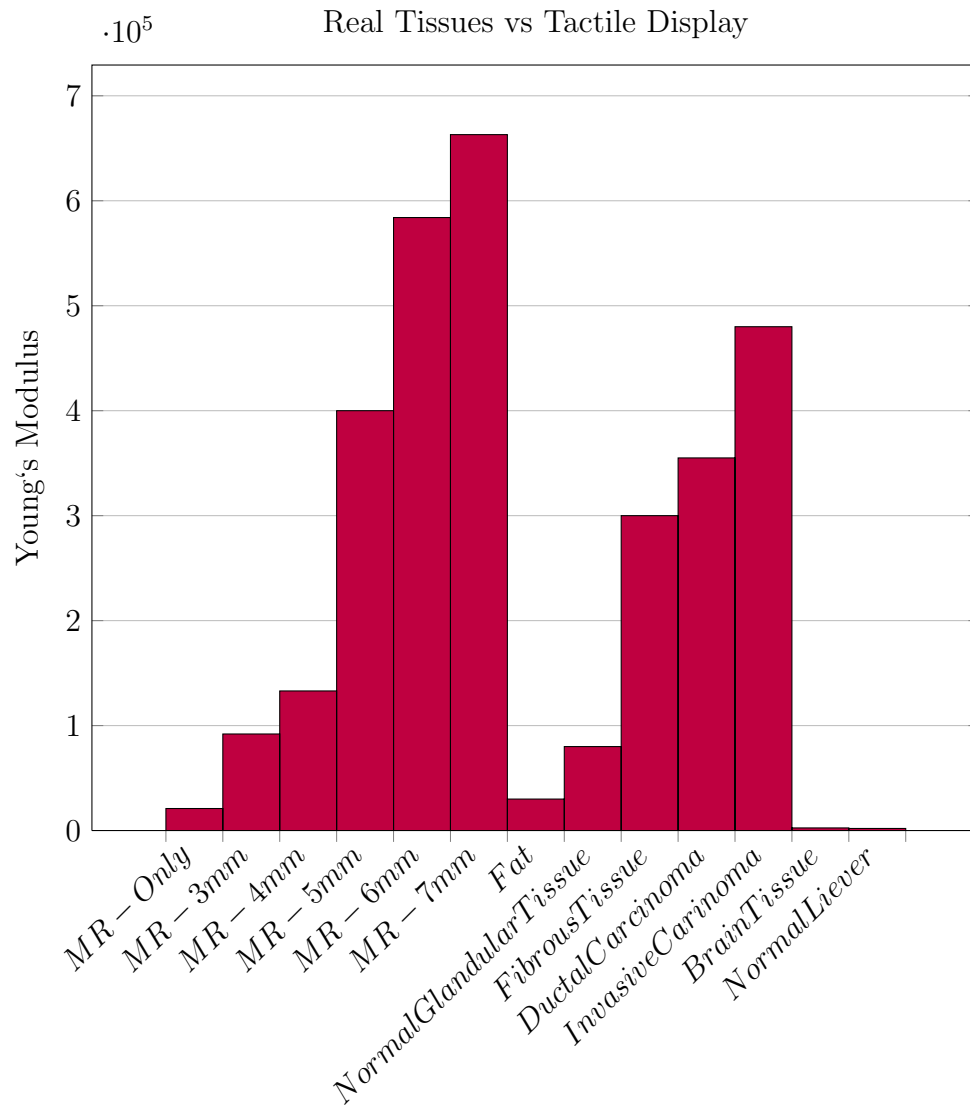


FIGURE 5.5: Plot stiffness versus magnet distance: the highest stiffness is generated by the 4 mm acrylic plate.

To choose the thickness of the acrylic base structure has been followed this procedure. The stiffness reached by the device is not proportional to the quantity of MR fluid used: the distance attenuates the magnetic field and the iron particles as well, hence should be found the right trade off between the thickness of PMMA case and the stiffness module to be reached. In this experiment are evaluated various thicknesses that the display can have. The protocol provides, for a chosen magnet, a preload of 0.1 N and a stoke of 80% of the total thickness of the acrylic plate for different position of the magnet ranging from 4 mm distance up to when the magnet's top surface reaches the bottom acrylic plate. The blue line defines the limit before which the stiffness displayed is not due to the magnetorehological properties of the fluid but is a result of the mechanical behaviour of the membrane and glycerin: to overcome this phenomena a preload of 0.1 N is applied.



Now that the thickness of the acrylic plate has been chosen it's time to select the dimension of the magnet. The desired dimension of the spot is 5 mm in diameter but to make the proper choice different information should be gathered. In fact the magnet has to generate both the spot and enough stiffness as well. The stiffness, equivalently the Young's module, should be comparable to the one of the real tissues. To have an idea of the module has been looked up in the literature different values of Young's Module of tissues or human body parts [40–43]. All the information are summarized in the following graph and compared with the Young's Module reached with different magnet's dimension¹

¹All the magnet have the same diameter and height: $D \times H$ with $D = H$.

One chosen the speed of 30 mm/s of compression, the PDMS membrane of 1000-RPM and 4 mm thick structure has been analyzed the spatial distribution of the repulsive force generated by different magnets. The test has been repeated 5 times to prove the repeatability of the display and each magnet's resulting spatial resolution compared. The procedure has been the following: with 0.1 N of preload have been measured all the points along the longitudinal axis of the display at steps of 1 mm as shown in figure 5.6.

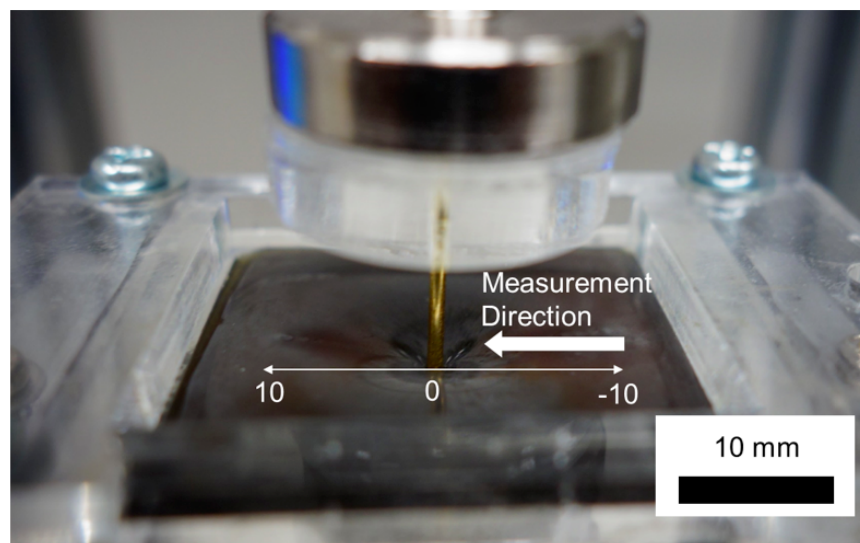


FIGURE 5.6: Measurement position and direction.

The repulsive force generated, hence the Young's Module, is proportional to the dimension of the magnet since the magnetic flux intensity is growing with the dimension of the magnet's surface but also the FWHM is increasing as well. Full width at half maximum (FWHM) is an expression of the extent of a function, given by the difference between the two extreme values of the independent variable at which the dependent variable is equal to half of its maximum value. An increment of this value causes a loss of spatial resolution to the system since the gaussian generated is larger. The following graphs refer to this phenomenon and the are summarized in figure 5.12.

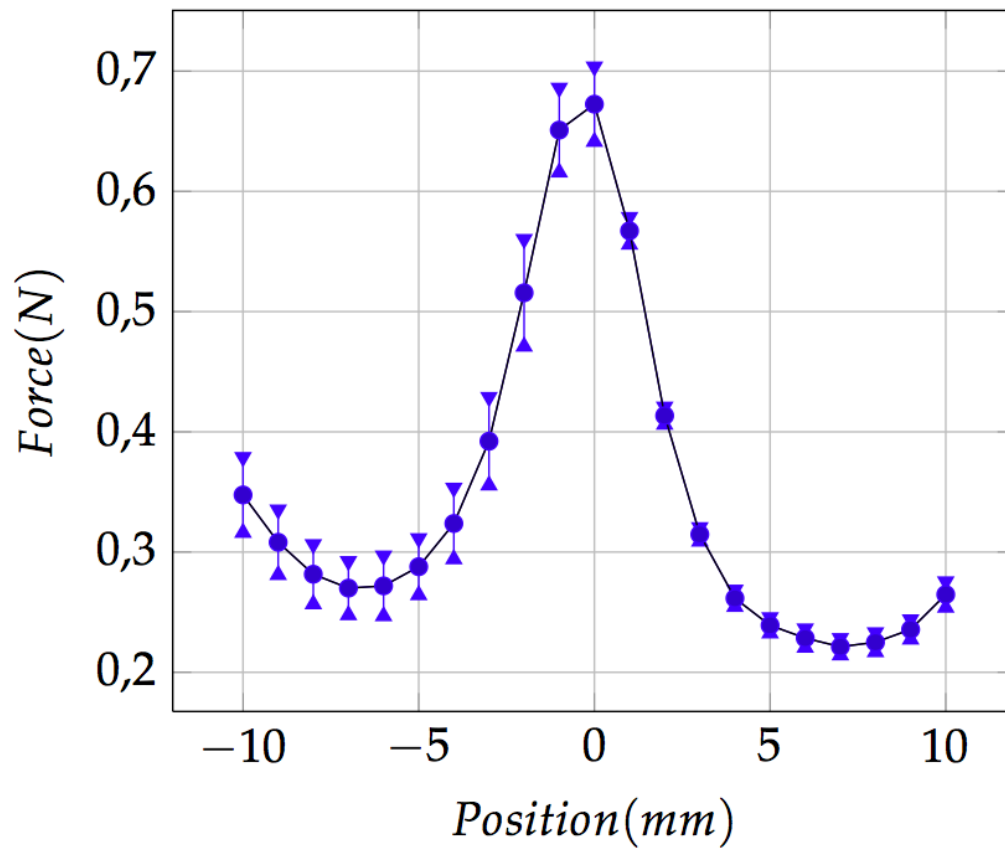


FIGURE 5.7: 3x3 mm diameter force's distribution.

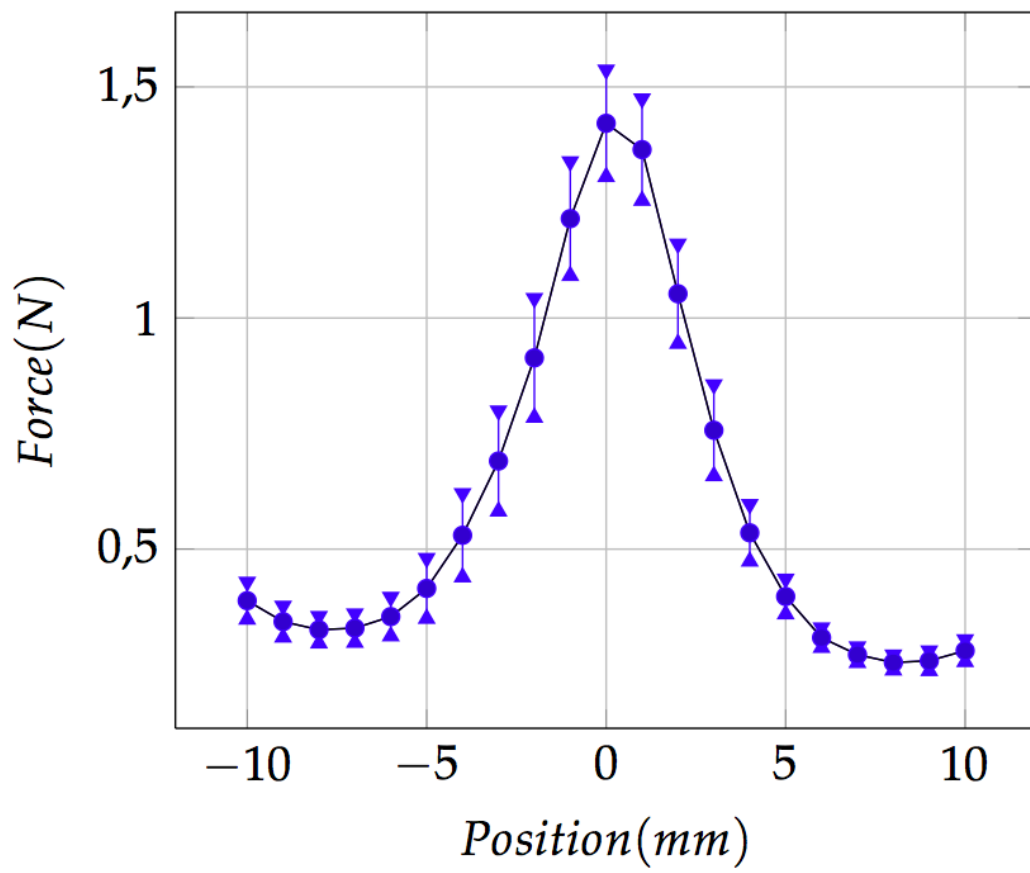


FIGURE 5.8: 4x4 mm diameter force's distribution.

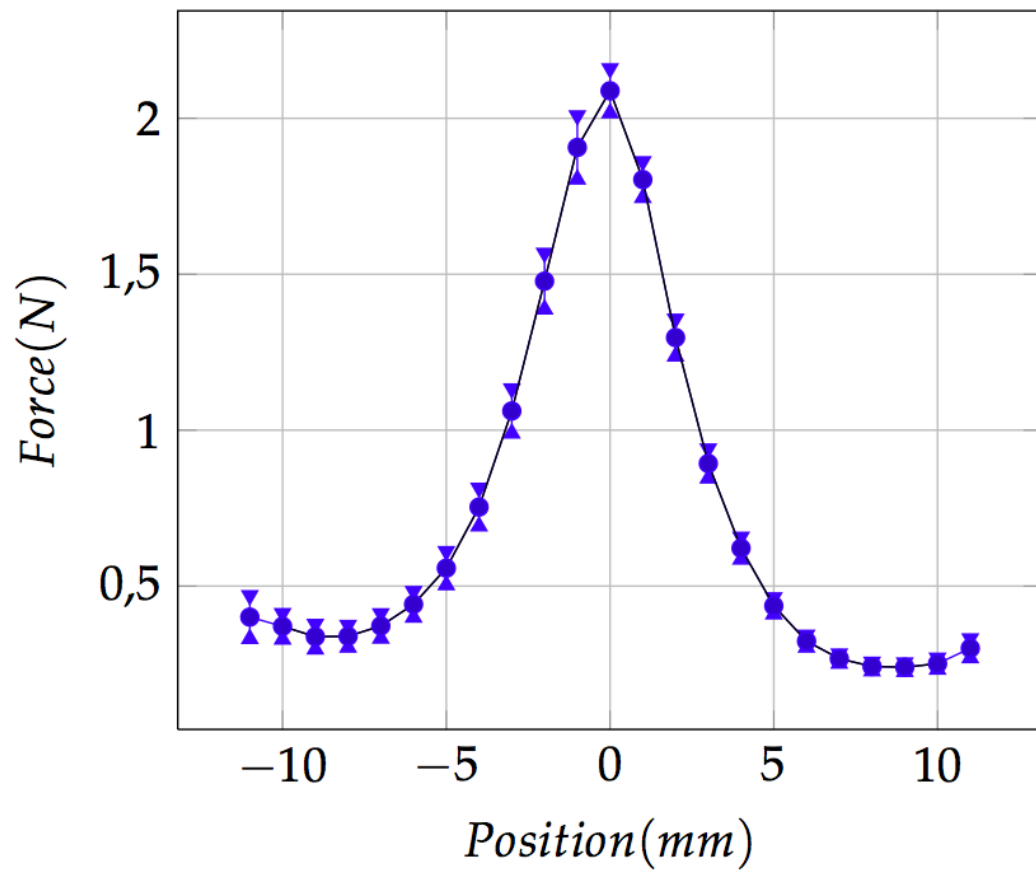


FIGURE 5.9: 5x5 mm diameter force's distribution.

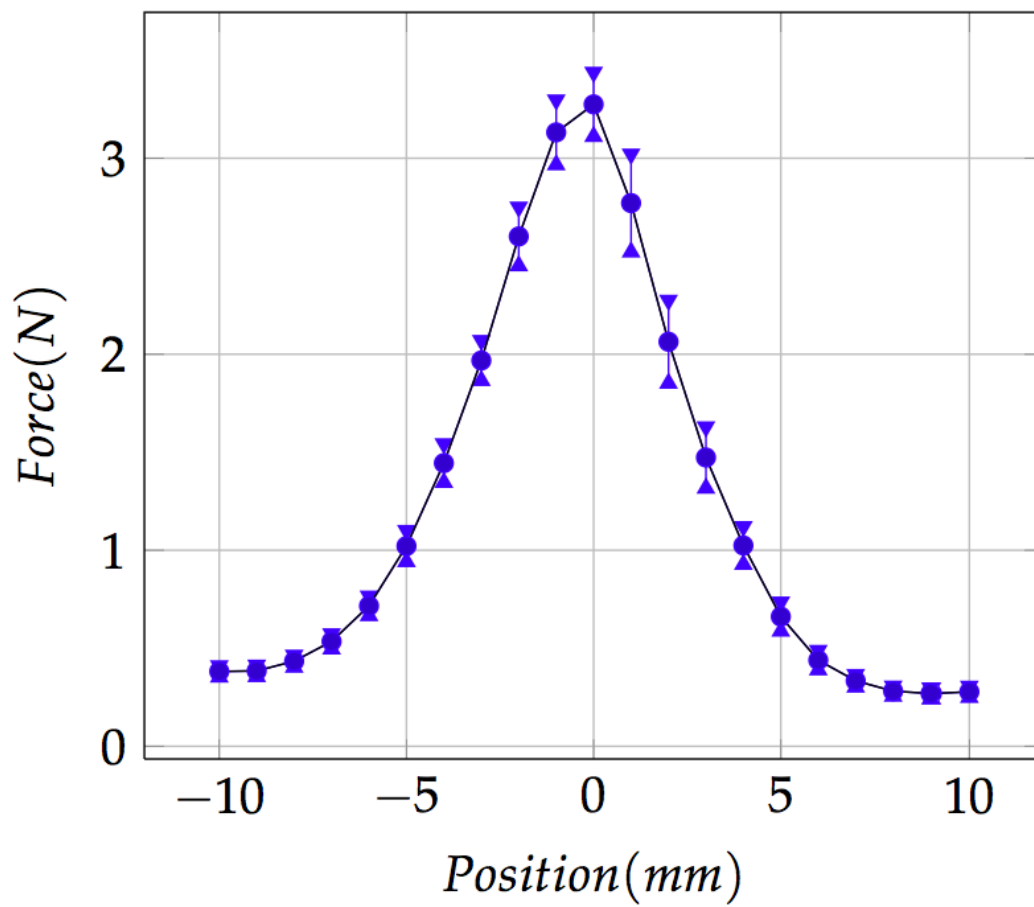


FIGURE 5.10: 6x6 mm diameter force's distribution.

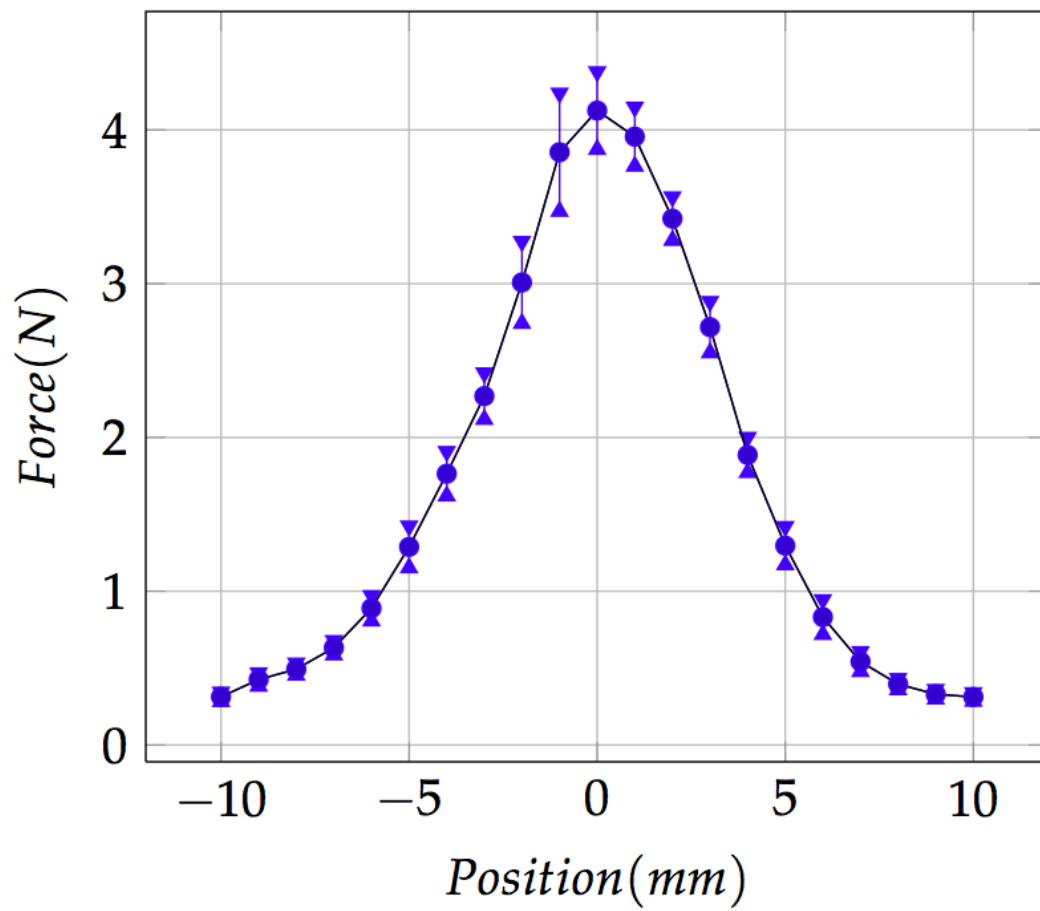


FIGURE 5.11: 7x7 mm diameter force's distribution.

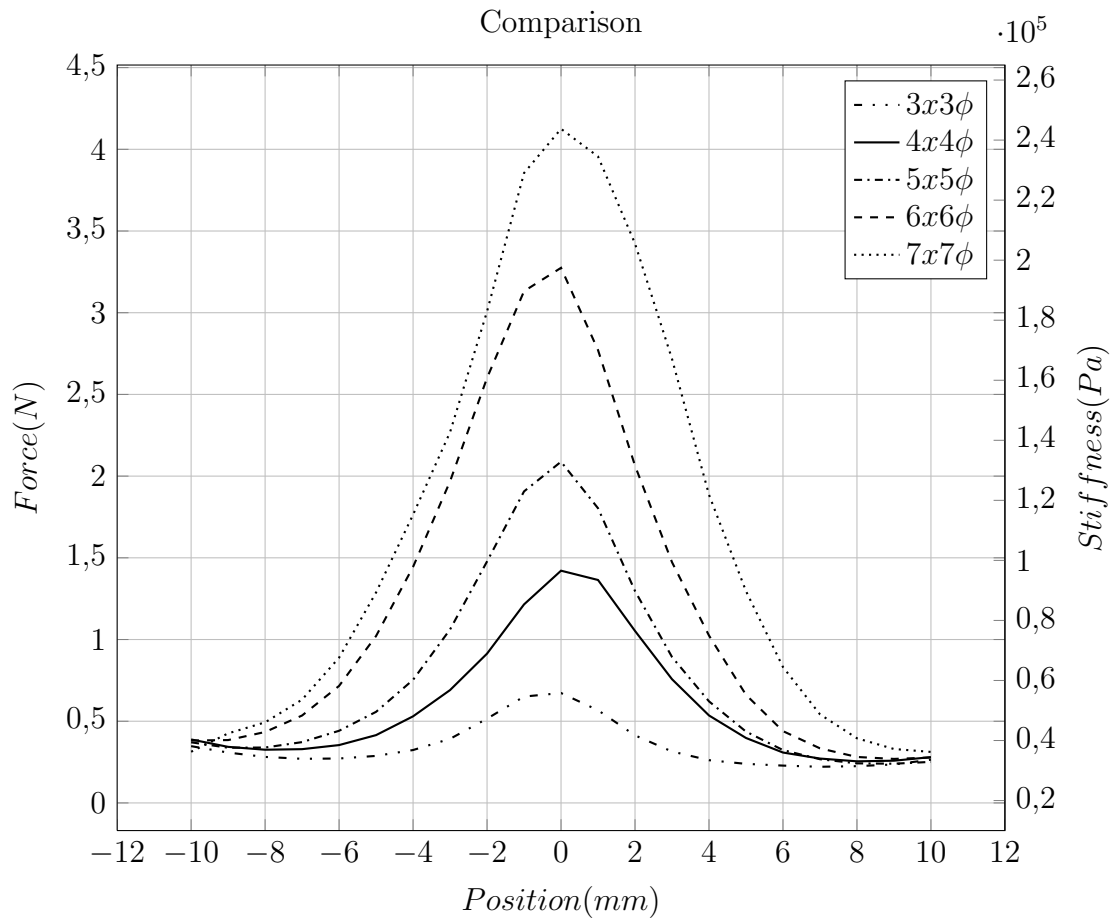
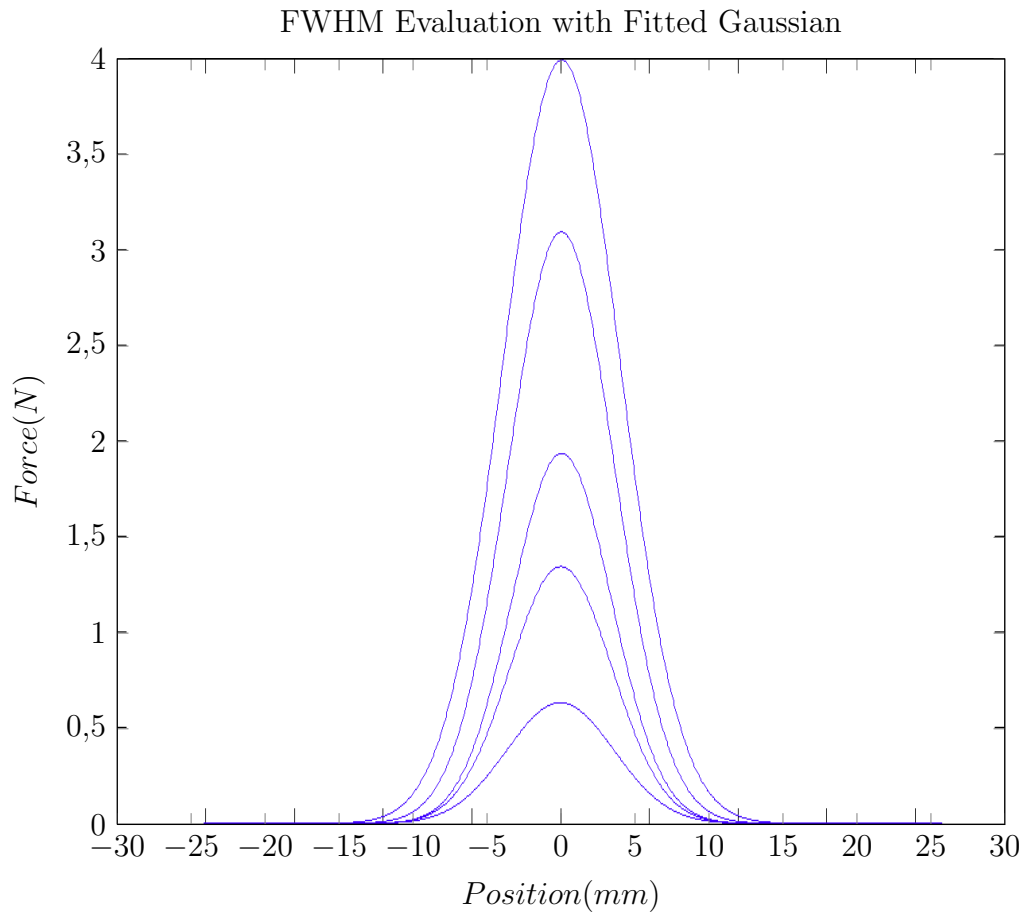
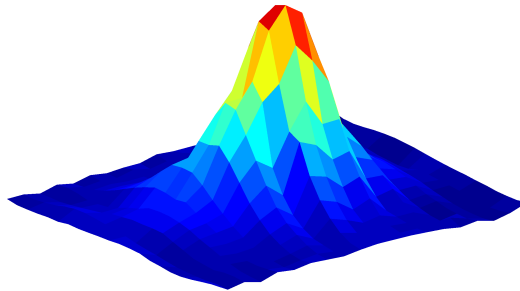


FIGURE 5.12: The information are then summarized in one graph where is possible to compare the maximum repulsive force (stiffness or equivalently Young's Module) and the FWHM.

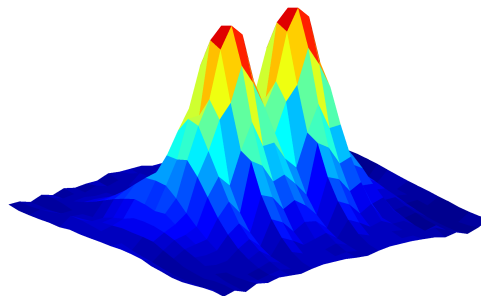
From the raw data of figure 5.12 is not easy to extrapolate the information of the full width at half maximum (FWHM). Thus, with the fitting toolbox in Matlab™ the data have been fitted with curves of the 3rd order. The values obtained are the following:



FWHM Evaluation			
Magnet diameter [mm]			
4	5	6	7
6.8 mm	7.0 mm	7.8 mm	8.4 mm



(a) Single magnet 3D distribution.



(b) Two magnets 3D distribution. The two spots are distinguishable since their distance is at the FWHM's value.

FIGURE 5.13: 3D qualitative Young's Modulus distribution.

Concluding from the results, the right trade off between the Young's Modulus generated and the value of the FWHM is with 5x5 mm neodymium magnets. Figure 5.13 shows a 3D distribution of the repulsive force generated by the tactile display, in other words the distribution of the Young's Modulus caused by the magnetic field in the magnetical properties of the MR fluid.

Chapter 6

Conclusions

6.1 Open topics and future directions

DU_E to a short research period few ideas were not fully realized but are still ongoing. These topics such as the shielding of magnetic field as discussed in chapter 2, the septa for MR's particles containment and the usage of iron nanoparticles have been partially analyzed but not sufficient data have been collected due to a lack of time.

For example has never been studied the idea of substituting the usage of PDMS with Photocurable perfluoropolyethers (PFPEs) which is liquids at room temperature and can be photocured into microfabricated devices. It exhibits low surface energy, low modulus and low toxicity fitting perfectly the intended application. In fact the PDMS septa were too hard to press and the tactile feeling unpurified by the septa's structure, which is not acceptable. If a material similar to PDMS but with a density comparable to the one of MR fluid would be used the presence of septa it would not be noticed, yet maintaining their confining capability.

Other example of future developments is the fabrication of the MR fluid itself. In the matter of fact is possible to choose whether purchasing the MR fluid or not. Buying separately glycerin and iron particles is possible to have control on the ratio of the two components. Thus, if the ratio provided by the company is not fully satisfying the request is possible to improve the dumping and mechanical properties of the purchased liquid or create a new one as well.

Another study ongoing is the variation of the bottom acrylic plate to increase the effective magnetic field applied to the particles inside the chamber. In addition on what already done in chapter 4 reducing as much as possible the thickness of the plate it has been studied the behavior of placing an iron disc perpendicularly to each magnet. In fact using the ferromagnetic properties of the iron it's possible to reply the magnetic field applied at the bottom of the display directly inside the chamber containing the MR fluid as shown in figure.

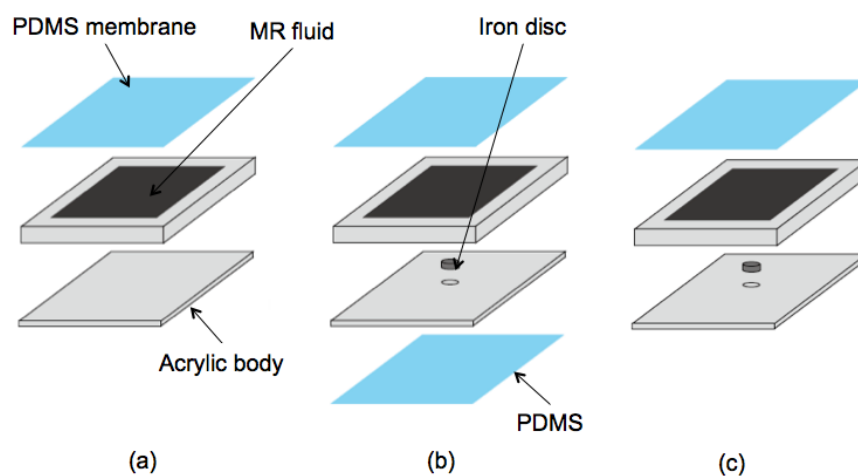


FIGURE 6.1: (a) shows the basic tactile display. To improve the spatial resolution of the device is possible to use an iron disc bonded with PDMS membrane (b) or glued directly inside the bottom acrylic plate (c).

Normally the electromagnetic field spread out in the space and becomes weak very quickly with the inverse of the cubic distance. In the presence of an external magnetic field a ferromagnetic material exhibits a characteristic ordered alignment of its magnetic dipoles. So basically the magnetic field strength permeates easily through the iron and emerges virtually on top of the disc with the same strength. The final effect is a translation of the intensity reached at the bottom of the plate directly inside the MR chamber eliminating the attenuation caused by the distance, as getting rid of the thickness of the bottom acrylic plate.

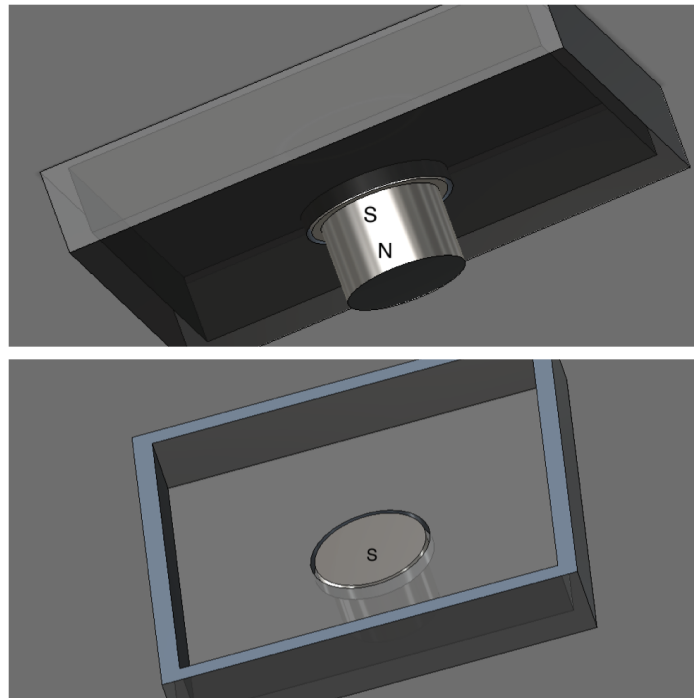


FIGURE 6.2: Detail of the ferromagnetic effect on the iron disc that traslate the same magnetic field from the top of the magnet inside the chamber.

The consequences of using this technique are the following. If the value of Young's modulus satisfies the requirements and there is no need to change the magnetic intensity, the advantage gained eliminating the thickness of the acrylic plate is used to reduce the size of the magnet getting the same magnetic intensity. On the other side keeping the same 5x5 mm diameter neodymium magnets higher magnetic field in contact with iron particles is achieved hence higher stiffness or equivalently Young's modulus is displayed.

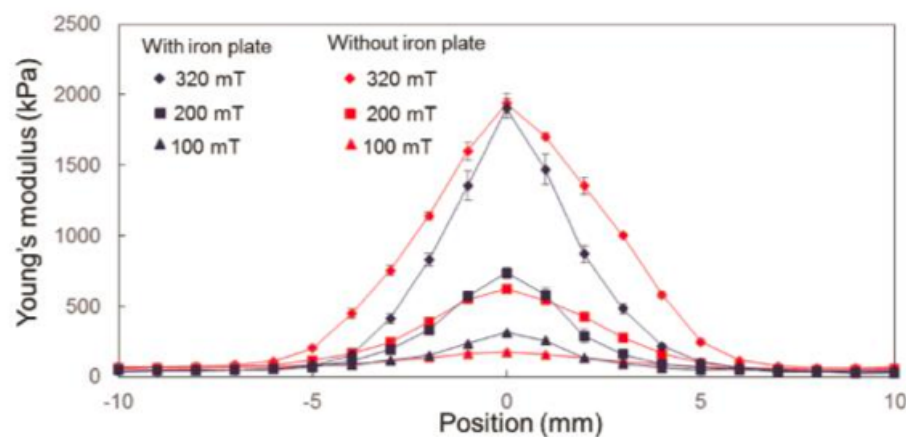


FIGURE 6.3: Picture shows Young's Modulus distribution. Using the iron disc the highest stiffness' value is substantially increased.

Another interesting point is the increase of the spatial resolution. As already discussed the magnetic flux lines exiting for the top of the magnet are forced to pass through the disc and the flux is better confined avoiding to spread in the neighborhood, thus the spot-like pixel on the display is smaller. The confirmation of what mentioned above is shown in the experimental results of Mr. Hiroki Ishizuka¹ [44]: an improvement of the Q-factor of the stiffness distribution and an higher Young's modulus displayed.

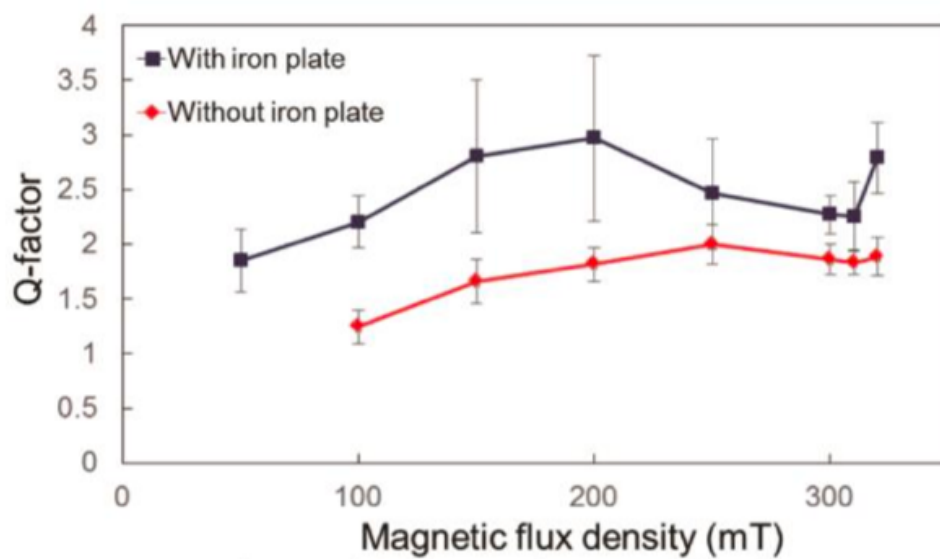


FIGURE 6.4: Relation of Q-factor with magnetic flux intensity. The Q-factor, hence the shape of the stiffness distribution is improved with the use of the iron disc.

Last but not least open topic is the quantification of tactile feeling to understand the real tactile sensation that the operator has when touches the display. As it is easily understandable the subjective tactile feeling is really hard to quantify but Mr. Hiroki Ishizuka [44] represents the benefit of using iron plate on the determination of the spot on the display with a subjective tests.

¹PhD student at Department of Mechanical Engineering at Keio University and project's fellow.

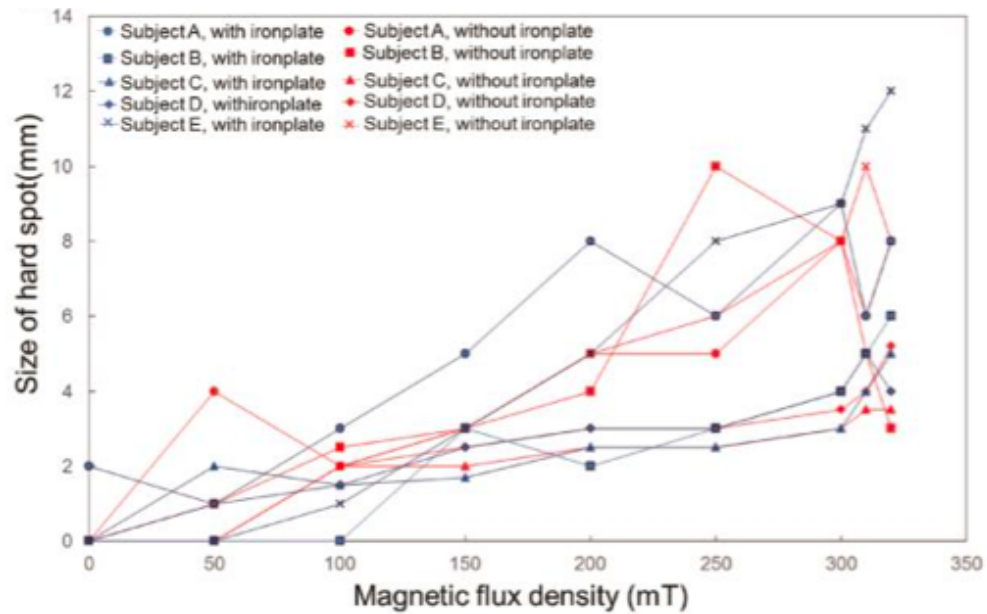


FIGURE 6.5: Subjective sensations on spot's size displayed in relation with the magnetic flux intensity.

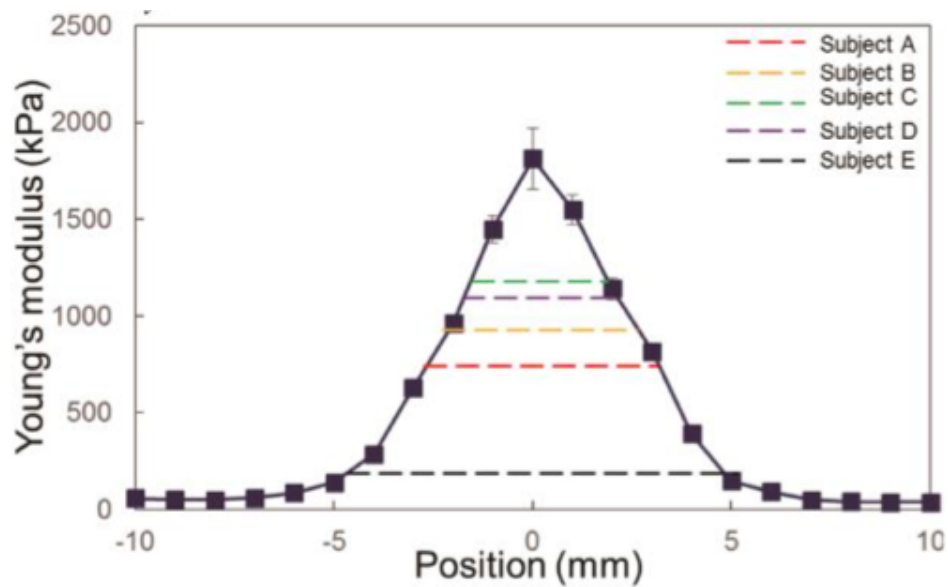


FIGURE 6.6: Picture shows the minimum detectable stiffness at 310 mT.

6.2 Final conclusions on the device

In the previous chapter it has been followed a line of draft that ended up designing a device that is the initial point for future experiments and of course for further improvements. Generically speaking the parameters that primarily affected the design of the tactile display were and still are:

- **Low complexity device:** when a device has to be engineered if it's not complex is not a deficit but an add value on the final product. Complexity especially in precise device is synonymous of high number of components and delicate parts, hence high probability of breakage. Moreover, if the device is simple it might be easier to reproduce it for testing.
- **Good spatial resolution:** especially in medical field the spatial resolution is fundamental. Higher is the spatial resolution, higher is the capability of the system to distinguish and detect smaller diseases. Let's take as an example the tumor detection: failure to distinguish also the smallest lymph node is not acceptable.
- **Delay in processing the information:** real time applications are of course preferred for immediate diagnosis without the necessity of post processing or expectation of results.
- **Repeatability and accuracy:** the results as showed in chapter 5 have to be repeatable and accurate, hence the results has to be always the same and always as close as possible to the correct one.
- **Efficiency and effectiveness:** long and interesting discussion might be opened on this topic. This two concept refer to each other: an object could be effective in what is designed for but might do it in a very inefficient way and vice versa. For example let's take a car with gasoline engine that drives people from point A to point B: the car could be really effective since all people reach the destination in a short time but it might be with high rate of pollution and high consumption, thus reaches point B not efficiently. On the other hand the car could be efficient in reaching point B if it is batteries-powered but at the same time being ineffective since it takes long time and stops to charge the engine. Balancing and trading off the efficiency and effectiveness could be made for tactile display as well.

The tactile display in object is not concluded since is just the first idea to start a wider and more complex project to enable virtual palpation in telesurgery and diagnosis using an endoscope connected with the MR display. Referring to the previous list final conclusions are the following. The display designed is very simple and its assembly is not time consuming (2 days more or less).

The spatial resolution using magnetorheological (MR) fluid and 5-millimeter diameter neodymium magnet is about 7 mm (referred to FWHM), which is consistent with the 5 mm diameter of the smallest lymph node and higher of the 40 mm of stiffness display in prior work [45]. When MR fluid reacts against an external magnetic field and changes its mechanical property the display through the PDMS membranes can create a hard spot in soft surfaces, like a tumor in tissues. The hardness of the spot is within the values of natural tissues [46] and can range of several hundreds of kPa, as show in the istogram of chapter 5. Using voice coil actuator for magnet positioning the action is fast enough to consider negligible the delay of implementation. Even though in previous chapter have been presented different software solutions and the correspondent hardware implementations the time available has not been sufficient to test them and the work has been kept as an open topic. As figures 5.7, 5.8, 5.9, 5.10 and 5.11 show the hardness displayed along the device has a small standard deviation and it is stable, hence a good repeatability has been achieved. MEMS technologies have been of great help for the design of the device ranging from the spin coating techniques for the study of the membrane to the design of the septa up now and will be in the future.

Nowadays CT scan and endoscopes are used to detect tumors. However, CT scan cannot detect tumors smaller than 5 mm and endoscopes can only observe tumors on the surfaces. Since tumors are stiffer than normal tissues, palpation is still considered to be effective and for this reason, tactile displays presented in this thesis has valuable characteristics in this field. Of course after more studies and improving the tactile display will be integrated in a bigger project to create an independent system composed of a MEMS based on-tip sensor which get mechanical information of tissues and send them to tactile device to be displayed. Once a complete device is achieved it could be integrated in existing devices as surgery assistant robots for medical real-time diagnosis.

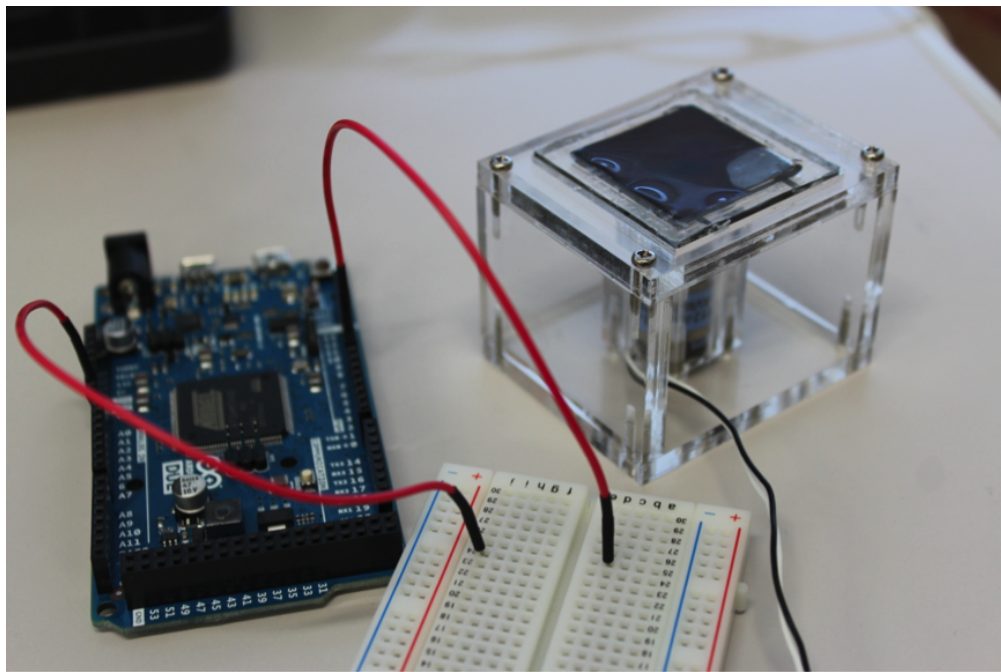


FIGURE 6.7: Tactile display with tunable stiffness and magnetorehological fluid filled-in based on voice coil actuation.

Appendix A

Conference Paper

5. Micro-Actuators
(Please chose category)

0929
Reference number from
(website confirmation)

Display of Stiffness Distribution Using Encapsulated Magnetorheological Fluid

Hiroki Ishizuka¹, Nicolo Lorenzoni² and Norihisa Miki^{1,3}
¹Keio University, Japan
²Politecnico di Milano, Italy
³JST PRESTO, Japan

This paper demonstrates a tactile display to present spatial distribution of stiffness using magnetorheological (MR) fluid. MR fluid reacts against the external magnetic field and changes its mechanical property. The display encapsulates MR fluid with flexible PDMS membranes and can create a hard spot in soft surfaces, like a tumor in tissues. We investigated the mechanical properties of the manufactured display and experimentally revealed that the hardness and size of the hard spot could be controlled by the applied magnetic field. We conducted tactile experiments using the developed display. The hard spot was successfully displayed to all the subjects, where discrepancy in the spot sizes answered by the subjects was investigated. The ultimate goal of our work is to enable palpation in telesurgery and diagnosis using an endoscope using the proposed display.

CT scan and endoscopes are used to detect tumors. However, CT scan cannot detect tumors smaller than 5 mm and endoscopes can only observe tumors on the surfaces. Since tumors are stiffer than normal tissues, palpation is considered to be effective. For this purpose, tactile displays that can present stiffness distribution several hundreds of kPa with a high resolution of millimeter or less are demanded, where MEMS technologies will be of great help. The spatial resolution of a stiffness display in prior work was 40 mm [1].

MR fluid is a mixture of magnetic iron particles 10 μm in diameter and poly- α -olefin with a weight ratio of 80wt%. When a magnetic field is applied, the particles form clusters and the fluid changes its mechanical property. Figure 1 shows the schematic image of the proposed device. MR fluid is encapsulated with PDMS membranes 100 μm in thickness. Our group has been working on liquid encapsulation into MEMS devices [2]. We also designed a display that has an iron cylinder 3 mm in diameter and 1 mm in height in the bottom plate, which confines the magnetic field and increases the resolution of the display. Figures 2 and 3 show the fabrication process and a photo of the device.

Figure 4 shows the spatial distributions of stiffness of the two devices obtained in compression tests when a permanent magnet 5 mm in diameter was positioned below the bottom plate. The magnetic field was controlled by the gap between the plate and the magnet. The stiffness was highest above the center of the magnet and decreased with the distance from the center. The stiffness increases with the magnetic field. The stiffness of tumor is reported to be in the range from 480 to 600 kPa [3], which the proposed device successfully covered. The distribution was sharper with the iron cylinder, which we evaluated by Q-factor, as shown in Figure 5.

We attempted to correlate the mechanical properties of the device with human tactile sensations. Five subjects touched the device with their index fingers and were requested to answer the size of the hard spot. As shown in Figure 6, the display could present hard spots to all the subjects. Two sources for the individual differences were considered. First, the minimum stiffness that the subject could recognize could differ. As shown in Figure 7(a), the minimum detectable stiffness determines the size of the hard spot. Second, the sizes they answered were different from the physical sizes. The vertical axis of Figure 7(b) is the normalized size by the size they answered when the magnetic field was 310 mT. The smaller individual difference was shown than in Figure 6. These characteristics of human tactile sensation need to be further analyzed for practical application of the proposed MEMS stiffness distribution display.

Word count: 598

Submitting author: H. Ishizuka, Keio University, 3-14-1 Hiyoshi, Kohoku-ku, Yokohama, 223-8522 Japan
Tel: +81-45-563-1141; Fax: +81-45-566-1495; E-mail:ishizuka1314@a3.keio.jp

References

- [1] Chu, HL and Min, GJ, *Sensors 11* (2011), pp. 2845-2856.
- [2] Hotta, Y, Zhang, Y and Miki, N, *MEMS 2011*, pp. 573-576.
- [3] Krouskop TA, Wheeler TM, Kaller F et al, *Ultrason Image 20* (1998), pp. 260-274

Appendix B

Journal Paper

Bulletin of the JSME

Vol.000, No.00, 2013

Mechanical Engineering Journal

Tactile display for stiffness distribution using Magneto-rheological fluid

Hiroki Ishizuka*, Nicolo Lorenzoni** and Norihisa Miki*

*Department of Mechanical Engineering, Keio University
3-14-1 Hiyoshi Kohoku-ku, Yokohama, Kanagawa 223-8522, Japan
E-mail: Ishizuka1314@a3.keio.jp

** Department of Electronics, Information and Bioengineering, Politecnico di Milano
Piazza Leonardo Da Vinci, 32, Milano 201-33, Italy

Abstract

This paper demonstrates a tactile display to present distribution of stiffness using Magneto-rheological (MR) fluid. CT scan and endoscopes are used to diagnosis intravital conditions. However, CT scan cannot detect tumor smaller than 5 mm, and endoscope can only diagnosis surface of tissue. It is well known that tumor is stiffer than normal tissue. If doctors press intravital tissue, they can detect tumors that have never detected. To reproduce stiffness of intravital tissue, tactile display that can present stiffness distribution on the order of 600 kPa with a high resolution of 5 millimeter will be needed. We propose tactile display with MR fluid that is changed by applied magnetic field. We investigated mechanical properties of the tactile display, and compared them to human subject's tactile sensation. At first, we measured distributions of resistance force with two probes and calculated elastic modulus. Diameter of one is 1mm, another is 4.6 mm. From experimental results, proposed display successfully created normal tissue stiffness and tumor tissue stiffness. We found force distribution was similar shape compared with applied magnetic field distribution with 1 mm probe and force distribution was like Gaussian distribution with 4.6 mm probe. Next, we attempted to compare mechanical properties of the display with human tactile sensation. As experimental method, five subjects touched the device with their finger, and answered the size of created hard spot. From experimental results, we found the difference among subjects and that they felt the size got smaller by decrease of magnetic field.

Keywords : Tactile display, Human Interface, MR fluid, Liquid Encapsulation, Elastic modulus, MEMS, Tumor tissue, Normal tissue

1. Introduction

Recently, CT scan and endoscope are used to diagnose patient's intravital condition. These minimal invasiveness and faculty to detect tumors tissue early on progression of focus contribute to quality of life. However, these equipment have faults. CT scan cannot detect tumor smaller than 5 mm. Endoscope can diagnose only surface of tissue, so cannot detect tumor inside tissue.

Generally, it is well known that stiffness of tissue changes by progress of focus and tumor tissue is two times stiffer than normal tissue (Krouskop, et al., 1998). It is said that doctors can distinguish tumor and normal tissue by their fingers. If doctors palpation patient's intravital tissue, they will detect tumor tissue by difference of stiffness. Then, doctors can detect tumors that is on position they have never detected more early on progress of focus.

For this purpose, devices to present stiffness of tissue in doctor's finger during diagnosis will be needed. To present tactile sensation to doctor's finger, use of tactile displays is considered. Many groups reported tactile display to present stiffness. These tactile displays are based on electro-rheological fluid, air pressure and diratancy fluid (Taylor, et al., 1998; Hongbing, et al., 2013; Saga, et al., 2009). These tactile displays can only display one stiffness or has resolution of stiffness distribution bigger than 40 mm.

To solve this problem, we propose tactile display with MR fluid. MR fluid is one of functional fluids and changes mechanical property by applied magnetic field. Some groups presented tactile display tactile display with MR fluid.

Bibliography

- [1] *PNAS*, 2013.
- [2] VAN ERP J. Vibrotactile spatial acuity on the torso: effects of location and timing parameters. *Haptic Interfaces for Virtual Environment and Teleoperator Systems*, Joint Eurohaptics Conference and Symposium:80 – 85, 2005.
- [3] Thorsten A. Kern. Engineering haptic devices: A beginner’s guide for engineers. 2009.
- [4] Jerzy Kaleta Daniel Lewandowski Rafał Mech and Piotr Zajac. Smart magnetic composites. *Institute of Materials Science and Applied Mechanics Wrocław University of Technology Poland*.
- [5] Yasunari Hotta Yuhua Zhang and Norihisa Miki. A flexible capacitive sensor with encapsulated liquids as dielectrics. *Micromachines*, (3):137–149, 2012.
- [6] Junpei Watanabe Hiroaki Ishikawa Xavier Arouette and Norihisa Miki. Surface texture and pseudo tactile sensation displayed by a mems-based tactile display. 2012.
- [7] Oshimichi Ami Hiroto Tachikawa Naoki Takano. Formation of polymer microneedle arrays using soft lithography.
- [8] Takashi Sakamoto and Noriyuki Hori. New pwm schemes based on the principle of equivalent areas. 2002.
- [9] Aristotle. *De anima*. ca. 350 BC.
- [10] Sharon Assaf. The ambivalence of the sense of touch in early modern prints.
- [11] Wolf U. Aristoteles’ nikomachische ethik. 2007.
- [12] Kant Immanuel. *Anthropologie in pragmatischer hinsicht*. 1983.

-
- [13] Yanju Liu J. D. Ngu R. I. Davidson P. M. Taylor. Tactile display array based on magnetorheological fluid. .
- [14] A. Bicchi (Senior Member IEEE) M. Raugi R. Rizzo and N. Sgambelluri. Analysis and design of an electromagnetic system for the characterization of magneto-rheological fluids for haptic interfaces.
- [15] Goethals P. Sette M. M. Reynaerts D. Brussel E. V. Flexible elastoresistive tactile sensor for minimally invasive surgery. *Springer, Berlin/Heidelberg*, page 573–579, 2008.
- [16] A. Kern T. A. Eicher D. Schemmer B. Schlaak H. F. Inkoman Ruse. An intracorporal manipulator for minimally invasive surgery. *In Proceedings Biomedizinische Technik*, 2006.
- [17] Gescheider G. Psychophysics: the fundamentals. *Lawrence Erlbaum Associates*, (3rd ed.), 1997.
- [18] Merriam. Neuroscience. *Webster Medical Dictionary*.
- [19] Robles De La Torre G. Virtual reality: Touch / haptics. *Sage Encyclopedia of Perception*, Thousand Oaks CA, Sage Publications 2009.
- [20] V.G. Chouvardas A.N. Miliou M.K. Hatalis. Tactile displays: Overview and recent advances.
- [21] Yanju Liu J. D. Ngu R. I. Davidson P. M. Taylor. Tactile display array based on magnetorheological fluid. .
- [22] Chul Hee Lee and Min-Gyu Jang. Virtual surface characteristics of a tactile display using magneto-rheological fluids.
- [23] Dr. John Cuppoletti. Metal ceramic and polymeric composites for various uses.
- [24] P. M. Taylor D. M. Pollet et al. Advances in an electrorheological fluid based tactile array. *Displays*, pages 135– 141, 1998.
- [25] Zsolt Varga Genoveva Filipcsei and Miklos Zrinyi. *Polymer*, pages 227–233, 2006.
- [26] Fu-Ming Hsu Guang-Yu Liu and Weileun Fang. Mems structure with tunable stiffness using the magnetorheological effect.

- [27] Rajendrani Mukhopadhyay. When pdms isn't the best.
- [28] Junpei Watanabe Hiroaki Ishikawa Xavier Arouette Yasuaki Matsumoto and Norihisa Miki. Demonstration of vibrational braille code display using large displacement micro-electro-mechanical systems actuators.
- [29] Yoshiyuki Okayama Keijiro Nakahara Xavier Arouette Takeshi Ninomiya Yasuaki Matsumoto Yoshinori Orimo Atsushi Hotta Masaki Omiya and Norihisa Miki. Characterization of a bonding-in-liquid technique for liquid encapsulation into mems devices.
- [30] Khiem NB Matsumoto K and Shimoyama I. Polymer thin film deposited on liquid for varifocal encapsulated liquid lenses. *Appl. Phys.*, (93):124101, 2008.
- [31] Yong K Eun K Soo K and B yeong. Low temperature epoxy bonding for wafer level mems. *Sensors Actuators*, (143):323–8, 2008.
- [32] YangL-J WangH-H YangP-C ChungY CandShenT. New packaging method using pdms for piezoresistive pressure sensors. *Sensors Mater*, (19), 2007.
- [33] A novel wafer-level hermetic packaging for mems devices. *IEEE Trans. Adv. Packag*, (30):616–21, 2007.
- [34] Ko H Park S Choi B Lee A and Cho D. Wafer-level hermetic packaged microaccelerometer with fully differential bicmos interface circuit. *Sensors Actuators*, pages 25–33, 137 2007.
- [35] Takegawa Y Baba T Kokudo T and Suzuki Y. Wafer-level packaging for micro-electro-mechanical systems using surface activated bonding. *Japan. J. Appl. Phys.*, (1 46):2768–70, 2007.
- [36] Kim B et al. Long-term and accelerated life test in gofa novel single-wafer vacuum encapsulation for mems resonators. *J. Microelectromech. Syst.*, (15): 1446–56, 2006.
- [37] Chen L Chang J Hsu C and Cheng. Fabrication and performance of mems-based pressure sensor packages using patterned ultra-thick photoresists. *Sensors*, (9):6200–18, 2009.
- [38] V.G. Chouvardas A.N. Miliou M.K. Hatalis. Tactile displays: Overview and recent advances. 2007.

-
- [39] Yoshimichi Ami Hiroto Tachikawa Naoki Takano. Formation of polymer microneedle arrays using soft lithography. 2011.
- [40] Thomas A. Krouskop Thomas M. Wheeler Faouzi Kallel Braian S. Garra and Timothy Hall. Elastic moduli of breast and prostate tissues under compression. *Ultrasonic imaging*, (20):260–274, 1998.
- [41] Sui Huang and Donald E. Ingber. Cell tension, matrix mechanics, and cancer development. 2005.
- [42] Wendy F. Liu and Christopher S. Chen. Engineering biomaterial to control cell function. 2005.
- [43] Takeshi Matsumura Takashi Oosaka Naoyuki Murayama Tsuyoshi Shiina Kouji Waki Yoshiko Yamamoto. Realtime tissue elastography. *Medix*, (41), 2009.
- [44] Hiroki Ishizuka Nicolo Lorenzoni and Norihisa Miki. Display of stiffness distribution using encapsulated magnetorheological fluid.
- [45] Chu HL and Min GJ. *Sensors 11*, pages 2845–2856, 2011.
- [46] Krouskop TA Wheeler TM Kaller F et al. *Ultrason Image*, (20):260–274, 1998.